

# R/V MIRAI Cruise Report MR23-05 Leg1

Interdisciplinary study of atmosphere-ocean-ecosystem variability  
in the western North Pacific

Western tropical and subtropical North Pacific  
June 28, 2023–July 20, 2023

Edited by Akira Nagano



Japan Agency for Marine–Earth Science and Technology  
(JAMSTEC)

## Contents

1. Cruise information
  - 1.1 Cruise ID
  - 1.2 Name of vessel
  - 1.3 Title of cruise
  - 1.4 Chief scientist
  - 1.5 Cruise period
  - 1.6 Ports of departure / call / arrival
  - 1.7 Research area
  - 1.8 Research map
  
2. Overview and observation summary
  - 2.1 Overview
  - 2.2 Observation summary
  - 2.3 Scientists and technical staffs
  - 2.4 Crew members
  - 2.5 Cruise log
  
3. Research/development activities
  - 3.1 General observations
    - 3.1.1 Meteorological observations
      - 3.1.1.1 Surface meteorological observations
      - 3.1.1.2 Ceilometer
  
    - 3.1.2 Ocean observations
      - 3.1.2.1 Shipboard ADCP
      - 3.1.2.2 Underway surface water monitoring
  
    - 3.1.3 Geophysical surveys
      - 3.1.3.1 Sea surface gravity
      - 3.1.3.2 Sea surface three-component magnetic field
      - 3.1.3.3 Swath bathymetry
  
  - 3.2 Mooring observations
    - 3.2.1 Kuroshio Extension Observatory (KEO) mooring -Time-series sediment trap observation-
    - 3.2.2 Philippine Sea mooring
    - 3.2.3 ADCP subsurface moorings
  
  - 3.3 Ocean observation platforms
    - 3.3.1 Wave Glider observation
    - 3.3.2 Flux drifting buoy observation
    - 3.3.3 Air-sea momentum flux observation
    - 3.3.4 Communication tests by multipurpose observation floats and radiosondes
    - 3.3.5 Virtual mooring drone observation
    - 3.3.6 Argo float observation (core)
    - 3.3.7 Argo float observation for air-sea interaction research
    - 3.3.8 Smart CARTHE drifter observation

- 3.4 CTD
  - 3.5 Water sampling
    - 3.5.1 Salinity
    - 3.5.2 Dissolved oxygen concentration
    - 3.5.3 Nutrients
    - 3.5.4 Dissolved inorganic carbon
    - 3.5.5 Total alkalinity
    - 3.5.6 Inorganic iodine
    - 3.5.7 Volatile organic iodine
    - 3.5.8 Phytoplankton pigments
    - 3.5.9 Photosynthesis–irradiance parameters of phytoplankton
    - 3.5.10 Transparent exopolymer particles
  - 3.6 Marine snow catcher observation
  - 3.7 GPS radiosonde observation
  - 3.8 C-band weather radar observation
  - 3.9 Disdrometer observation
    - 3.9.1 Optical disdrometer
    - 3.9.2 Micro rain radar
  - 3.10 Microwave radiometer observation
  - 3.11 Atmospheric composition in the marine boundary layer
    - 3.11.1 Trace gases and aerosols in the marine boundary layer
    - 3.11.2 Experiment for ozone reaction with seawater
    - 3.11.3 Greenhouse gases observation
  - 3.12 GNSS precipitable water
  - 3.13 Lidar observation
  - 3.14 Aerosol optical characteristics measured by shipborne sky radiometer
  - 3.15 Three-dimensional wind and sonic temperature observation for eddy-covariance momentum and heat fluxes observation
4. Notice on using

## **1 General information**

### **1.1 Cruise ID**

MR23-05 Leg1

### **1.2 Name of vessel**

R/V MIRAI

### **1.3 Title of cruise**

Interdisciplinary study of atmosphere-ocean-ecosystem variability in the western North Pacific

### **1.4 Chief scientist**

Akira Nagano, Senior Scientist

Center for Coupled Ocean-Atmosphere Research (CCOAR),

Research Institute for Global Change (RIGC),

Japan Agency for Marine-Earth Science and Technology (JAMSTEC)

### **1.5 Cruise period**

June 28, 2023 – July 20, 2023

### **1.6 Ports of departure / call / arrival**

Shimizu, Japan (Departure: June 28, 2023)

Koror, Palau (Call: July 13, 2023)

Shimizu, Japan (Arrival: July 20, 2023)

### **1.7 Research area**

The western tropical and subtropical North Pacific

### 1.8 Research map

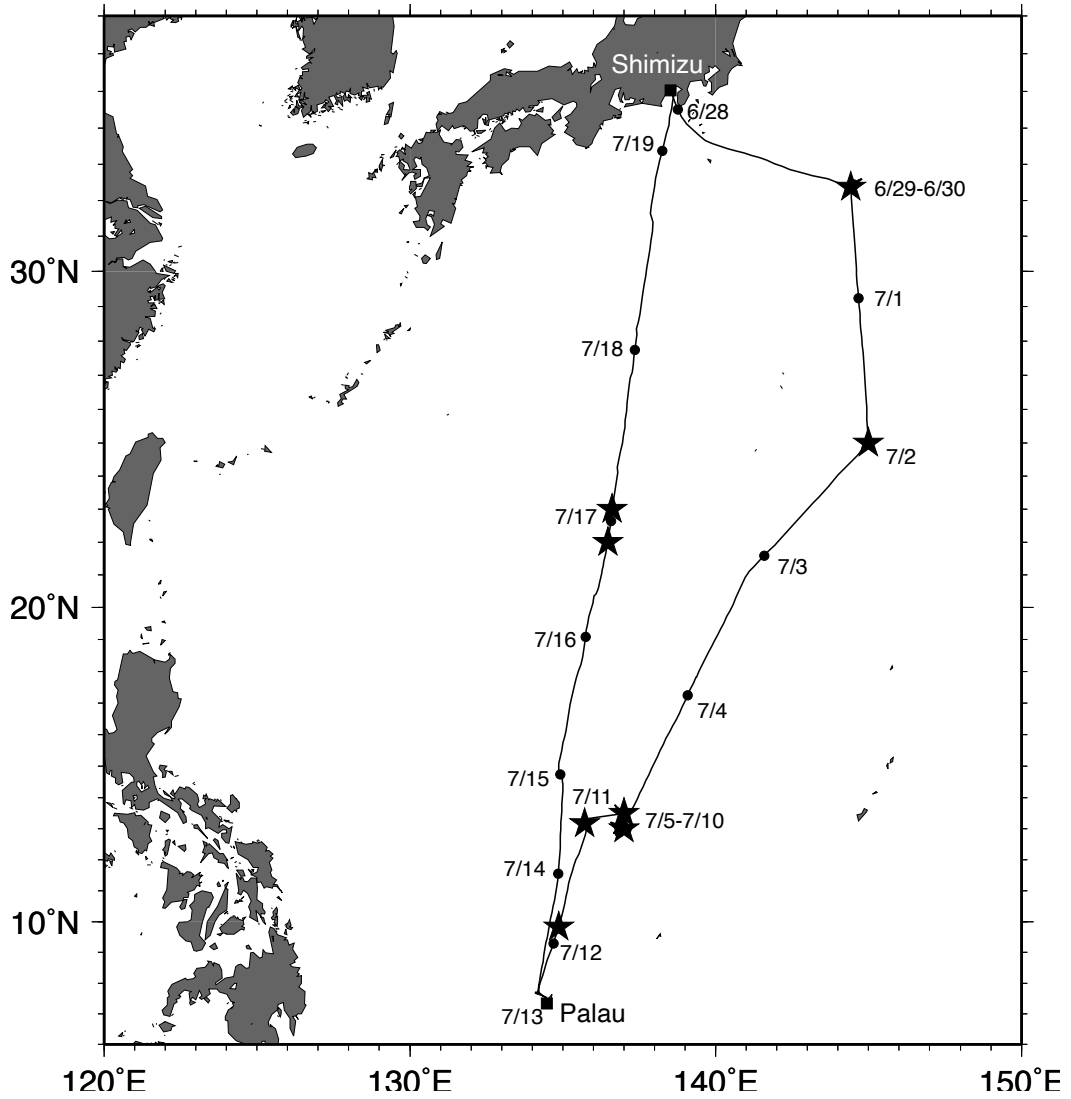


Figure 1.8-1 MR23-05 Leg1 cruise track (solid line). Stars and dots indicate observation sites and SMT (UTC+9hr) 00:00 positions of the R/V MIRAI, respectively.

## 2 Overview and observation summary

### 2.1 Overview

The western North Pacific is an effective sink of carbon dioxide due to primary production by algae and others. The study of the nutrients supply process which owes to biological production is critical to understand the ecosystem and carbon circulation and to predict their future states. In addition, the ocean plays a key role in the global climate through the teleconnection of El Niño/Southern Oscillation (ENSO) and the Pacific decadal oscillation (PDO). In particular, the warm water pool located at the western Pacific has the highest sea surface temperature (SST) in the ocean all over the world. Therefore, the ocean and atmosphere interaction in this region is important for the climate variability.

This cruise was conducted to understand the biogeochemical processes and air-sea interaction in the tropical and subtropical western North Pacific. For these purposes, we performed deployment and recovery of the Kuroshio Extension observatory (KEO) sediment-trap mooring, the Philippine Sea mooring (PHSMO) buoy, acoustic Doppler current profiler (ADCP) subsurface moorings as the main mission. The buoy observations are advantageous for analyses of the long-term variabilities. In addition, we carried out other observations, such as by using a conductivity-temperature-depth (CTD) and other sensors, water sampling, radiosondes, ocean observation platforms, and other meteorological instruments.

### 2.2 Observation summary

Kuroshio Extension Observatory (KEO) mooring deployment	1 site
KEO mooring recovery	1 site
Philippine Sea Mooring (PHSMO) mooring buoy	1 site
PHSMO mooring buoy recovery	1 site
ADCP mooring deployment	2 sites
ADCP mooring recovery	2 sites
Wave Glider	1 site
CTD including water sampling	12 casts
Radiosonde	56 launched
Argo float observation	5 sites
Surface meteorology	continuous
Doppler radar observation	continuous
Shipboard ADCP observation	continuous
Geophysical observation	continuous

Surface temperature, salinity and dissolved oxygen measurements

by intake method

continuous

\*\*\* Other specially designed observations have been carried out successfully

## 2.3 Scientists and technical staffs

Name		Affiliation	Occupation
Akira	Nagano	JAMSTEC	Chief Scientist
Iwao	Ueki	JAMSTEC	Scientist
Masaki	Katsumata	JAMSTEC	Scientist
Makio	Honda	JAMSTEC	Scientist
Kazuhiko	Matsumoto	JAMSTEC	Scientist
Fumikazu	Taketani	JAMSTEC	Scientist
Takashi	Sekiya	JAMSTEC	Scientist
Kensuke	Watari	JAMSTEC	Engineer
Masahiro	Kaku	JAMSTEC	Engineer
Hiroshi	Matsubara	NTT Space Environment and Energy Laboratories	Scientist
Hongwei	Qin	AORI, The University of Tokyo	Scientist
Tianchang	Cui	Hokkaido University	Scientist
Yutaro	Murakami	Nippon Marine Enterprises	Technical Staff
Ryo	Oyama	Nippon Marine Enterprises	Technical Staff
Hiroki	Ushiromura	Marine Works Japan	Technical Staff
Masaki	Furuhata	Marine Works Japan	Technical Staff
Makito	Yokota	Marine Works Japan	Technical Staff
Masaki	Yamada	Marine Works Japan	Technical Staff
Kango	Fukuyama	Marine Works Japan	Technical Staff
Keita	Hayashi	Marine Works Japan	Technical Staff
Nobuhiro	Fujii	Marine Works Japan	Technical Staff
Htet Aung	Tun	Marine Works Japan	Technical Staff
Aine	Yoda	Marine Works Japan	Technical Staff
Katsunori	Sagishima	Marine Works Japan	Technical Staff
Nagisa	Fujiki	Marine Works Japan	Technical Staff
Masahiro	Orui	Marine Works Japan	Technical Staff
Misato	Kuwahara	Marine Works Japan	Technical Staff
Shiori	Ariga	Marine Works Japan	Technical Staff
Yuko	Miyoshi	Marine Works Japan	Technical Staff
Takuya	Izutsu	Marine Works Japan	Technical Staff

## 2.4 Crew members

Name		Rank or Rating
Akihisa	Tsuji	Master
Hiroyuki	Kato	Chief Officer
Shozo	Fujii	1 <sup>st</sup> Officer
Yasuhito	Iida	2 <sup>nd</sup> Officer
Natsuko	Sakurai	3 <sup>rd</sup> Officer
Kazuhiko	Kaneda	Chief Engineer
Yoichi	Yasue	1 <sup>st</sup> Engineer
Ryuzo	Mikami	2 <sup>nd</sup> Engineer
Genta	Takeya	3 <sup>rd</sup> Engineer
Yosuke	Komaki	Chief Radio Operator
Kazuyoshi	Kudo	Boatswain
Tsuyoshi	Sato	Quarter Master
Shuji	Komata	Quarter Master
Kenji	Nakae	Quarter Master
Hideyuki	Okubo	Quarter Master
Satoshi	Shimpo	Quarter Master
Shohei	Uehara	Quarter Master
Yuki	Oishi	Sailor
Shin	Ito	Sailor
Ryota	Kume	Sailor
Iori	Terasaki	Sailor
Hiroyuki	Oishi	No.1 Oiler
Takuya	Watanabe	Oiler
Daiki	Sato	Oiler
Tsuyoshi	Uchiyama	Assistant Oiler
Kyotaro	Maruyama	Assistant Oiler
Marina	Shimizu	Assistant Oiler
Tatsunari	Onoue	Chief Steward
Toshiyuki	Asano	Steward
Kenichi	Okumura	Steward
Kanjuro	Murakami	Steward
Hodaka	Wakizaka	Steward
Yuta	Hangai	Steward

## 2.5 Cruise log

SMT (UTC + 9 hr)		UTC		Event logs		
Date	Time	Date	Time			
06.28 (Wed)	09:00	06.28 (Wed)	00:00	Departure from Shimizu, Japan		
	10:38		01:38	Start of sea surface water sampling		
	13:15		04:15	Start of continuous observations		
	14:30		05:30	Emergency drill		
	20:30		11:30	Radiosonde		
06.29 (Thu)	00:00	06.29 (Thu)	15:00	Radiosonde		
	02:30		17:30	Start of Doppler radar observation		
	08:30		23:30	Radiosonde		
	13:40-16:48		04:40-07:48	Recovery of the KEO sediment-trap mooring		
	14:30		05:30	Radiosonde		
06.30 (Fri)	20:30	06.30 (Fri)	11:30	Radiosonde		
	02:30		17:30	Radiosonde		
	06:59-08:02		21:59-23:02	CTD-Shallow/water sampling at KEO site (32°-27.43'N, 144°-31.93'E, 500 m)		
	08:24-10:02		23:24-25:02	MSC-Shallow/Deep at KEO site		
	08:30		23:30	Radiosonde		
	10:28-14:33		01:28-05:33	CTD-Deep/water sampling at KEO site (32°-27.37'N, 144°-31.60'E, 5760 m)		
	14:30		05:30	Radiosonde		
	14:46-18:21		05:46-07:21	Deployment of the KEO sediment-trap mooring (32°-21.95'N, 144°-25.17'E, 5785 m)		
	20:30		11:30	Radiosonde		
	07.01 (Sat)		02:30	07.01 (Sat)	17:30	Radiosonde
08:30		23:30	Radiosonde			
14:30		05:30	Radiosonde			
20:30		11:30	Radiosonde			
07.02 (Sun)	08:00-09:04	07.02 (Sun)	23:00-24:04	CTD-Shallow/water sampling at KEOS site (24°-59.98'N, 144°-59.98'E, 400 m)		
	09:18-10:32		00:18-01:32	MSC-Shallow/Deep at KEOS site		
	09:47		00:47	Radiosonde		
	10:58-14:26		01:58-05:26	CTD-Deep/water sampling at KEOS site (24°-59.89'N, 145°-00.06'E, 5042 m)		
	14:29		05:29	Installation of an Argo float		
	20:28		11:28	Radiosonde		
	07.03 (Mon)		09:40	07.03 (Mon)	00:40	Radiosonde
07.04 (Tue)	20:30	07.04 (Tue)	11:30	Radiosonde		
	20:24		11:30	Radiosonde		
07.05 (Wed)	08:30	07.05 (Wed)	23:30	Radiosonde		
	09:11		00:11	Installation of a Wave Glider		
	13:04		04:04	Installation of a MOF		
	13:08-16:33		04:08-07:33	CTD-Deep/water sampling at PHSMO site (13°-07.52'N, 136°-53.11'E, 5135 m)		
	14:30		05:30	Radiosonde		
	14:57		05:57	Radiosonde for communication with MOF		
	16:35		07:35	Installation of an Argo float		
	20:30		11:30	Radiosonde		
	07.06 (Thu)		02:22	07.06 (Thu)	17:22	Radiosonde
			08:00-09:01		23:00-24:01	CTD-Shallow/water sampling at PHSMO site (13°-00.00'N, 136°-59.86'E, 500 m)
08:30		23:30	Radiosonde			
09:05-		00:05-	MSC-Shallow/Deep at PHSMO site			

	10:24		01:24	
	13:20		04:20	Installation of JAMSTEC flux surface buoy
	13:24		04:24	Installation of JAMSTEC flux surface buoy
	13:27		04:27	Installation of Kindai flux surface buoy
	14:30		05:30	Radiosonde
	20:30		11:30	Radiosonde
07.07 (Fri)	02:22		17:22	Radiosonde
	08:30		23:30	Radiosonde
	08:33-13:48		23:30-28:48	Deployment of the new PHSMO buoy (12°-53.61'N, 136°-54.31'E, 5246 m)
	14:26	07.07 (Fri)	05:26	Radiosonde
	14:30-14:58		05:30-05:58	CTD-Shallow at PHSMO site (12°-53.73'N, 136°-54.70'E, 500 m)
	15:14		06:14	Installation of a VM drone
	20:30		11:30	Radiosonde
07.08 (Sat)	22:22		13:30	Radiosonde for communication with MOF
	02:30		17:30	Radiosonde
	08:05-13:42		23:05-28:42	Recovery of the old PHSMO buoy
	08:30		23:30	Radiosonde
	14:30	07.08 (Sat)	05:30	Radiosonde
	16:31		07:31	Recovery of the VM drone
07.09 (Sun)	20:29		11:29	Radiosonde
	02:30		17:30	Radiosonde
	07:59-10:18		22:59-25:18	Recovery of old ADCP_S mooring
	08:28		23:28	Radiosonde
	13:11-14:46	07.09 (Sun)	04:11-05:46	Deployment of new ADCP_S mooring (12°-58.99'N, 137°-08.27'E, 5032 m)
	14:22		05:22	Radiosonde
07.10 (Mon)	20:30		11:30	Radiosonde
	02:30		17:30	Radiosonde
	07:59-08:53		22:59-23:53	CTD-Shallow/water sampling (13°-30.86'N, 137°-03.03'E, 250 m)
	08:30		23:30	Radiosonde
	09:25-12:05	07.10 (Mon)	00:25-03:05	Recovery of old ADCP_N mooring
	12:14		03:14	Installation of a MOF
	13:41-15:56		04:41-05:56	Deployment of new ADCP_N mooring (13°-29.96'N, 137°-03.97'E, 5039 m)
	13:27		04:27	Radiosonde for communication with MOF
	14:30		05:30	Radiosonde
	16:31		07:31	Radiosonde for communication with MOF
07.11 (Tue)	20:30		11:30	Radiosonde
	02:30		17:30	Radiosonde
	08:22		23:22	Radiosonde
	08:28-09:39		23:28-24:39	CTD-Shallow/water sampling (13°-10.23'N, 135°-43.09'E, 500 m)
	09:41-12:04	07.11 (Tue)	00:41-03:04	MSC-Shallow/Deep
	10:20		01:20	Radiosonde for communication with MOF
	13:45		04:45	Recovery of JAMSTEC flux surface buoy
	14:14		05:14	Recovery of JAMSTEC flux surface buoy
	14:30		05:14	Radiosonde
	15:16		06:16	Recovery of Kindai flux surface buoy
	16:46		07:46	Radiosonde for communication with MOF
07.12 (Wed)	20:30		11:30	Radiosonde
	02:30		17:30	Radiosonde
	08:00-09:02		23:00-24:02	CTD-Shallow/water sampling (9°-49.76'N, 134°-51.64'E, 500 m)
	08:52		23:52	Radiosonde

	09:04 16:00	07.12 (Wed)	00:04 07:00	Installation of an Argo float Stop of sea surface water sampling Stop of continuous observations
07.13 (Thu)	09:00 14:00 17:00	07.13 (Tue)	00:00 05:00 08:00	Arrival at Koror, Palau Departure from Koror Start of sea surface water sampling Start of continuous observations
07.14 (Fri)	19:03 20:30		10:03 11:30	Radiosonde for communication with MOF Radiosonde
07.15 (Sat)	08:15 09:25 15:26 15:37 16:30 20:30	07.15 (Sat)	23:15 00:25 06:26 06:37 07:30 11:30	Deployment of the VM drone Recovery of the Wave Glider Recovery of the VM drone Installation of a MOF Radiosonde for communication with MOF Radiosonde
07.16 (Sun)	20:30	07.16 (Sun)	11:30	Radiosonde
07.17 (Mon)	07:58- 08:34 08:35 13:55- 14:25 14:25 14:28 20:30		22:58- 23:34 23:35 04:55- 05:25 05:25 05:28 11:30	CTD-Shallow (21°-59.95'N, 136°-27.95'E, 500 m) Installation of an Argo float CTD-Shallow (22°-59.92'N, 136°-37.42'E, 500 m) Installation of an Argo float Installation of two smart CARTHE drifters Radiosonde
07.18 (Tue)	02:30 08:30 14:30 20:30	07.17 (Mon)	05:25 05:25 05:28 11:30 17:30 23:30 05:30 11:30	Radiosonde Radiosonde Radiosonde Radiosonde Radiosonde Radiosonde
07.19 (Wed)	02:30 08:30 09:00	07.18 (Tue)	05:30 11:30 17:30 23:30	Radiosonde Radiosonde Radiosonde Radiosonde
		07.19 (Wed)	00:00	Stop of sea surface water sampling Stop of continuous observations
07.20 (Thu)	09:00			Arrival at Shimizu, Japan

### 3. Research/development activities

#### 3.1 General observations

##### 3.1.1 Meteorological observations

##### 3.1.1.1 Surface meteorological observations

Akira NAGANO	(JAMSTEC)	- Principal investigator
Yutaro MURAKAMI	(NME)	- Operation leader
Ryo OYAMA	(NME)	
Yosuke KOMAKI	(NME)	- MIRAI crew

##### (1) Objectives

Surface meteorological parameters are observed as a basic dataset of the meteorology. These parameters provide the temporal variation of the meteorological condition surrounding the ship.

##### (2) Instruments and methods

Surface meteorological parameters were observed during this cruise. In this cruise, we used two systems for the observation.

##### i) MIRAI Surface Meteorological observation (SMet) system

Instruments of SMet system are listed in Table 3.1.1.1-1 and measured parameters are listed in Table 3.1.1.1-2. Data were collected and processed by KOAC-7800 weather data processor made by Koshin-Denki, Japan. The data set consists of 6 seconds averaged data.

##### ii) Shipboard Oceanographic and Atmospheric Radiation (SOAR) measurement system

SOAR system designed by BNL (Brookhaven National Laboratory, USA) consists of major five parts.

- a) Analog meteorological data sampling with CR1000 logger manufactured by Campbell Inc., Canada - wind, pressure, and rainfall (by a capacitive rain gauge (CRG)) measurement.
- b) Digital meteorological data sampling from individual sensors - air temperature, relative humidity and rainfall (by optical rain gauge (ORG)) measurement.
- c) Radiation data sampling with CR1000X logger manufactured by Campbell Inc., Radiometers designed by Hukseflux Thermal Sensors B.V. Netherlands. – short and long wave downward radiation measurement.
- d) Photosynthetically Available Radiation (PAR) and Ultraviolet Irradiance (UV) sensor manufactured by Biospherical Instruments Inc., USA. – PAR and UV measurement.
- e) Scientific Computer System (SCS) developed by NOAA (National Oceanic and Atmospheric Administration, USA) - centralized data acquisition and logging of all data sets. SCS recorded radiation, air temperature, relative humidity, CR1000, ORG and PAR data. SCS composed Event data (JamMet) from these data and ship's navigation data every 6 seconds. Instruments and their locations are listed in Table 3.1.1.1-3 and measured parameters are listed in Table 3.1.1.1-4.

##### iii) Quality control

For the quality control as post processing, we checked the following sensors, before and after the cruise.

- a) Young Rain Gauge (SMet and SOAR)  
Inspect of the linearity of output value from the rain gauge sensor to change input value by adding fixed quantity of test water.
- b) Barometer (SMet and SOAR)

- Comparison with the portable barometer value, PTB220, VAISALA
- c) Thermometer (air temperature and relative humidity) (SMet and SOAR)  
Comparison with the portable thermometer value, HMP70, VAISALA

(3) Preliminary results

Figure 3.1.1.1-1 show the time series of the following parameters;

- Wind (SOAR)
- Air temperature (SMet)
- Relative humidity (SMet)
- Precipitation (SOAR, CRG)
- Short/long wave radiation (SOAR)
- Barometric Pressure (SMet)
- Sea surface temperature (SMet)
- Significant wave height (SMet)

(4) Data archives

These obtained data will be submitted to JAMSTEC Data Management Group (DMG).

(5) Remarks (Times in UTC)

- i) The following periods, data acquisition was suspended due to within the territorial sea of Palau.  
07:00UTC 12 Jul. 2023 – 08:00UTC 13 Jul. 2023
- ii) The following period, Sea surface temperature of SMet data were available.  
01:39UTC 28 Jun. 2023 – 06:58UTC 12 Jul. 2023  
08:00UTC 13 Jul. 2023 – 00:00UTC 19 Jul. 2023

Table3.1.1.1-1. Instruments and installation locations of the MIRAI Surface Meteorological observation system

Sensors	Type	Manufacturer	Location (altitude from surface)
Anemometer	KS-5900	Koshin Japan	Denki, Foremast (25 m)
Tair/RH with aspirated radiation shield	HMP155 43408 Gill	Vaisala, Finland R.M. Young, USA	Compass deck (21 m) starboard side and port side
Thermometer: SST	RFN2-0	Koshin Japan	Denki, 4th deck (-1m, inlet -5m)
Barometer	Model-370	Setra System, USA	Captain deck (13 m) weather observation room
Capacitive rain gauge	50202	R. M. Young, USA	Compass deck (19 m)
Optical rain gauge	ORG-815DS	Osi, USA	Compass deck (19 m)
Radiometer (short wave)	MS-802	Eko Seiki, Japan	Radar mast (28 m)
Radiometer (long wave)	MS-202	Eko Seiki, Japan	Radar mast (28 m)
Wave height meter	WM-2	Tsurumi-seiki, Japan	Bow (10 m) Stern (8 m)

Table3.1.1.1-2. Parameters of the MIRAI Surface Meteorological observation system

Parameter	Units	Remarks
1 Latitude	degree	
2 Longitude	degree	
3 Ship's speed	knot	MIRAI log
4 Ship's heading	degree	MIRAI gyro
5 Relative wind speed	m/s	6sec./10min. averaged
6 Relative wind direction	degree	6sec./10min. averaged
7 True wind speed	m/s	6sec./10min. averaged
8 True wind direction	degree	6sec./10min. averaged
9 Barometric pressure	hPa	adjusted to sea surface level 6sec. averaged
10 Air temperature (starboard)	degC	6sec. averaged
11 Air temperature (port)	degC	6sec. averaged
12 Dewpoint temperature (starboard)	degC	6sec. averaged
13 Dewpoint temperature (port)	degC	6sec. averaged
14 Relative humidity (starboard)	%	6sec. averaged
15 Relative humidity (port)	%	6sec. averaged
16 Sea surface temperature	degC	6sec. averaged
17 Precipitation intensity (optical rain gauge)	mm/hr	hourly accumulation
18 Precipitation (capacitive rain gauge)	mm/hr	hourly accumulation
19 Down welling shortwave radiation	W/m <sup>2</sup>	6sec. averaged
20 Down welling infra-red radiation	W/m <sup>2</sup>	6sec. averaged
21 Significant wave height (bow)	m	hourly
22 Significant wave height (stern)	m	hourly
23 Significant wave period (bow)	second	hourly
24 Significant wave period (stern)	second	hourly

Table3.1.1.1-3. Instruments and installation locations of SOAR system

Sensors (Meteorological)	Type	Manufacturer		Location
Anemometer	05106	R.M. Young, USA		foremast (25 m)
Barometer	PTB210	Vaisala, Finland		foremast (23 m)
with pressure port	61002 Gill	R.M. Young, USA		foremast (24 m)
Rain gauge	50202	R.M. Young, USA		foremast (24 m)
Tair/RH	HMP155	Vaisala, Finland		foremast (23 m)
with aspirated radiation shield	43408 Gill	R.M. Young, USA		foremast (24 m)
Optical rain gauge	ORG-815DR	Osi, USA		foremast (24 m)
Sensors (Radiation)	Type	Manufacturer		Location *
Radiometer (short wave)	SR20	Hukseflux	Thermal	foremast (25 m)
		Sensors	B.V., Netherlands	
Radiometer (long wave)	IR20	Hukseflux	Thermal	foremast (25 m)
		Sensors	B.V., Netherlands	
Sensor (PAR&UV)	Type	Manufacturer		Location *
PAR&UV sensor	PUV-510	Biospherical Inc., USA	Instruments	Navigation deck (18m)

\*Location: Altitude from surface

Table3.1.1.1-4. Parameters of SOAR system (JamMet)

Parameter	Units	Remarks
1 Latitude	degree	
2 Longitude	degree	
3 SOG	knot	
4 COG	degree	
5 Relative wind speed	m/s	
6 Relative wind direction	degree	
7 Barometric pressure	hPa	
8 Air temperature	degC	
9 Relative humidity	%	
10 Precipitation intensity (optical rain gauge)	mm/hr	
11 Precipitation (capacitive rain gauge)	mm/hr	reset at 50 mm
12 Down welling shortwave radiation	W/m <sup>2</sup>	
13 Down welling infrared radiation	W/m <sup>2</sup>	
14 PAR	microE/cm <sup>2</sup> /sec	
15 UV 305 nm	microW/cm <sup>2</sup> /nm	
16 UV 320 nm	microW/cm <sup>2</sup> /nm	
17 UV 340 nm	microW/cm <sup>2</sup> /nm	
18 UV 389 nm	microW/cm <sup>2</sup> /nm	

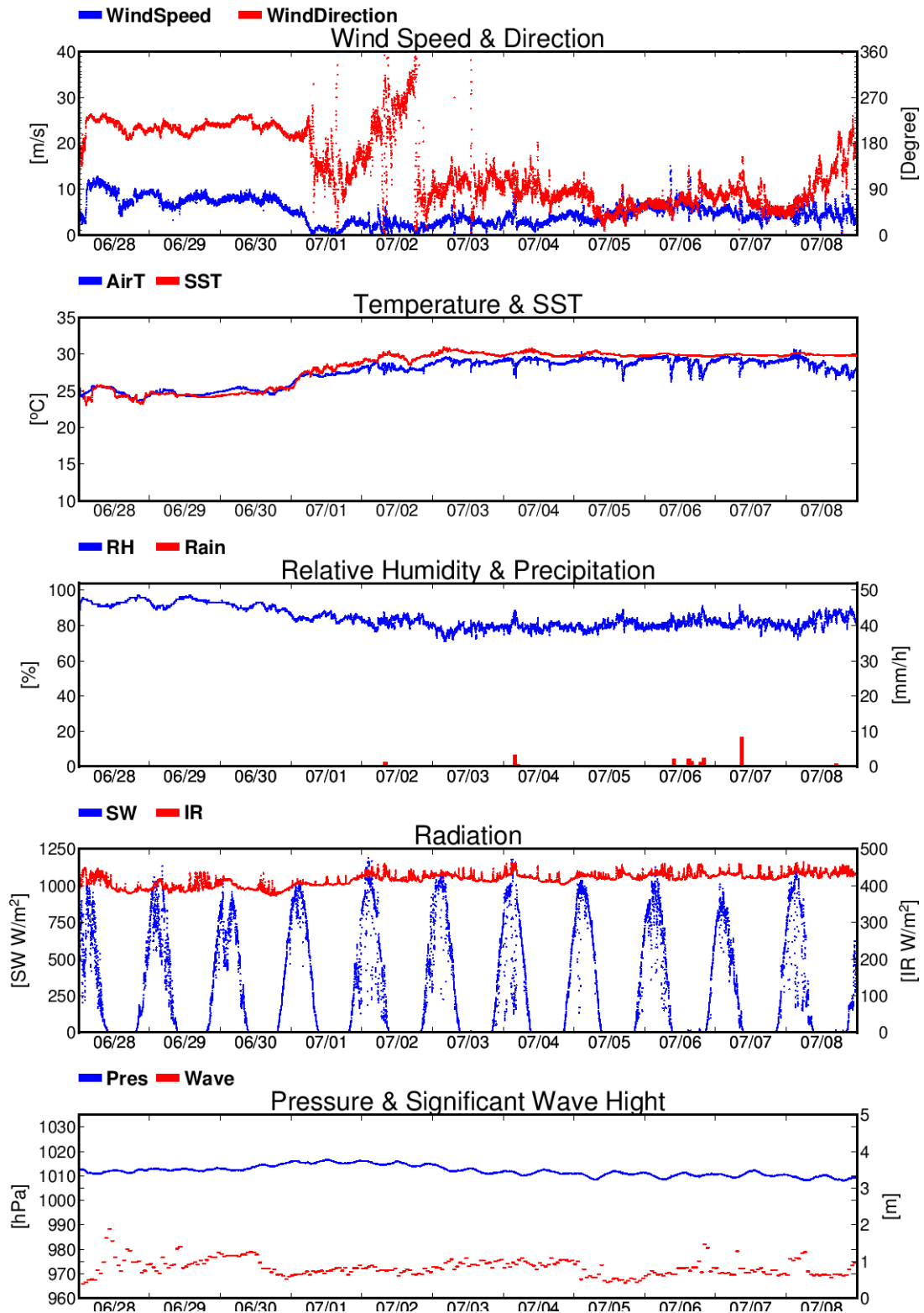


Figure 3.1.1.1-1 Time series of surface meteorological parameters during MR23-05Leg1

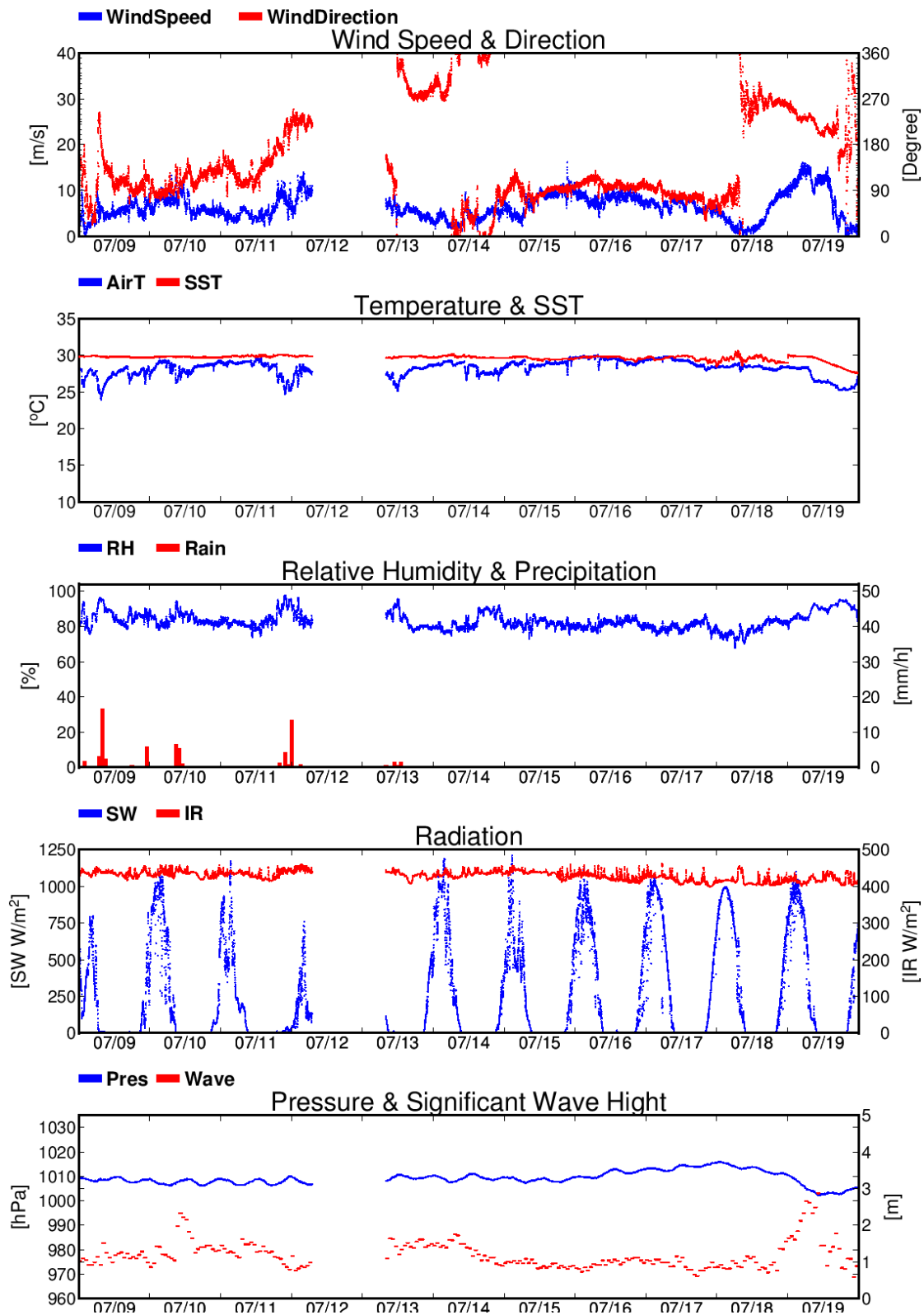


Figure 3.1.1.1-1 (Continued)

### 3.1.1.2 Ceilometer

Akira NAGANO	(JAMSTEC)	- Principal Investigator
Yutaro MURAKAMI	(NME)	- Operation Leader
Ryo OYAMA	(NME)	
Yosuke KOMAKI	(NME)	- MIRAI Crew

#### (1) Objectives

The information of cloud base height and the liquid water amount around cloud base is important to understand the process on formation of the cloud. As one of the methods to measure them, the ceilometer observation was carried out.

#### (2) Instruments and methods

Cloud base heights and backscatter profiles were observed by ceilometer (CL51, VAISALA, Finland). On the archive dataset, cloud base heights and backscatter profiles were recorded with a resolution of 10 m.

#### i) Parameters

- a) Cloud base height [m].
- b) Backscatter profile, sensitivity, and range normalized at 10 m resolution.
- c) Estimated cloud amount [oktas] and height [m]; Sky Condition Algorithm.

#### ii) The measurement configurations are shown in Table 3.1.1.2-1.

Table 3.1.1.2-1 The measurement configurations

Property	Description
Laser source	Indium Gallium Arsenide (InGaAs) Diode
Transmitting center wavelength	910±10 nm at 25 degC
Transmitting average power	19.5 mW
Repetition rate	6.5 kHz
Detector	Silicon avalanche photodiode (APD)
Responsibility at 905 nm	65 A/W
Cloud detection range	0 – 13 km
Measurement range	0 – 15 km
Resolution	10 m in full range
Sampling rate	36 sec.
	Cloudiness in octas (0 – 9)
	0 Sky Clear
	1 Few
Sky Condition	3 Scattered
	5 – 7 Broken
	8 Overcast
	9 Vertical Visibility

(3) Preliminary results

Figure 3.1.1.2-1 show the time-series of the lowest, second and third cloud base height during the cruise.

(4) Data archives

These obtained data will be submitted to JAMSTEC Data Management Group (DMG).

(5) Remarks (Times in UTC)

i) The following periods, data acquisition was suspended due to within the territorial sea of Palau.

07:00UTC 12 Jul. 2023 – 08:00UTC 13 Jul. 2023

ii) Window cleaning

00:15UTC 04 Jul. 2023

01:13UTC 15 Jul. 2023

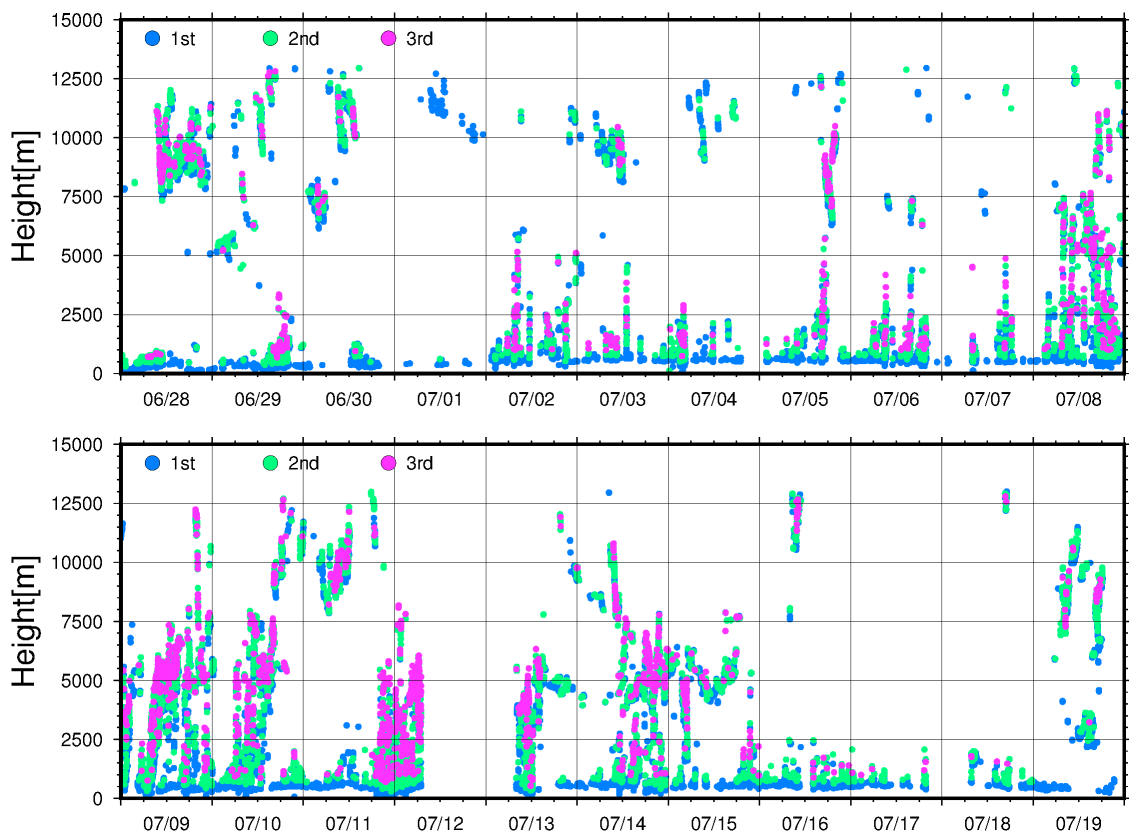


Figure 3.1.1.2-1 Time series of cloud base height during MR23-05Leg1

### 3.1.2 Ocean observations

#### 3.1.2.1 Shipboard ADCP

Akira NAGANO	(JAMSTEC)	- Principal investigator
Yutaro MURAKAMI	(NME)	- Operation leader
Ryo OYAMA	(NME)	
Yosuke KOMAKI	(NME)	- MIRAI crew

##### (1) Objectives

To obtain continuous measurement data of the current profile along the ship's track.

##### (2) Instruments and methods

Upper ocean current measurements were made during this cruise, using the hull-mounted Acoustic Doppler Current Profiler (ADCP) system. For most of its operation, the instrument was configured for water-tracking mode. Bottom-tracking mode, interleaved bottom-ping with water-ping, was made to get the calibration data for evaluating transducer misalignment angle in the shallow water. Major parameters for the measurement, Direct Command, are shown in Table 3.1.2.1-1. The system consists of following components;

- i) Ocean Surveyor for vessel-mount ADCP (frequency 76.8 kHz; Teledyne RD Instruments, USA) has been installed to the R/V MIRAI. It has a phased-array transducer with single ceramic assembly and creates 4 acoustic beams electronically. We mounted the transducer head rotated to a ship-relative angle of 45 degrees azimuth from the keel.
- ii) For heading source, we use ship's gyro compass (Tokyo Keiki, Japan), continuously providing heading to the ADCP system directory. Additionally, we have Inertial Navigation Unit (Phins, Ixblue, France) which provide high-precision heading, attitude information, pitch and roll. They are stored in ".N2R" data files with a time stamp.
- iii) Differential GNSS system (StarPack-D, Fugro, Netherlands) providing precise ship's position.
- iv) We used VmDas software version 1.50.19 (TRDI) for data acquisition.
- v) To synchronize time stamp of ping with Computer time, the clock of the logging computer is adjusted to GPS time server by using NTP (Network Time Protocol).
- vi) Fresh water is charged in the sea chest to prevent bio fouling at transducer face.
- vii) The sound speed at the transducer does affect the vertical bin mapping and vertical velocity measurement, and that is calculated from temperature, salinity (constant value; 35.0 PSU) and depth (6.5 m; transducer depth) by equation in Medwin (1975).
- viii) Data were configured for "8 m" layer intervals starting about 19m below sea surface. Data were recorded every ping as raw ensemble data (.ENR). Additionally, 30 seconds averaged data were recorded as short-term average (.STA). 300 seconds averaged data were long-term average (.LTA), respectively.

Table 3.1.2.1-1 Major parameters

---

Bottom-Track Commands	
BP = 001	Pings per Ensemble (almost less than 1,300m depth)
Environmental Sensor Commands	
EA = 04500	Heading Alignment (1/100 deg)
ED = 00065	Transducer Depth (0 – 65535 dm)
EF = +001	Pitch/Roll Divisor/Multiplier (pos/neg) [1/99 - 99]
EH = 00000	Heading (1/100 deg)
ES = 35	Salinity (0–40 pp thousand)
EX = 00000	Coordinate Transform (Xform:Type; Tilts; 3Bm; Map)
EZ = 10200010	Sensor Source (C; D; H; P; R; S; T; U)
	C (1): Sound velocity calculates using ED, ES, ET (temp.)
	D (0): Manual ED
	H (2): External synchro
	P (0), R (0): Manual EP, ER (0 degree)
	S (0): Manual ES
	T (1): Internal transducer sensor
	U (0): Manual EU
EV = 0	Heading Bias (1/100 deg)
Timing Commands	
TE = 00:00:02.00	Time per Ensemble (hrs:min:sec.sec/100)
TP = 00:02.00	Time per Ping (min:sec.sec/100)
Water-Track Commands	
WA = 255	False Target Threshold (Max) (0-255 count)
WC = 120	Low Correlation Threshold (0-255)
WD = 111 100 000	Data Out (V; C; A; PG; St; Vsum; Vsum^2; #G; P0)
WE = 1000	Error Velocity Threshold (0–5000 mm/s)
WF = 0800	Blank After Transmit (cm)
WN = 100	Number of depth cells (1–128)
WP = 00001	Pings per Ensemble (0–16384)
WS = 800	Depth Cell Size (cm)
WV = 0390	Radial Ambiguity Velocity (cm/s)

(3) Preliminary results

Horizontal velocity along the ship’s track is presented in Fig.3.1.2.1-1. In vertical direction, the data are averaged from 35 to 60 m

(4) Data archives

These obtained data will be submitted to JAMSTEC Data Management Group (DMG).

(5) Remarks (Times in UTC)

Data acquisition was suspended due to within the territorial sea of Palau during the following periods: 06:50UTC 12 Jul. 2023 – 08:05UTC 13 Jul. 2023.

**MR23-05 Leg1 Cruise**  
*15min. Average / Layer : 35-60m*

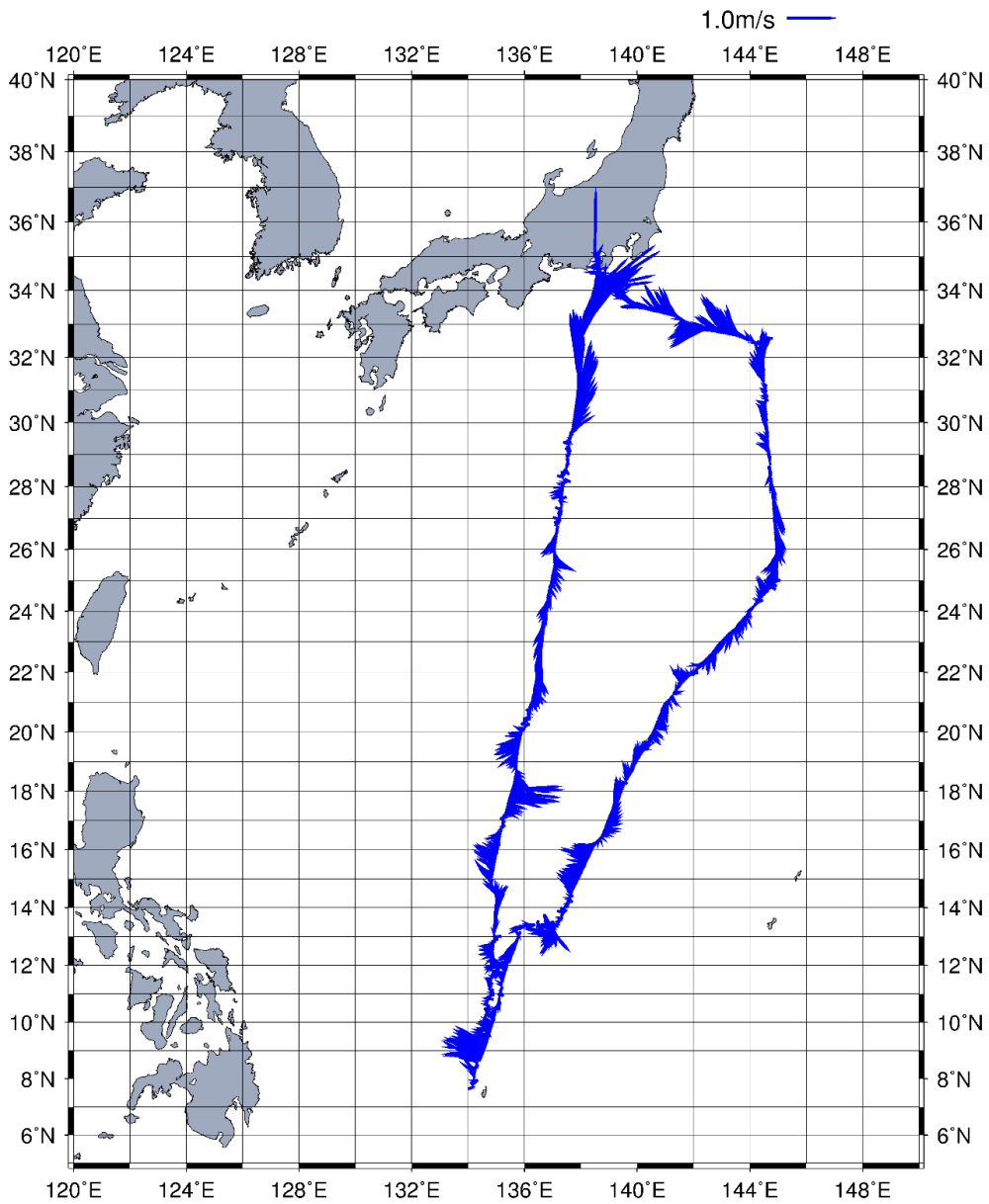


Figure 3.1.2.1-1. Horizontal Velocity along the ship's track in this cruise.  
(15 min. Average / Layer: 35-60 m)

### 3.1.2.2 Underway surface water monitoring

Kazuhiko MATSUMOTO	(JAMSTEC)	- Principal investigator
Katsunori SAGISHIMA	(MWJ)	
Misato KUWAHARA	(MWJ)	- Operation leader

#### (1) Objective

Our purpose is to obtain temperature, salinity, dissolved oxygen, fluorescence, and total dissolved gas pressure data continuously in near-sea surface water.

#### (2) Parameters

- Temperature
- Salinity
- Dissolved oxygen
- Fluorescence
- Turbidity
- Total dissolved gas pressure

#### (3) Instruments and Methods

The Continuous Sea Surface Water Monitoring System (Marine Works Japan Co. Ltd.) has six sensors and automatically measures temperature, salinity, dissolved oxygen, fluorescence, turbidity and total dissolved gas pressure in near-sea surface water every one minute. This system is located in the “sea surface monitoring laboratory” and connected to shipboard LAN-system. Measured data, time, and location of the ship were stored in a data management PC. Sea water was continuously pumped up to the laboratory from an intake placed at the approximately 4.5 m below the sea surface and flowed into the system through a vinyl-chloride pipe. The flow rate of the surface seawater was adjusted to  $10 \text{ dm}^3 \text{ min}^{-1}$ .

##### a. Instruments

###### Software

Seamoni-kun Ver.1.20

###### Sensors

Specifications of the each sensor in this system are listed below.

###### Temperature and Conductivity sensor

Model:	SBE-45, SEA-BIRD ELECTRONICS, INC.
Serial number:	4552788-0264
Measurement range:	Temperature $-5 \text{ }^\circ\text{C} - +35 \text{ }^\circ\text{C}$ Conductivity $0 \text{ S m}^{-1} - 7 \text{ S m}^{-1}$
Initial accuracy:	Temperature $0.002 \text{ }^\circ\text{C}$ Conductivity $0.0003 \text{ S m}^{-1}$
Typical stability (per month):	Temperature $0.0002 \text{ }^\circ\text{C}$ Conductivity $0.0003 \text{ S m}^{-1}$
Resolution:	Temperature $0.0001 \text{ }^\circ\text{C}$ Conductivity $0.00001 \text{ S m}^{-1}$

###### Bottom of ship thermometer

Model:	SBE 38, SEA-BIRD ELECTRONICS, INC.
Serial number:	3852788-0457

Measurement range:  $-5\text{ }^{\circ}\text{C} - +35\text{ }^{\circ}\text{C}$   
 Initial accuracy:  $\pm 0.001\text{ }^{\circ}\text{C}$   
 Typical stability (per 6 month):  $0.001\text{ }^{\circ}\text{C}$   
 Resolution:  $0.00025\text{ }^{\circ}\text{C}$

Dissolved oxygen sensor

Model: RINKO II, JFE ADVANTECH CO. LTD.  
 Serial number: 0035  
 Measuring range:  $0\text{ mg L}^{-1} - 20\text{ mg L}^{-1}$   
 Resolution:  $0.001\text{ mg L}^{-1} - 0.004\text{ mg L}^{-1}$  ( $25\text{ }^{\circ}\text{C}$ )  
 Accuracy: Saturation  $\pm 2\%$  F.S. (non-linear) (1 atm,  $25\text{ }^{\circ}\text{C}$ )

Fluorescence & Turbidity sensor

Model: C3, TURNER DESIGNS  
 Serial number: 2300707  
 Measuring range: Chlorophyll in vivo  $0\text{ }\mu\text{g L}^{-1} - 500\text{ }\mu\text{g L}^{-1}$   
 Minimum Detection Limit: Chlorophyll in vivo  $0.03\text{ }\mu\text{g L}^{-1}$   
 Measuring range: Turbidity  $0\text{ NTU} - 1500\text{ NTU}$   
 Minimum Detection Limit: Turbidity  $0.05\text{ NTU}$

Total dissolved gas pressure sensor

Model: HGTD-Pro, PRO OCEANUS  
 Serial number: 36-296-10  
 Temperature range:  $-2\text{ }^{\circ}\text{C} - 50\text{ }^{\circ}\text{C}$   
 Resolution:  $0.0001\%$   
 Accuracy:  $0.01\%$  (Temperature Compensated)  
 Sensor Drift:  $0.02\%$  per year max ( $0.001\%$  typical)

(4) Observation log

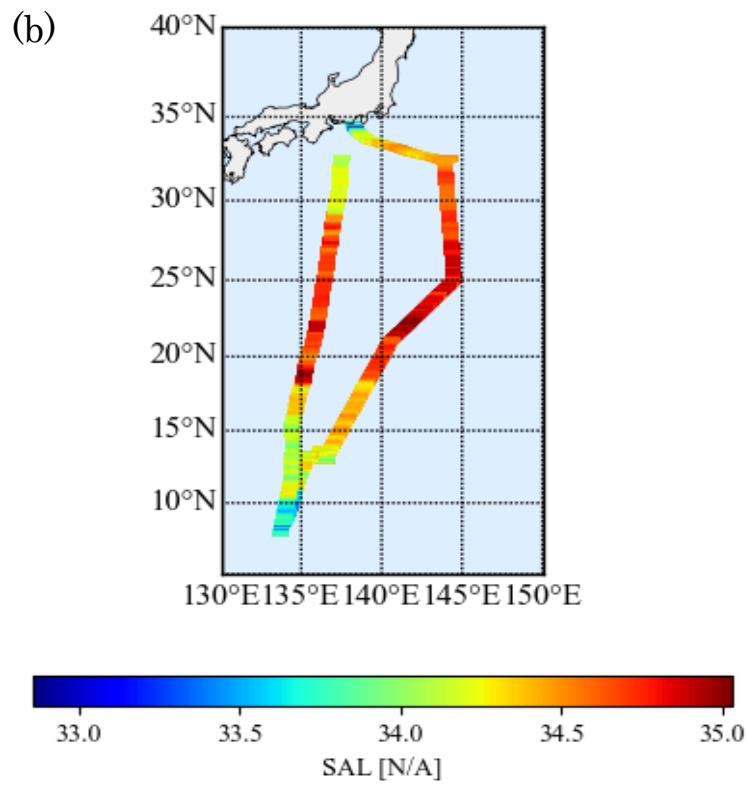
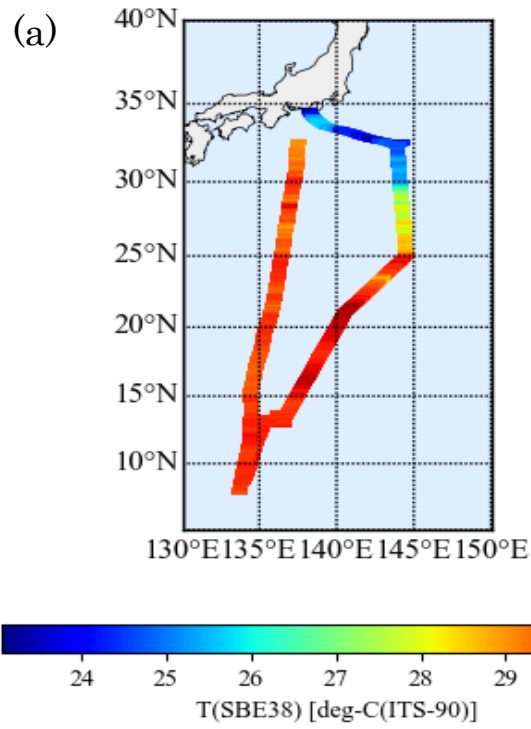
Periods of measurement, maintenance, and problems during this cruise are listed in Table 3.1.2.2-1.

Table 3.1.2.2-1 Events list of the Sea surface water monitoring during MR23-05Leg1

System Date [UTC]	System Time [UTC]	Events	Remarks
2023/06/28	02:30	All the measurements started and data was available.	Start
2023/07/12	06:59	All the measurements stopped.	Pump up stopped
2023/07/13	08:47	All the measurements started and data was available.	Logging restart
2023/07/13	09:10-10:32	Total dissolved gas pressure was no data. Salinity, Dissolved oxygen, Fluorescence, Turbidity was bad data.	HGTD-Pro Maintenance
2023/07/13	10:33	All the measurements data was available.	
2023/07/19	00:00	All the measurements stopped.	End

We took the surface water samples from this system once a day to compare sensor data with bottle data of salinity. The results are shown in Fig. 3.1.2.2-2. All the salinity samples were

analyzed by the Model 8400B “AUTOSAL” manufactured by Guildline Instruments Ltd. (see section 3.5.1).



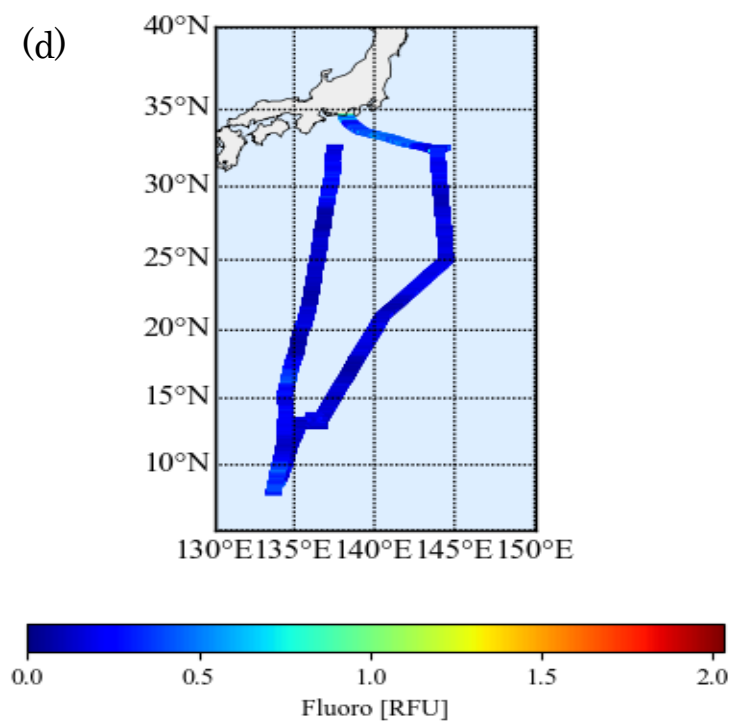
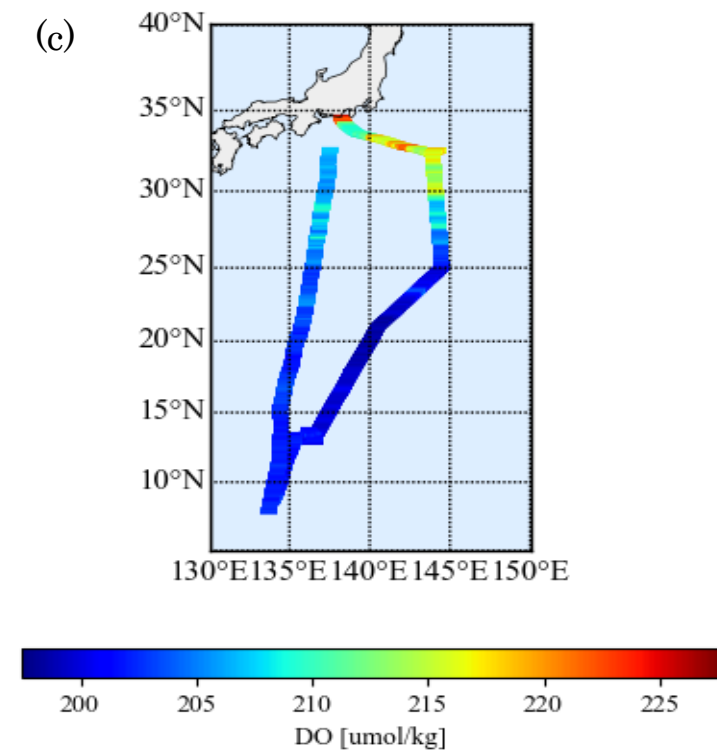


Figure 3.1.2.2-1 Spatial and temporal distribution of (a) temperature, (b) salinity, (c) dissolved oxygen, and (d) fluorescence in MR23-05Leg1 cruise.

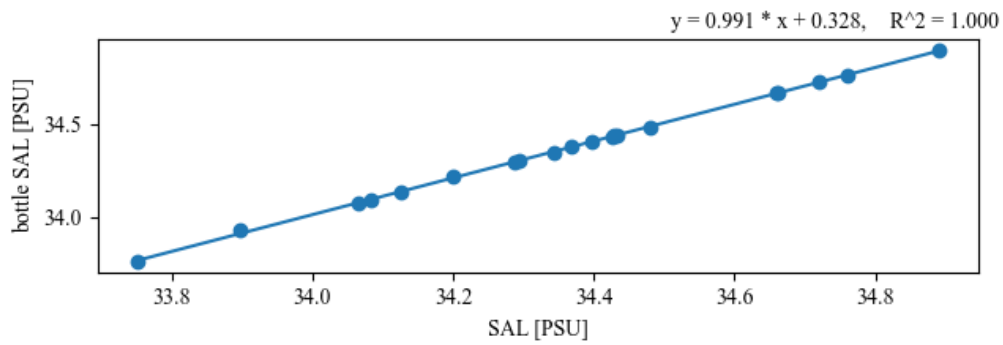


Figure 3.1.2.2-2 Correlation of salinity between sensor data and bottle data.

(5) Data archives

These data obtained in this cruise will be submitted to the Data Management Group (DMG) of JAMSTEC, and will be opened to the public via “Data Research System for Whole Cruise Information in JAMSTEC (DARWIN)” in JAMSTEC web site.

<<http://www.godac.jamstec.go.jp/darwin/e>>

### 3.1.3 Geophysical surveys

#### 3.1.3.1 Sea surface gravity

Akira NAGANO	(JAMSTEC)	- Principal investigator
Yutaro MURAKAMI	(NME)	- Operation leader
Ryo OYAMA	(NME)	
Yosuke KOMAKI	(NME)	- MIRAI crew

##### (1) Objectives

The local gravity is an important parameter in geophysics and geodesy. We collected gravity data at the sea surface.

##### (2) Instruments and methods

We measured relative gravity using LaCoste and Romberg air-sea gravity meter S-116 (Micro-G LaCoste, LLC) during this cruise. Parameters of gravity meter are as follows:

$$\begin{aligned} &\text{Relative Gravity [CU: Counter Unit]} \\ &[\text{mGal}] = (\text{coef1: } 0.9946) * [\text{CU}] \end{aligned}$$

##### (3) Preliminary result

Absolute gravity table was shown in Table.3.1.3.1-1.

Table 3.1.3.1-1 Absolute gravity table

No.	Date m/d	UTC hh:mm	Port	Absolute Gravity [mGal]	Sea Level [cm]	Ship Draft [cm]	Gravity at Sensor *1 [mGal]	S-116 Gravity [mGal]
#1	6/26	07:11	Shimizu Fujimi No.6-7	979730.02	180	646	979730.83	12001.64
#2	7/20	22:49	Shimizu Sodeshi No.1_11	979728.98	157	605	979729.60	12001.37

$$*1: \text{Gravity at Sensor} = \text{Absolute Gravity} + \text{Sea Level} * 0.3086 / 100 + (\text{Draft} - 530) / 100 * 0.2222$$

##### (4) Data Archive

These obtained data will be submitted to JAMSTEC Data Management Group (DMG).

##### (5) Remarks (Times in UTC)

Data acquisition was suspended due to within the territorial sea of Palau during the following period: 07:00UTC 12 Jul. 2023 – 08:00UTC 13 Jul. 2023

### 3.1.3.2 Sea surface three-component magnetic field

Akira NAGANO	(JAMSTEC)	- Principal investigator
Yutaro MURAKAMI	(NME)	- Operation leader
Ryo OYAMA	(NME)	
Yosuke KOMAKI	(NME)	- MIRAI Crew

#### (1) Objectives

Measurement of magnetic force on the sea is required for the geophysical investigations of marine magnetic anomaly caused by magnetization in upper crustal structure. We measured geomagnetic field using a three-component magnetometer during this cruise.

#### (2) Instruments and methods

A shipboard three-component magnetometer system (Tierra Tecnica SFG2018) is equipped on-board the R/V MIRAI. Three-axes flux-gate sensors with ring-cored coils are fixed on the fore mast. Outputs from the sensors are digitized by a 20-bit A/D converter (1 nT/LSB), and sampled at 8 times per second. Ship's heading, pitch, and roll are measured by the Inertial Navigation System (INS) for controlling attitude of a Doppler radar. Ship's position and speed data are taken from LAN every second.

#### Principle of ship-board geomagnetic vector measurement

The relation between a magnetic-field vector observed on-board,  $\mathbf{Hob}$ , (in the ship's fixed coordinate system) and the geomagnetic field vector,  $\mathbf{F}$ , (in the Earth's fixed coordinate system) is expressed as:

$$\mathbf{Hob} = \mathbf{A} * \mathbf{R} * \mathbf{P} * \mathbf{Y} * \mathbf{F} + \mathbf{Hp} \quad (\text{a})$$

where,  $\mathbf{R}$ ,  $\mathbf{P}$  and  $\mathbf{Y}$  are the matrices of rotation due to roll, pitch and heading of a ship, respectively.  $\mathbf{A}$  is a 3 x 3 matrix which represents magnetic susceptibility of the ship, and  $\mathbf{Hp}$  is a magnetic field vector produced by a permanent magnetic moment of the ship's body.

Rearrangement of Eq. (a) makes

$$\mathbf{R} * \mathbf{Hob} + \mathbf{Hbp} = \mathbf{R} * \mathbf{P} * \mathbf{Y} * \mathbf{F} \quad (\text{b})$$

where  $\mathbf{R} = \mathbf{A}^{-1}$ , and  $\mathbf{Hbp} = -\mathbf{R} * \mathbf{Hp}$ . The magnetic field,  $\mathbf{F}$ , can be obtained by measuring  $\mathbf{R}$ ,  $\mathbf{P}$ ,  $\mathbf{Y}$  and  $\mathbf{Hob}$ , if  $\mathbf{R}$  and  $\mathbf{Hbp}$  are known. Twelve constants in  $\mathbf{R}$  and  $\mathbf{Hbp}$  can be determined by measuring variation of  $\mathbf{Hob}$  with  $\mathbf{R}$ ,  $\mathbf{P}$  and  $\mathbf{Y}$  at a place where the geomagnetic field,  $\mathbf{F}$ , is known.

#### (3) Preliminary result

The results will be published after primary processing.

#### (4) Data Archive

These obtained data will be submitted to JAMSTEC Data Management Group (DMG).

#### (5) Remarks

i) For calibration of the ship's magnetic effect, we made a "figure-eight" turn (a pair of

clockwise and counter-clockwise rotation). These calibrations were carried out as below.

10:00UTC 29 Jun. 2023 – 10:28UTC 29 Jun. 2023 (32°-36'N, 144°-47'E)

08:55UTC 05 Jul. 2023 – 09:22UTC 05 Jul. 2023 (12°-54'N, 136°-52'E)

ii) Data acquisition was suspended due to within the territorial sea of Palau during the following period: 07:00UTC 12 Jul. 2023 – 08:00UTC 13 Jul. 2023.

### 3.1.3.3 Swath bathymetry

Akira NAGANO	(JAMSTEC)	- Principal investigator
Yutaro MURAKAMI	(NME)	- Operation leader
Ryo OYAMA	(NME)	
Yosuke KOMAKI	(NME)	- MIRAI crew

#### (1) Objectives

The R/V MIRAI is equipped with a Multi narrow Beam Echo Sounding system (MBES), SEABEAM 3012 Model (L3 Communications ELAC Nautik). The objective of MBES is collecting continuous bathymetric data along ship's track to make a contribution to geological and geophysical investigations and global datasets.

#### (2) Instruments and methods

The "SEABEAM 3012 Model" on the R/V MIRAI was used for bathymetry mapping during this cruise. To get accurate sound velocity of water column for ray-path correction of acoustic multibeam, we used Surface Sound Velocimeter (SSV) data to get the sea surface (6.62 m) sound velocity, and the deeper depth sound velocity profiles were calculated by temperature and salinity profiles from CTD and Argo float data by the equation in Del Grosso (1974) during the cruise. Table 3.1.3.3-1 shows system configuration and performance of SEABEAM 3012 system.

Table 3.1.3.3-1 SEABEAM 3012 System configuration and performance

Frequency:	12 kHz
Transmit beam width:	2.0 degree
Transmit power:	4 kW
Transmit pulse length:	2 to 20 msec
Receive beam width:	1.6 degree
Depth range:	50 to 11,000 m
Beam spacing:	Equi-Angle
Number of beams:	301 beams
Swath width:	60 to 150 degrees (max)
Depth accuracy:	< 1 % of water depth (average across the swath)

#### (3) Preliminary Result

The results will be published after primary processing.

#### (4) Data Archive

These obtained data will be submitted to JAMSTEC Data Management Group (DMG).

#### (5) Remarks

i) The period of data acquisition.

02:47UTC 28 Jun. 2023 – 23:50UTC 18 Jul. 2023

ii) Data acquisition was suspended during the following periods:

09:36UTC 30 Jun. 2023 – 11:19UTC 30 Jun. 2023 (ANS system operation)

06:50UTC 12 Jul. 2023 – 08:05UTC 13 Jul. 2023 (Within the territorial sea of Palau)

## 3.2 Mooring observations

### 3.2.1 Kuroshio Extension Observatory (KEO) mooring -Time-series sediment trap observation-

Makio HONDA	(JAMSTEC)
Masaki FURUHATA	(MWJ)
Hiroki USHIROMURA	(MWJ)
Keita HAYASHI	(MWJ)
Kango FUKUYAMA	(MWJ)

#### (1) Objective

Based on the comparison study of biogeochemistry in the northwestern North Pacific eutrophic subarctic region and oligotrophic subtropical region (“K2S1 project” in 2010–2013), it was clarified that surface biological activity (primary productivity) in the subtropical region is comparable to or slightly larger than that in the subarctic region (Special issue of *Journal of Oceanography* vol.72 no.3 2016; Honda et al. 2017) although particulate organic carbon in the subarctic region is transported to the deep efficiently (Honda 2020). In order to verify the support mechanism of biological activity, that is the mechanism of nutrient supply, time-series sediment trap experiment was initiated in 2014 at about 4900 m of the station KEO. This station is the time-series station maintained by National Ocean and Atmosphere Administration (NOAA) Pacific Marine Environmental Laboratory (PMEL) (URL: <https://www.pmel.noaa.gov/ocs/data/disdell/>). Surface buoy with meteorological sensors and physical oceanographic sensors have been deployed at station KEO since 2004. Therefore, these time-series data of meteorology and physical oceanography can be utilized to interpret time-series variability in sediment trap data. Owing to simultaneous analysis of time-series data obtained by NOAA surface buoy and JAMSTEC sediment trap between 2014 and 2016, it was verified that mesoscale cyclonic eddy potentially plays a role in nutrient supplier (Honda et al. 2018). In order to evaluate other potential mechanisms such as typhoon and aeolian dust input, sediment trap experiment has been continued at station KEO. In 2022, KEO sediment trap mooring system with two sediment traps at 1800 m and 4900 m was deployed in December during the R/V MIRAI MR21-06 cruise.

#### (2) Recovery

On 29 June 2023, thanks to great efforts by cruise participants, marine technicians from Marine Works Japan Ltd. and ship crews from NME, sediment trap mooring system was successfully recovered although several grass floats were broken. Time-series sediment trap sample at both depths between January 2022 and April 2023 was successfully collected.

#### (3) Preliminary result: total mass flux

Onboard, heights of collected samples (settling particles) in collecting cups were measured roughly with scale (Fig. 3.2.1-1). Qualitatively, the peak of sinking particle was observed in March–April 2022 at both depths. On the other hand, 1800 m Fluxes after July 2022 were quite small. The Bottom of sediment trap cone (inlet of collecting cup) might be clogged unfortunately.

#### (4) Future analysis

The above preliminary result is qualitative. In order to evaluate settling particles quantitatively, on land laboratory, sediment trap sample will be pretreated (splitting, filtration, dry-up, pulverization) and major chemical components such as organic carbon, inorganic carbon, biogenic opal, CaCO<sub>3</sub> and Al will be analyzed.

#### (4) Data archive

Obtained data will be submitted to KEO sediment trap database (URL: [https://ebcrpa.jamstec.go.jp/egcr/e/oal/oceansites\\_keo/](https://ebcrpa.jamstec.go.jp/egcr/e/oal/oceansites_keo/)).

#### (5) References

- Honda MC, Matsumoto K, Fujiki T, Siswanto E, Sasaoka K, Kawakami H, Wakita M, Mino Y, Sukigara C, Kitamura M, Sasai Y, Smith SL, Hashioka T, Yoshikawa C, Kimoto K, Watanabe S, Kobari T, Nagata T, Hamasaki K, Kaneko R, Uchimiya M, Fukuda H, Abe O, Saino T (2017) Comparison of carbon cycle between the western Pacific subarctic and subtropical time-series stations: highlights of the K2S1 project. *J Oceanogr* 73:647-667. doi:10.1007/s10872-017-0423-3.
- Honda MC, Sasai Y, Siswanto E, Kuwano-Yoshida A, Aiki H, Cronin MF (2018) Impact of cyclonic eddies and typhoons on biogeochemistry in the oligotrophic ocean based on biogeochemical/physical/meteorological time-series at station KEO. *Progress in Earth and Planetary Science*. doi.org/10.1186/s40645-018-0196-3
- Honda MC (2020) Effective vertical transport of particulate organic carbon in the Western North Pacific Subarctic Region. *Front. Earth Sci.* 8:366. doi: 10.3389/feart.2020.00366

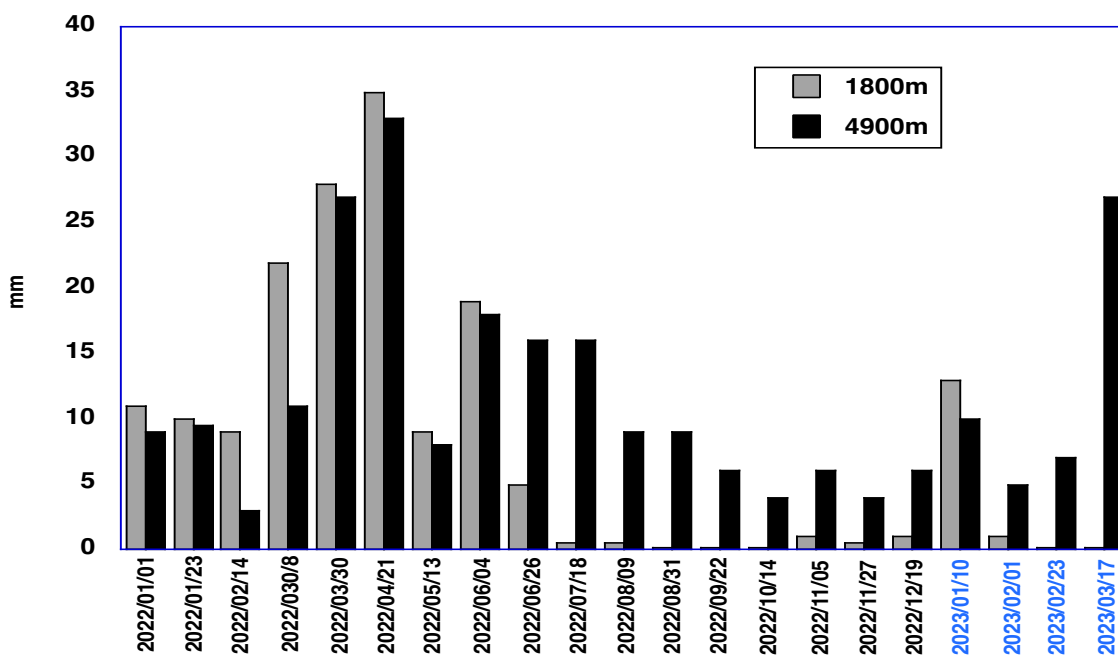


Figure 3.2.1-1 Seasonal variability in Total Mass flux (heights of collected material).

(6) Redeployment

After retrieving sample / data, replacement of new battery and initialization of schedule (Table 3.2.1-1), sediment trap mooring system with two sediment traps (~1000 m and 4800 m) was deployed on 30 June 2023 successfully. Designs of mooring system are shown in Fig. 3.2.1-2. Based on “positioning” with SSBL, determined anchor position is

**32°21.9458’N, 144°25.1682’E**  
**Water depth 5786 m**

Figure 3.2.1-3 is mooring position and ambient bathymetry.

It is planned that this mooring system will be recovered in October 2024 during the R/V MIRAI cruise.

Table 3.2.1-1 Time schedule of collection interval for both depths

Int (days)	
	22
1	2023/7/1 0:00
2	2023/7/23 0:00
3	2023/8/14 0:00
4	2023/9/5 0:00
5	2023/9/27 0:00
6	2023/10/19 0:00
7	2023/11/10 0:00
8	2023/12/2 0:00
9	2023/12/24 0:00
10	2024/1/15 0:00
11	2024/2/6 0:00
12	2024/2/28 0:00
13	2024/3/21 0:00
14	2024/4/12 0:00
15	2024/5/4 0:00
16	2024/5/26 0:00
17	2024/6/17 0:00
18	2024/7/9 0:00
19	2024/7/31 0:00
20	2024/8/22 0:00
21	2024/9/13 0:00
22	2024/10/5 0:00

# 2023 KEO BGC Deployment

Mooring Number : KEOBGC  
 Deployment Data : / / ~ /  
 Cruise No. : MR23-  
 Position : LAT - . N  
 LONG - . E  
 Depth : m

# KEO

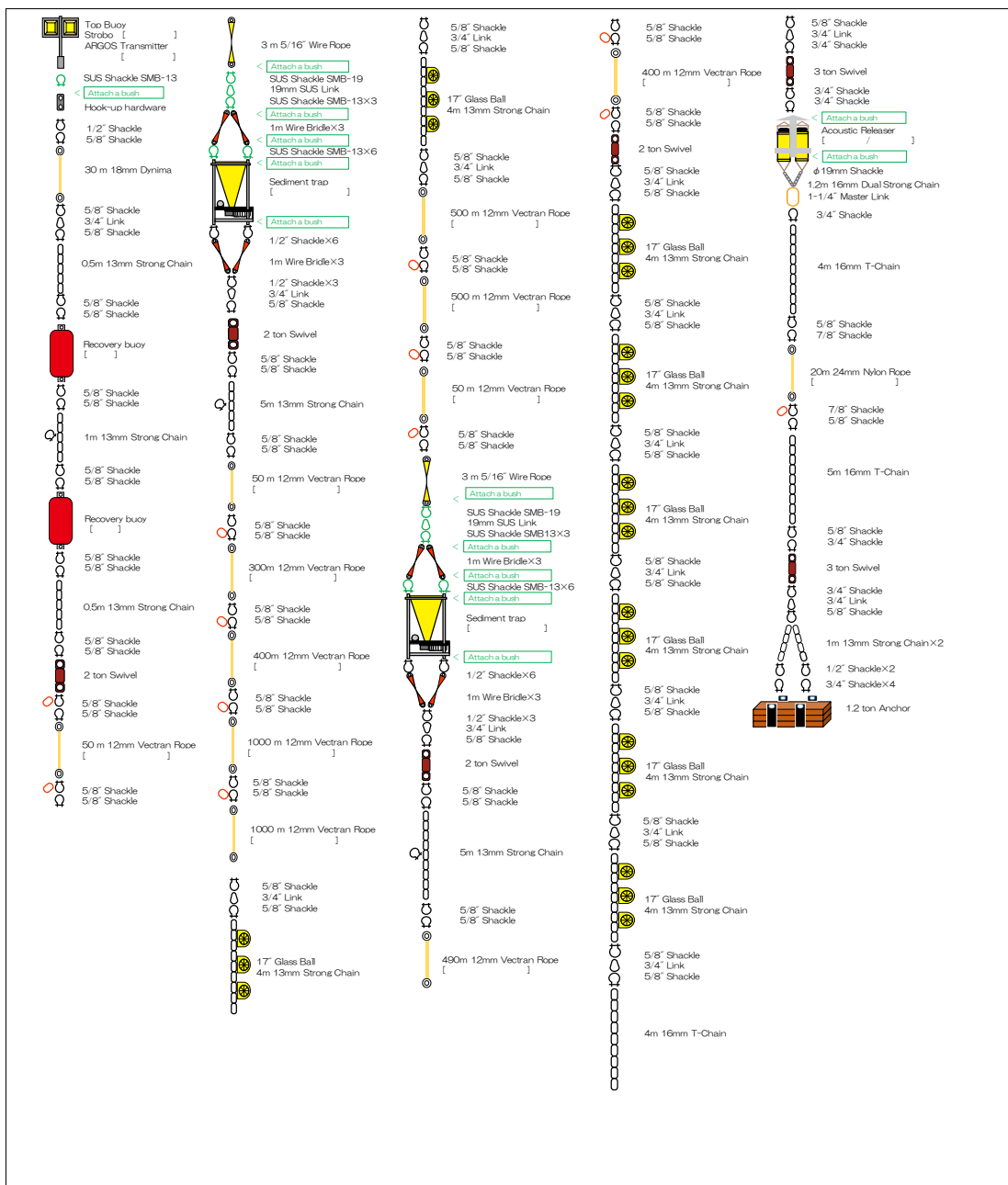


Fig. 3.2.1-2 KEO sediment trap mooring system.

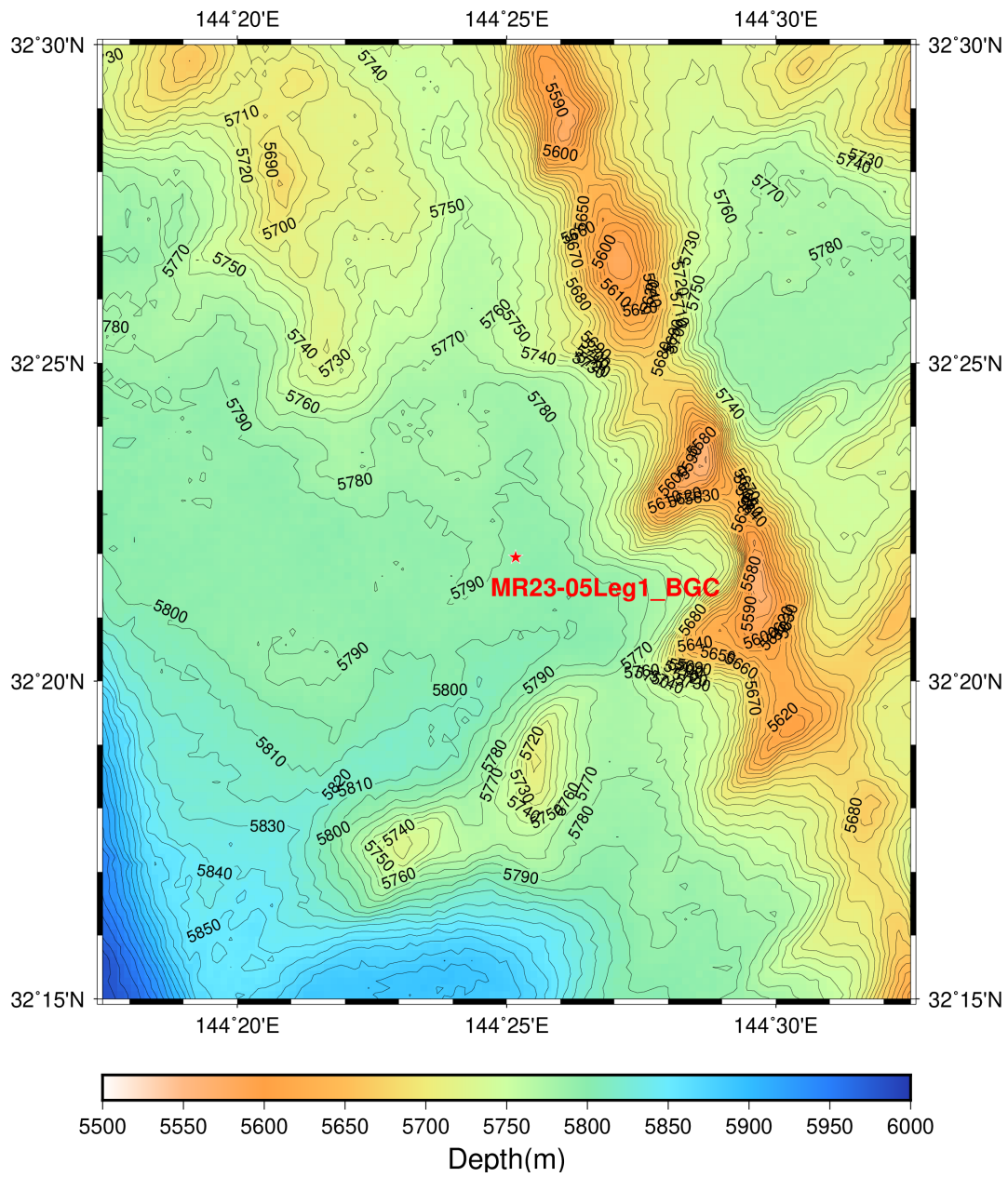


Fig. 3.2.1-3 Position of MR23-05KEO mooring system  
(32°-21.9458'N / 144°-25.1682'E).

### 3.2.2 Philippine Sea mooring

Iwao UEKI	(JAMSTEC)	- Principal investigator
Akira NAGANO	(JAMSTEC)	- Chief scientist
Kensuke WATARI	(JAMSTEC)	- Technical scientist
Masaki FURUHATA	(MWJ)	- Operation leader
Hiroki USHIROMURA	(MWJ)	- Technical leader
Makito YOKOTA	(MWJ)	- Technical staff
Masaki YAMADA	(MWJ)	- Technical staff
Kango FUKUYAMA	(MWJ)	- Technical staff

#### (1) Objectives

In the tropical Pacific and Kuroshio regions where the ocean and atmosphere variations play critical roles in the climate system, upper ocean and lower atmosphere monitoring system using moored buoy has been conducted. On the basis of the knowledge obtained from the buoy array data of the tropical Pacific, we further noticed that, in the Philippine Sea, there are other possible key areas where the variations are responsible for phenomena in the equatorial and Kuroshio regions such as ENSO (Hasegawa and Hanawa, 2007), ENSO-related salinity variation of the sea surface Kuroshio water (Nagano et al., 2014, 2017), and PDO (Nagano et al., 2022).

Also, other atmospheric and oceanic disturbances on various timescales such as typhoons, cold surges, seasonal march of the East Asian monsoon, and Madden-Julian Oscillation are present in the Philippine Sea (Nagano et al., 2018). Therefore, to further understand the air-sea interaction in the western North Pacific, JAMSTEC deployed a moored buoy at a site east of the Philippines (nominal 13°N, 137°E), corresponding to the northern edge of the western Pacific warm pool, and named PHSMO (Philippine Sea mooring) from December 2016.

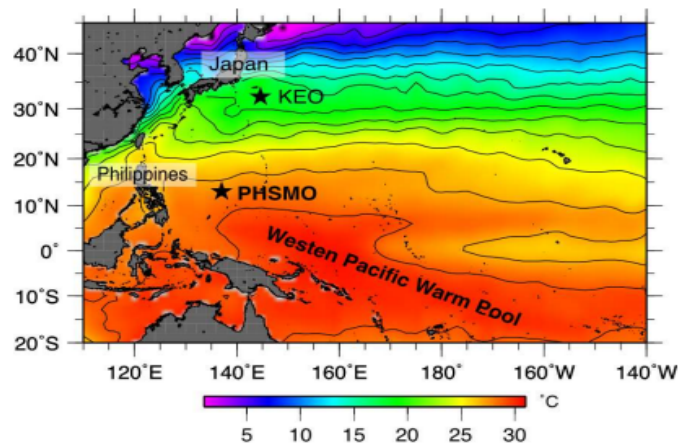


Figure 3. 2. 2-1 Map of sea surface temperature (°C) in the western tropical and northern subtropical Pacific in February 2017 from monthly NOAA Optimum Interpolation Sea Surface Temperature V2 data (Reynolds et al., 2007). Contour interval is 2 °C. KEO and PHSMO sites are indicated by stars.

This mooring is based on the m-TRITON system, deploying eastern Indian Ocean (Ueki et al., 2010), and K-TRITON buoy, which had been deployed in the Kuroshio Extension region from February 2008 to July 2013 (<http://www.jamstec.go.jp/iorgc/ocorp/ktsfg/data/jkeo/index.html>). The atmospheric and oceanic data observed by the mooring are publicly available in this web site.

In this cruise, the Philippine Sea mooring deployed during the R/V MIRAI MR21-03 cruise has been recovered, and the new one has been deployed during this cruise.

## (2) Measured parameters

The Philippine Sea mooring observes oceanic and meteorological variables by following sensors.

### Meteorological variables:

wind speed, direction, atmospheric pressure, air temperature, relative humidity, shortwave radiation, precipitation, and longwave radiation

### Oceanic variables:

Water temperature and conductivity sensors at depths of 1 m, 10 m, 20 m, 40 m, 60 m, 80 m, 90 m, 100 m, 110 m, 120 m, 180 m, 150 m, 200 m, 300 m, and 5000 m;

Depth (pressure) sensors at depths of 1 m, 10 m, 40 m, 80 m, 100 m, 120 m, 150 m, 180 m, 300m, and 5000 m;

Current meter at a depth of 1 m; and

Dissolved oxygen concentration at depths of 80 m, 100 m, 150 m, and 5000 m,

## (3) Instrument

Details of the instruments used on the Philippine Sea mooring are summarized as follow:

### Oceanic sensors

#### 1) CTD and CT

SBE-37 IM MicroCAT

A/D cycles to average:	4
Sampling interval:	600sec.
Measurement range, Temperature:	-5 - +35 deg-C
Measurement range, Conductivity:	0-7 S/m
Measurement range, Pressure:	0-full scale range

#### 2) CRN (Current meter)

Work Horse ADCP

Sensor frequency:	300 kHz
Sampling interval:	1 hour.

### Meteorological sensors

#### 1) Precipitation

R.M. YOUNG COMPANY MODEL50202/50203

Sampling interval:	600 sec.
--------------------	----------

2) Atmospheric pressure

PAROSCIENTIFIC. Inc. DIGIQUARTZ FLOATING BAROMETER

6000SERIES

Sampling interval: 600 sec.

3) Relative humidity/air temperature,

Shortwave radiation,

Longwave radiation,

Wind speed/direction

Sampling interval: 600sec.

(4) Location of deployed mooring

Nominal location: 13°N, 137°E

Mooring ID: 40505

Number on surface float: K03

Iridium ID number: 300434060153300

ARGOS backup PTT number: 29698, 27406

Deployed date: 7 Jul. 2023

Exact location: 12°53.61'N, 136°54.31'E

Depth: 5,246 m

(5) Location of recovered mooring

Nominal location: 13°N, 137°E

Mooring ID: 40504

Number on surface float: J06

Iridium ID number: 300434063013670

ARGOS backup PTT number: 30832

Deployed date: 12 Jun. 2021

Recovered date: 8 Jul. 2023

Exact location: 13°06.85'N, 136°56.38'E

Depth: 5,327 m

\*Dates and times are UTC and represent anchor drop times for deployments and acoustic releaser on deck times for recoveries.

### 3.2.3 ADCP subsurface moorings

Iwao UEKI	(JAMSTEC)	- Principal investigator
Hiroki USHIROMURA	(MWJ)	- Operation leader
Masaki FURUHATA	(MWJ)	
Makito YOKOTA	(MWJ)	
Masaki YAMADA	(MWJ)	
Kango FUKUYAMA	(MWJ)	

#### (1) Objectives

The purpose of the ADCP subsurface mooring is to get knowledge of physical process underlying the dynamics of the northern edge of the Pacific warm pool. We have been observing subsurface currents using ADCP moorings along the equator. In this cruise (MR23-05), we recovered moorings at the two sites of 13°N, 137°E and 13.5°N, 137°E and deployed new moorings at the same sites. These moorings also contribute to the multiplatform experiment combined with PHISMO, floats, Wave Gliders, drifting buoys and ship-based observations.

#### (2) Parameters

- Current profiles
- Echo intensity
- Pressure, temperature, and conductivity

#### (3) Methods

To acquire current profile in the subsurface layers above 2000 m, a Work Horse Long Ranger ADCP (Acoustic Doppler Current Profiler) was installed in a ball buoy as the top float of the mooring. A Seacat CTD was also installed at the bottom of the ball buoy to acquire pressure, temperature and salinity for correction of current profiles using sound speed and depth variability. Details of the instruments and their parameters are listed as follows:

##### 1) ADCP

Work Horse ADCP 75 kHz (Teledyne RD Instruments, Inc.)

Distance to first bin: 7.04 m

Pings per ensemble: 27

Time per ping: 6.66 seconds

Number of depth cells: 60

Bin length: 8.00 m

Sampling Interval: 3600 seconds

##### Recovered ADCP

- Serial Number: 24609 (Mooring No. 210613-13N137E)
- Serial Number: 2541 (Mooring No. 210614-13.5N137E)

##### Deployed ADCP

- Serial Number: 24614 (Mooring No. 230709-13N137E)
- Serial Number: 24620 (Mooring No. 230710-13.5N137E)

## 2) CTD

SBE-16 (Sea Bird Electronics Inc.)

Sampling Intervals: 3600 seconds

### Recovered CTD

- Serial Number: 1282 (Mooring No. 210613-13N137E)
- Serial Number: 1280 (Mooring No. 210614-13.5N137E)

### Deployed CTD

- Serial Number: 1279 (Mooring No. 230709-13N137E)
- Serial Number: 1286 (Mooring No. 230710-13.5N137E)

## 3) Other instruments

### (a) Acoustic Releaser (BENTHOS, Inc.)

#### Recovered Acoustic Releaser

- Serial Number: 636, 956 (Mooring No. 210613-13N137E)
- Serial Number: 663, 694 (Mooring No. 210614-13.5N137E)

#### Deployed Acoustic Releaser

- Serial Number: 632, 666 (Mooring No. 230709-13N137E)
- Serial Number: 693, 667 (Mooring No. 230710-13.5N137E)

### (b) Transponder (BENTHOS, Inc.)

#### Recovered Transponder

- Serial Number: 57114 (Mooring No. 210613-13N137E)
- Serial Number: 61940 (Mooring No. 210614-13.5N137E)

#### Deployed Transponder

- Serial Number: 67491 (Mooring No. 230709-13N137E)
- Serial Number: 57069 (Mooring No. 230710-13.5N137E)

### (c) ST-400A Xenon Flasher (MetOcean Data Systems)

#### Recovered Transponder

- Serial Number: A02-056 (Mooring No. 210613-13N137E)
- Serial Number: A02-057 (Mooring No. 210614-13.5N137E)

#### Deployed Transponder

- Serial Number: Z03-088 (Mooring No. 230709-13N137E)
- Serial Number: A02-066 (Mooring No. 230710-13.5N137E)

## (5) Recovery

We recovered two ADCP moorings which were deployed on 13 June 2021 at 13°N, 137°E and 14 June 2021 at 13.5°N, 137°E by the R/V MIRAI. The acquired data were retrieved from ADCP and CTD, and primary check was conducted.

The acquired current profiles were show in Figure 3.2.3-1 and 3.2.3-2 as time-depth sections for the zonal and meridional components.

(6) Deployment

At each mooring site, we deployed an ADCP mooring after recovery. Each ADCP was intended to install at about 2000 m depth. After deployments, we conducted acoustic calibration for mooring positions based on acoustic releases on each mooring.

The position of the mooring No. 230709-13N137E

Date: 07 Jul. 2023 Lat.: 12°-58.99'N Long.: 137°-08.27'E Depth: 5,032 m

The position of the mooring No. 230710-13.5N137E

Date: 07 Jul. 2023 Lat.: 13°-29.96'N Long.: 137°-03.97'E Depth: 5,039 m

(7) Data archive

All data will be opened at the following web page:

[https://www.jamstec.go.jp/ipobs/adcp/adcp\\_data.html](https://www.jamstec.go.jp/ipobs/adcp/adcp_data.html)

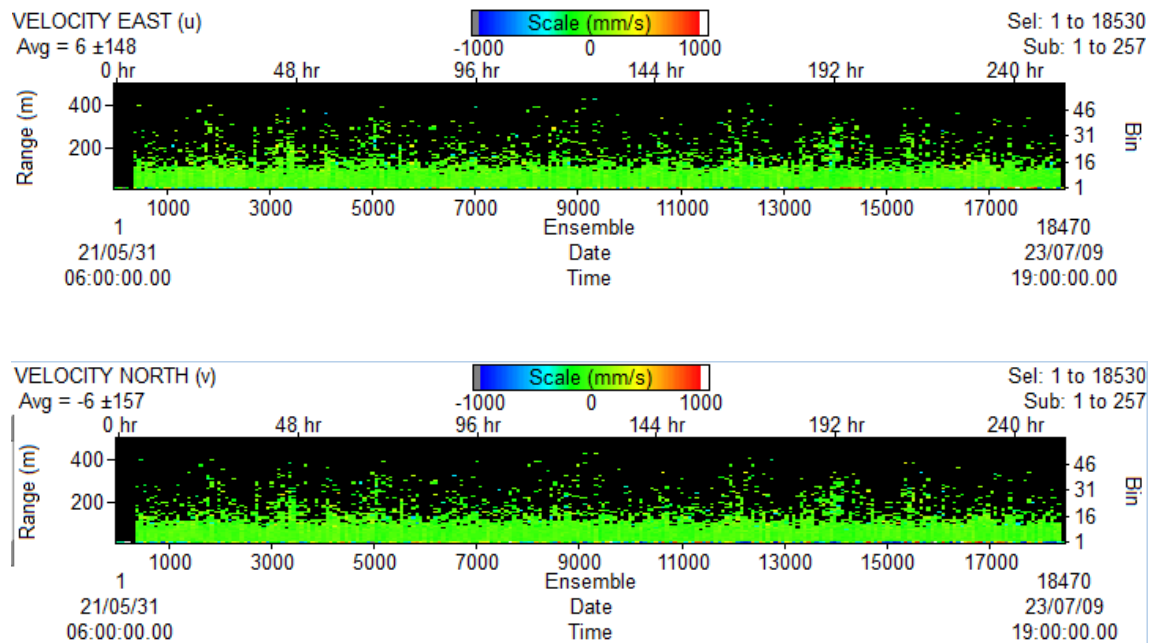


Figure 3.2.3-1 Time-depth sections of observed zonal (top panel) and meridional (bottom panel) currents obtained from ADCP mooring at 13°N, 137°E (2021/06/13–2023/07/09).

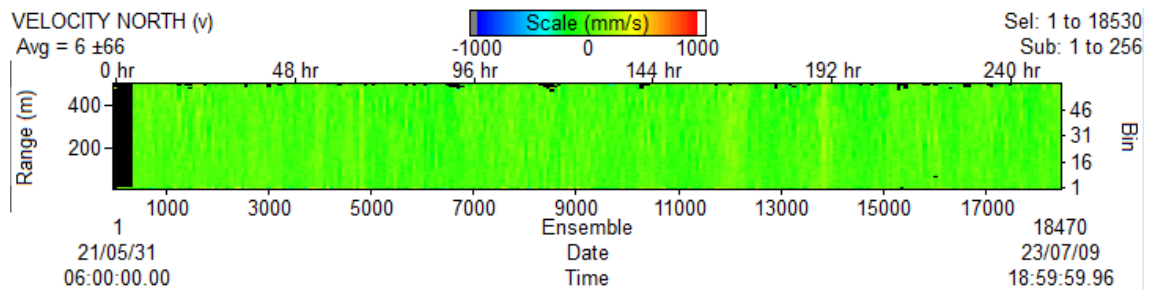
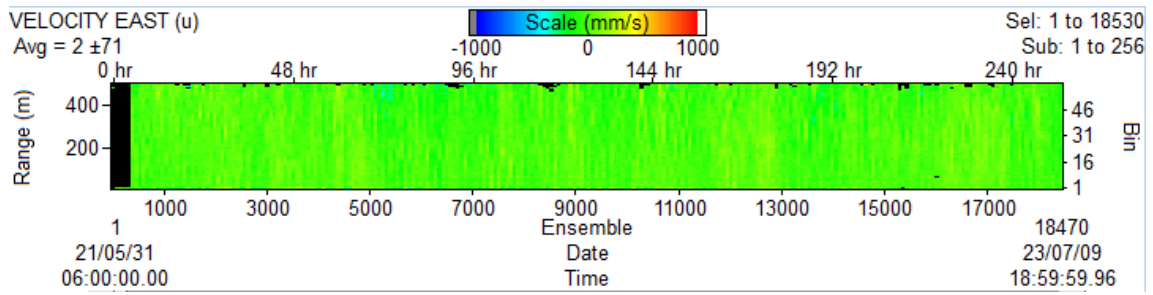


Figure 3.2.3-2 Time-depth sections of observed zonal (top panel) and meridional (bottom panel) currents obtained from ADCP mooring at 13.5°N, 137°E (2021/06/14–2023/07/10).

### 3.3 Ocean observation platforms

#### 3.3.1 Wave Glider observation

Iwao UEKI	(JAMSTEC)	- Principal investigator
Makito YOKOTA	(MWJ)	- Operation leader
Kango FUKUYAMA	(MWJ)	
Masaki FURUHATA	(MWJ)	
Masaki YAMADAY	(MWJ)	
Hiroki USHIROMURA	(MWJ)	
Keita HAYASHI	(MWJ)	
Nobuhiro FUJII	(MWJ)	
Tatsuya FUKUDA	(JAMSTEC)	- Not on board
Yasuhisa ISHIHARA	(JAMSTEC)	- Not on board
Takayuki HASHIMUKAI	(MWJ)	- Not on board
Shino SAKABE	(MWJ)	- Not on board
Tetsuya NAGAHAMA	(MWJ)	- Not on board

##### (1) Background and Objectives

Although there are many global air-sea flux products mainly based on Satellite observation and reanalysis, in situ observations by research vessels and mooring buoys are still essential. As a part of the TAO (Tropical Atmosphere and Ocean)/TRITON (Triangle trans-ocean buoy network) array, we have conducted the air-sea flux observation in the western Pacific and eastern Indian Ocean. The mooring observation has the advantage to acquire detailed direct measurement record at a fixed point, however it takes relatively high cost to keep many sites. Because of progress of the development of unmanned ocean surface vehicles, such as Wave Glider and Saildrone, we can use these vehicles as a platform for air-sea flux observation. Using the Wave Glider, we developed air-sea flux observing system.

We installed a Wave Glider (S/N: SV3-252) at the region around northern edge of Pacific warm pool to capture detailed structure of air-sea variables. The Wave Glider also used for evaluation for eddy covariance method of turbulent fluxes on moving platform. For that purpose, a 3-axis ultrasonic anemometer system was installed on the Wave Glider.

##### (2) Instrumentation

The Wave Glider is an autonomous ocean surface vehicle, which utilize both wave energy for propulsion and solar power for supporting on-board computing, communications and sensor payloads. It can travel tens of thousands of miles, collect data in the most demanding conditions, and deliver this data in real time. The Wave Glider consists of two-part architecture; surface float and underwater glider with umbilical cable (Fig. 3.3.1-1).

As payloads, we install three types of meteorological sensor units on the surface float; the Weather Station, Weather Transmitter, and JAMMET. The observed parameters are air temperature, relative humidity, barometric pressure, longwave radiation, shortwave radiation, wind direction, wind speed and rain fall amount. In terms of underwater sensors, temperature and conductivity sensors and ADCP were installed in the surface float and at the underwater glider. The observed parameters are ocean current within 120 m depth, temperature, conductivity and pressure. The acquired data are recorded on logger system and transmitted to land station via iridium satellite communication system.

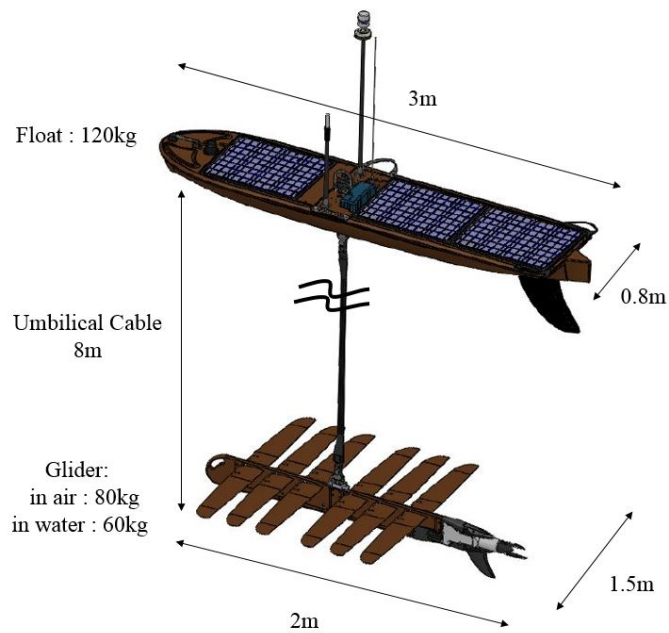


Figure 3.3.1-1 Wave Glider SV3 configuration (from Liquid Robotics Inc.)

### (3) Optional sensors

Three axis ultrasonic anemometer system was installed to the rear of the surface float (Fig. 3.3.1-2). The system includes motion sensor and logger in addition to three axis ultrasonic anemometer to conduct wind correction for motion of the Wave Glider. The system acquired 3-dimensional wind speed, speed of sound, and sonic temperature in every 0.05 sec. The acquired data are recorded on logger.

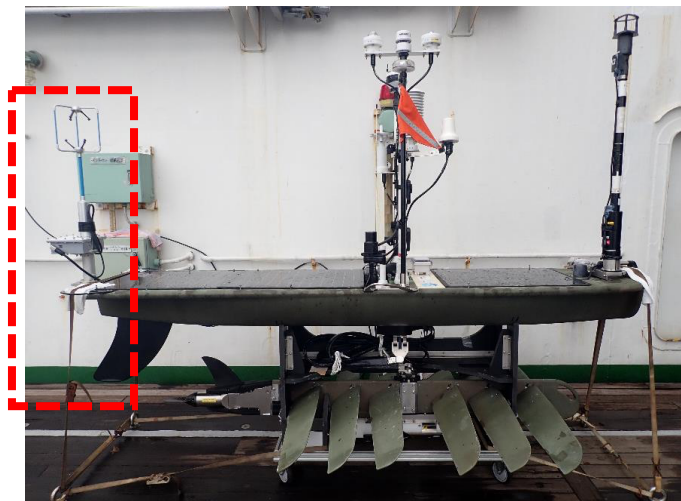


Figure 3.3.1-2 Three dimensions wind sensor system

### (4) Deployment and recovery

The Wave Glider was deployed from the R/V MIRAI on 05 Jul. 2023. And it was recovered by the R/V MIRAI on 15 Jul. 2023.

(5) Mission details

The Wave Glider conducted observation between 05 Jul. to 15 Jul. 2023. The Wave Glider went to 14 °N, 135°E (WP7) from 13.23°N, 137.08°E. After that it took a round trip between 14°N, 135°E to 15°N, 135°E (WP8) as shown in Fig. 3.3.1-3.

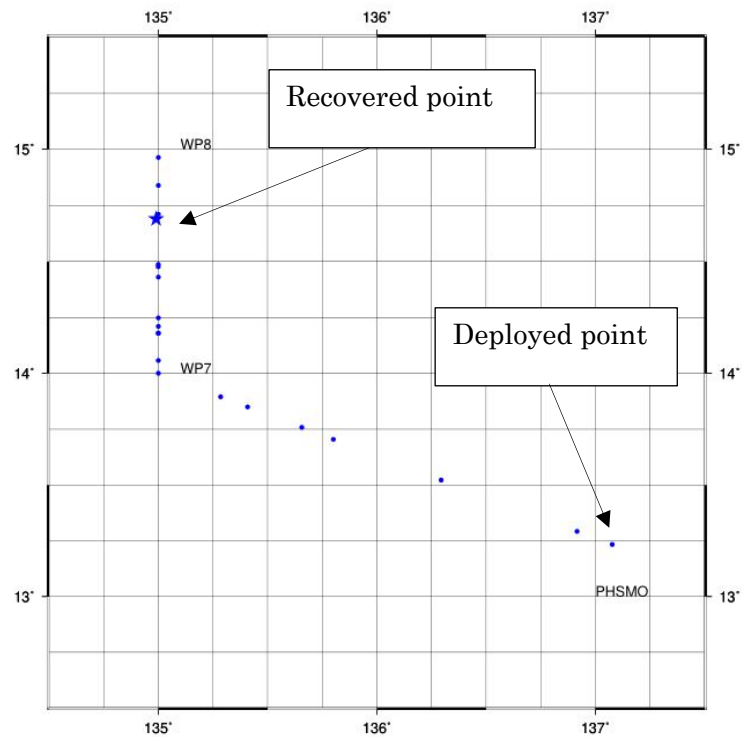


Figure 3.3.1-3 Cruise track of the Wave Glider during the mission from 05 Jul. to 15 Jul. 2023

(6) Preliminary Results

Time series of raw data acquired by the Wave Glider are shown in Fig. 3.3.1-4. As shown in these figures, measurements of each variable were well conducted. Through the entire mission period, easterly winds were dominant, and rain falls in night were frequently appeared. During the second half of the mission period, wind speed was increased with decreasing shortwave. Rain falls in daytime also appeared and surface salinity were decreased. Those features suggest influence of atmospheric disturbances.

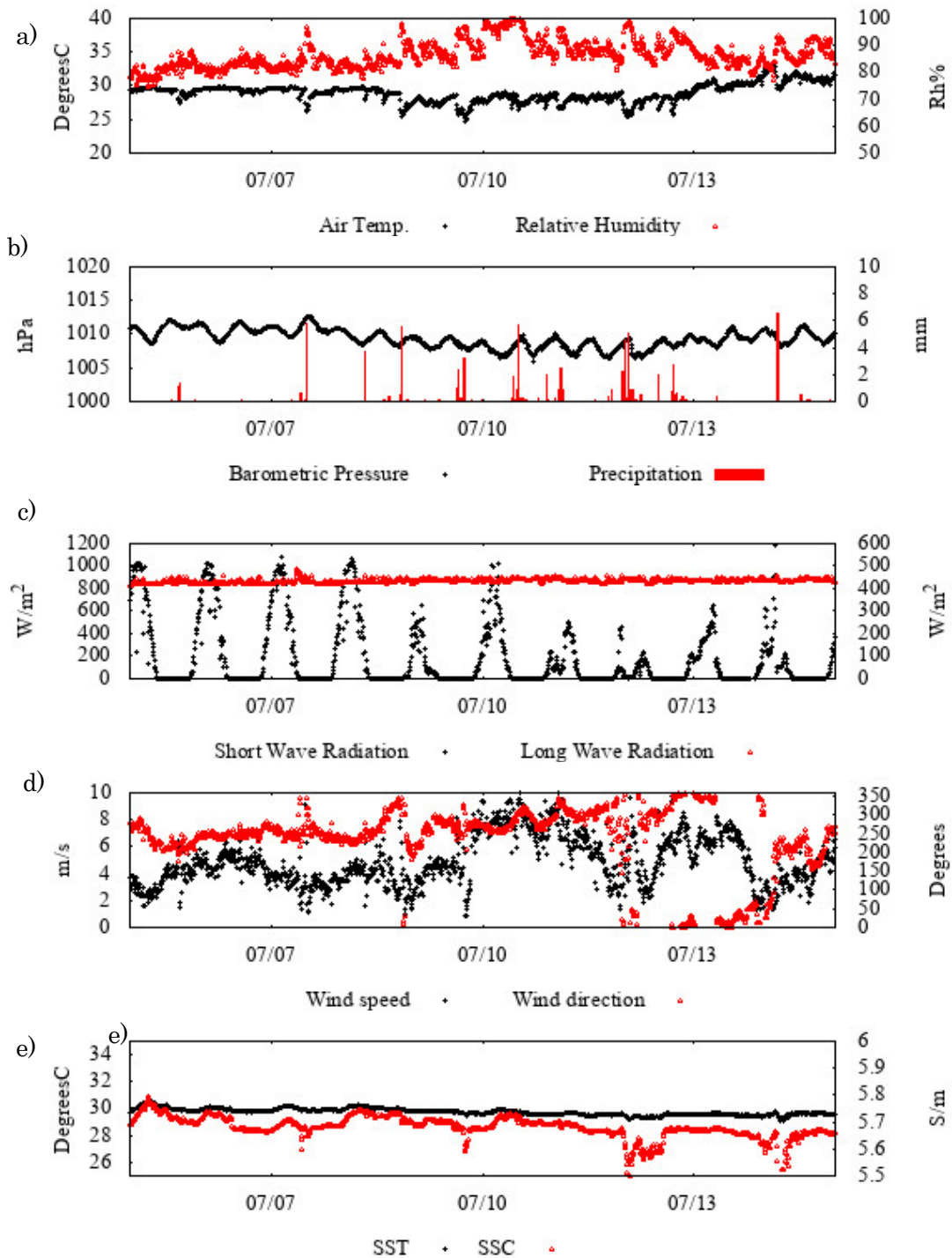


Figure 3.3.1-4 Results of observation by the Wave Glider. a) air temperature, relative humidity, b) barometric pressure, precipitation, c) Shortwave radiation, Longwave radiation, d) wind speed, wind direction, e) SST, SSC.

### 3.3.2 Flux drifting buoy observation

Iwao UEKI	(JAMSTEC)	- Principal investigator
Tatsuya FUKUDA	(JAMSTEC)	- Not on board
Makito YOKOTA	(MWJ)	

#### (2) Objectives

Exchange of momentum, heat, and mass between the ocean and atmosphere is recognized as important processes for atmospheric and oceanic circulation, but observational approaches to detailed processes are still insufficient, and understanding those processes through observation is widely required. According to those background, we have been enhancing our observations to improve our understanding of fundamental processes between the atmosphere and the ocean. As a part of those efforts, we are developing sea surface drifting buoy for momentum and heat fluxes (FDB). During this cruise, we conducted field experiment for those performance.

#### (3) Parameters

- Three-dimensional wind speed
- Sonic temperature
- Air temperature/Relative humidity
- Barometric pressure
- Conductivity, Temperature Pressure

#### (4) Methods

We installed two drifting buoys (FDB01 and FDB02) nearby PHISMO site (13.00°N, 136.97°E) on 06 July 2023 and recovered at 11 July 2023. For FDB02, we also installed a 6 meters rope with 10 TD sensors in 0.5 m intervals for observations of temperature profile within near the surface layer. Evaluations of correction schemes for wind speed and acquired fluxes will be done through comparisons with observations by PHISMO, Wave Glider and the R/V MIRAI.

#### (5) Preliminary results

The installed two FDBs were drifted northwestward as shown in Fig. 3. 3. 2-1. The both buoys took almost same track. According to observed values, easterly winds were dominant in entire observation period, whereas northerly (southerly) winds dominant in the first (second) half of the period. Associated with these wind variations, sensible heat flux derived by eddy covariance method became large when the wind speed intensified.

Evaluation of observation including correction method for pitch and roll of the buoy will be conducted after cruise.

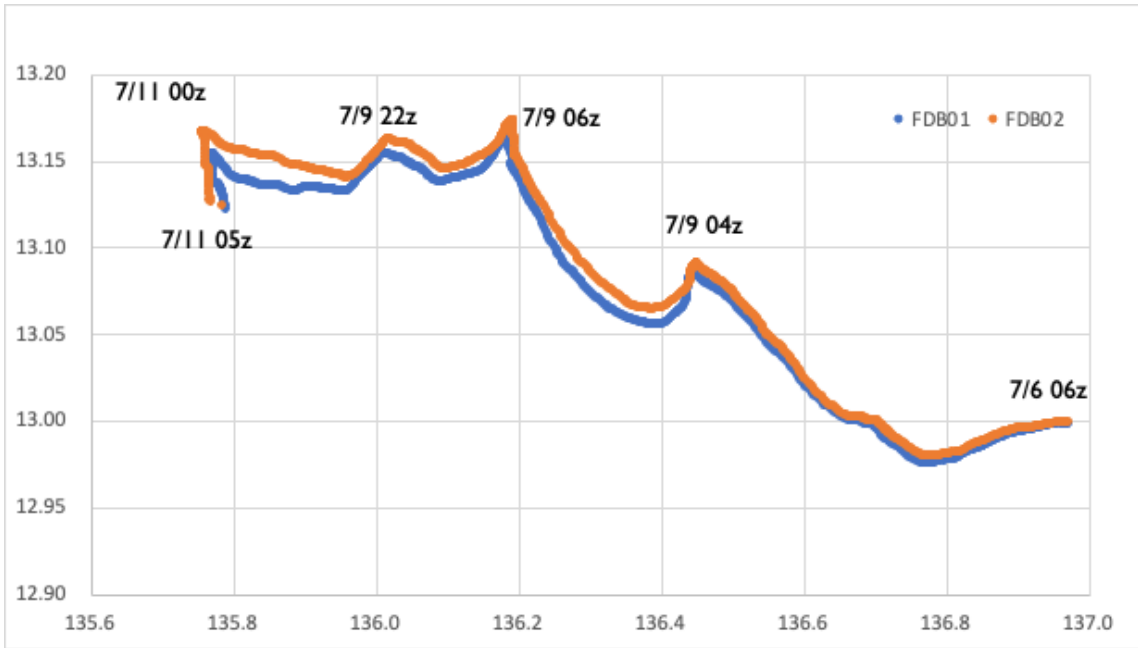


Figure 3.3.2-1 Locations of FDB01 (orange) and FDB02 (blue).

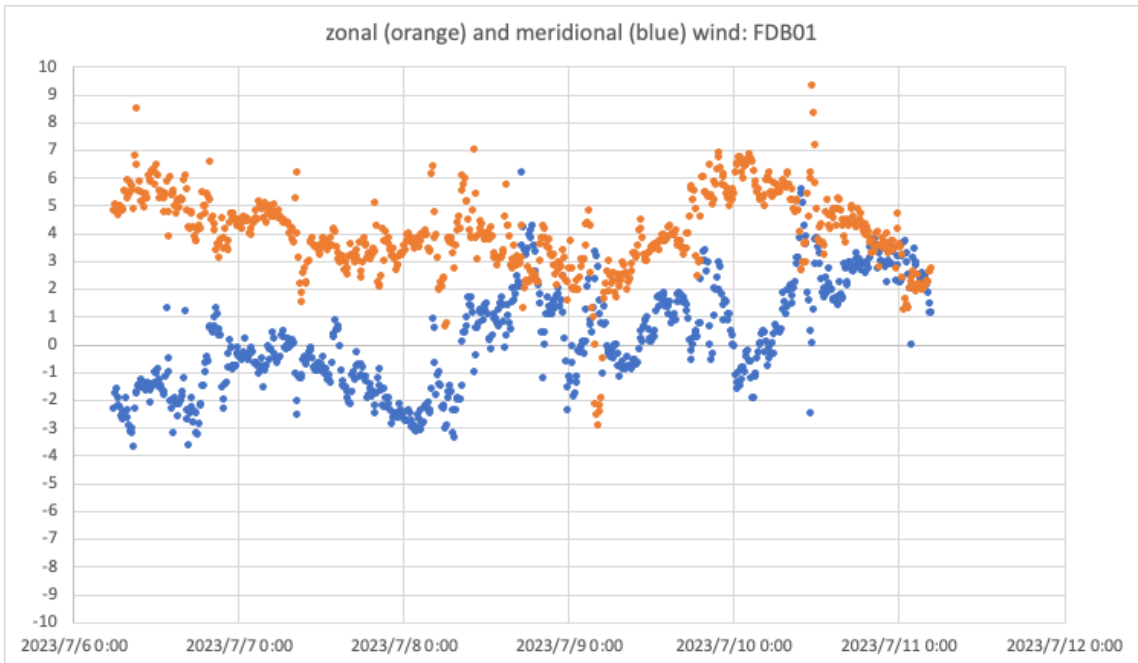


Figure 3.3.2-2 Time series of zonal (orange: positive values indicate easterly) and meridional (blue: positive values indicate southerly) winds observed by FDB01.

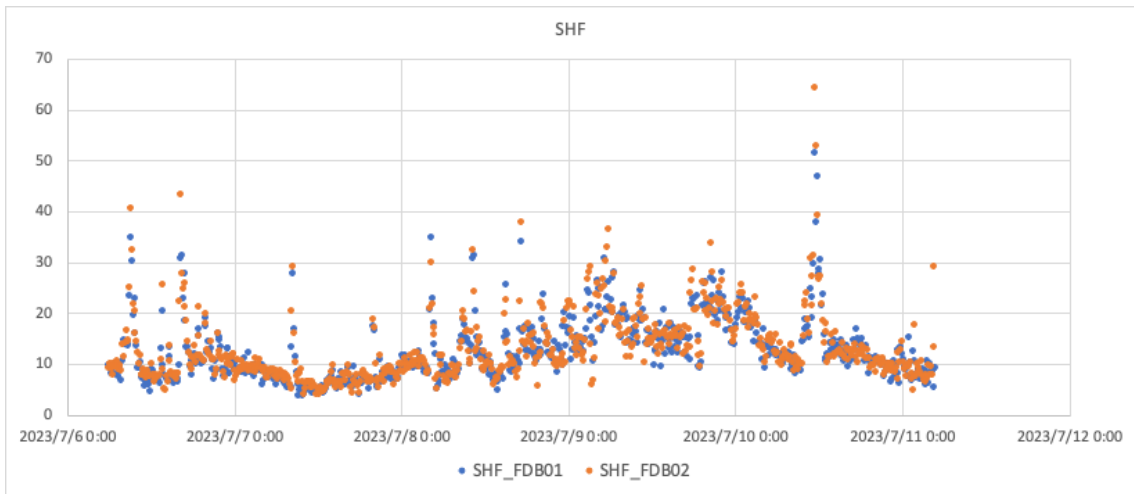


Figure 3.3.2-3 Time series of sensible heat flux based on eddy covariance method using acquired data from FDB01 (orange) and FDB02 (blue).

### 3.3.3 Air-sea momentum flux observation

Naoya SUZUKI (Kindai University) - Principal investigator  
Iwao UEKI (JAMSTEC)  
Atsutoshi IKEDA (Kindai University)

#### (1) Objective

The air-sea momentum flux has generally been estimated using the drag coefficient with the wind speed. However, there still exists considerable disagreement among investigators for the parameterization of the drag coefficient. Recently, air-sea momentum flux has been measured by many buoys designed specifically for air-sea interaction. The sizes of these buoys are very large and they cannot easily be deployed in open ocean. In this cruise, our objective is to measure the air-sea momentum flux using the small size buoy with an installed sonic anemometer in open ocean.

#### (2) Observation

The air-sea momentum flux was observed at around 13°N137°E for a period of 11 hours from 14:00 on 6th July to 1:00 on 7th July (Fig. 3.3.3-1). The iridium tracker was installed on the buoy, in order to obtain the location of the buoy. The buoy has a height of 1800 mm, the diameter of 800 mm, and the weight is 50 kg. Two horizontal and one vertical components of the wind velocity are recorded with a sampling frequency of 10 Hz. The motion of the buoy is measured using two IMU sensors to correct the wind component by the motion correction. By using the eddy correlation method with the wind component measurements, the friction velocity is obtained every 10 min. The significant wave height, wave height, wave period, and wave direction, etc. were measured every 1 hour by the GPS wave observation system on the buoy.



Figure 3.3.3-1

### 3.3.4 Communication tests by multipurpose observation floats and radiosondes

Kensuke WATARI	(JAMSTEC)
Masahiro KAKU	(JAMSTEC)
Hiroshi MATSUBARA	(NTT)
Yutaro MURAKAMI	(NME)
Ryo OYAMA	(NME)

#### (1) Background and objectives

In addition to remote sensing observations such as by satellites, in situ ocean observations are important for understanding the ocean-atmosphere interactions. Data sending and receiving networks by using Iridium Communication are innovative so as to enable communication at sea using small modems, but are still expensive in terms of communication costs and power consumption. NTT Space Environment Research Laboratories anticipated that low-cost and low-power networks can be realized by use of the 920 MHz LPWA satellite communication technique and apply them to ocean observations. In place of satellites, we launch radiosondes with the LPWA communication function and construct a virtual satellite network to communicate with multipurpose observation floats (MOFs), thereby demonstrating the usefulness of the LPWA satellite communication network for ocean observations. Besides, the experiments are conducted to verify the validity and practicality of this method as a communication test evaluation method, and the practicality of data transmission and reception using the LPWA communication in the real ocean.

#### (2) Instrumentation

A MOF is a small profiling float, which collects CTD data down to a depth of about 500 m. (Fig. 3.3.4-1). MOFs are deployed from the R/V MIRAI (Fig. 3.3.4-2), and autonomously dive and then stay at a specified depth. After drifting during designated times, the floats collect CTD profiles while ascending and transmit data at the sea surface. Instead of usually used Iridium communication, MOF used in the experiments are equipped with an LPWA communication module and antenna. Data transmission is performed through LPWA communication. In order to reduce the amount of communication, electrical conductivity, water temperature, and pressure data are merged and compressed, and the compressed data are sent. Additionally, radiosondes with relay function are used to communicate with MOFs in place of satellites or HAPS. (Fig. 3.3.4-3). Radiosondes are launched from the R/V MIRAI in the surfacing times of MOFs (Fig. 3.3.4-4). Signals relayed via radiosondes were received by a receiver installed to the R/V MIRAI. In addition to LPWA relay function, radiosondes can measure position, altitude, temperature, atmospheric pressure, humidity, and wind direction/speed using GPS and meteorological sensors. In the future, communication satellites and HAPS are to play the role of radiosondes (Fig. 3.3.4-5). For this reason, practical communication distances are measured by positions and altitudes relayed by radiosondes and surfaced positions of MOFs.

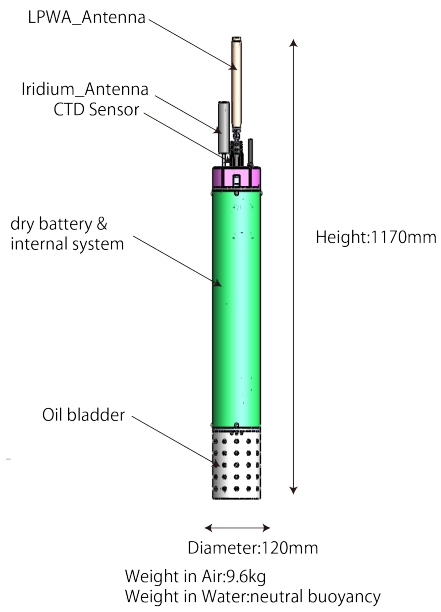


Figure 3.3.4-1 Diagram of a MOF.



Figure 3.3.4-2 Deployment of a MOF from the R/V MIRAI.

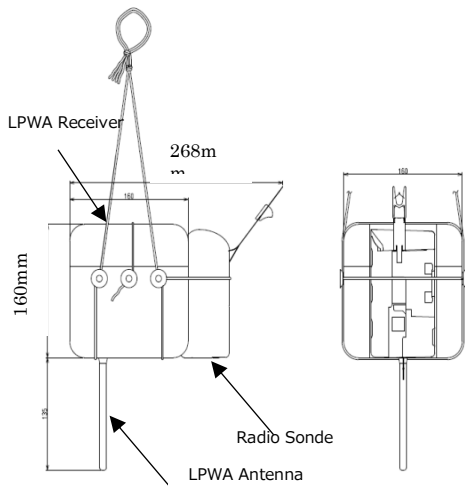


Figure 3.3.4-3 Schematics of an LPWA radiosonde



Figure 3.3.4-4 Launching of a balloon for radiosonde observation.

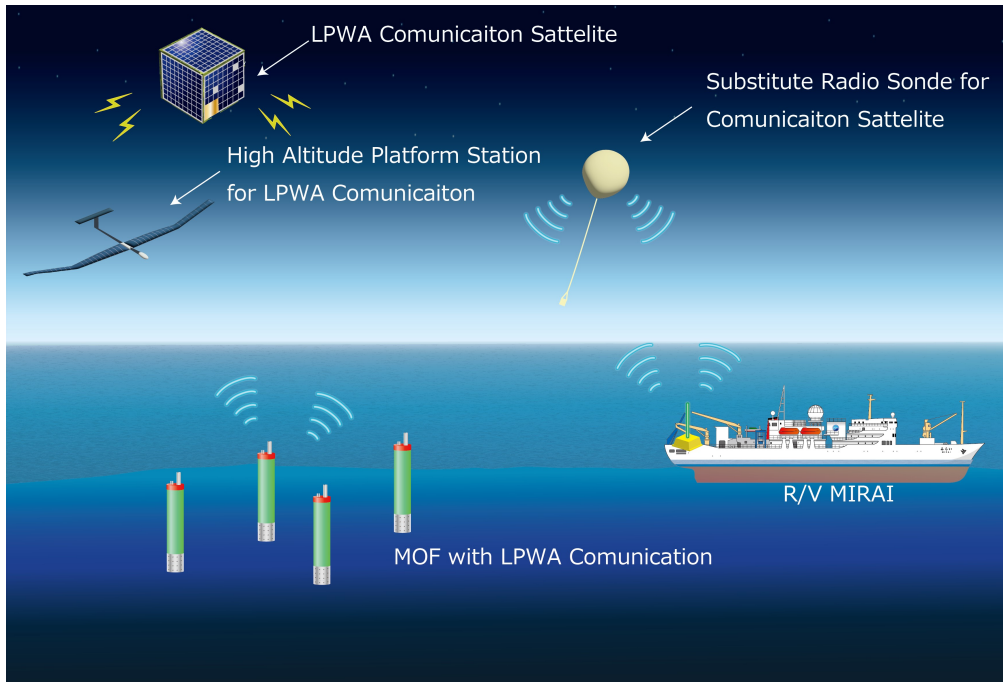


Figure 3.3.4-5 Overall picture of the MOF-LPWA experiment

(3) Deployment and recovery

A MOF was launched on July 5, 2023 and operated at sea until July 21. Tests of radiosonde launchings and communication were conducted on July 2, 3, and 5–15.

(4) Mission details

Three MOFs were used for the experimental observations. We launched 10 radiosondes and examined whether data reception was practicable, and determined distances between MOFs and radiosondes at the time of reception.

Table1. 3.3.4-1 Information of MOF deployments

Deployment date	Serial number	Deployment point	Target depth
2023/07/05	12	13°-07.51426'N 136°-53.07067'E	50 m
2023/07/10	13	13°-28.16565'N 137°-01.63834'E	100 m
2023/07/15	14	14°-47.45206'N 134°-51.80600'E	100 m

Table13.3.4-2 Information of LPWA radiosonde launchings

No.	Date	Launching time	S/N	Deployment point	Arrival height	Observation time
1	2023/07/02	09:43:00	7136300	25.00072°N 145.00249°E	24395 m	3h58m
2	2023/07/03	09:42:42	7136304	21.92309°N 141.9667°E	25517 m	2h40m
3	2023/07/05	14:47:57	7136301	13.1255°N 136.88459°E	24758 m	3h45m
4	2023/07/07	22:21:41	7136305	13.18816°N 136.64605°E	24151 m	2h34m
5	2023/07/10	13:26:55	7136297	13.54387°N 136.97418°E	24809 m	2h51m
6	2023/07/10	16:32:16	7136302	13.50002°N 137.06618°E	17006 m	4h18m
7	2023/07/11	10:20:09	7136296	13.16549°N 135.7279°E	25511 m	4h29m
8	2023/07/11	16:46:25	7136299	12.83336°N 135.7385°E	18552 m	5h37m
9	2023/07/14	19:03:42	7136298	13.00731°N 134.92648°E	22789 m	2h15m
10	2023/07/15	16:30:26	7136303	14.97919°N 134.86422°E	23270 m	3h49m

#### (5) Preliminary results

Figure 3.3.4-6 shows electrical conductivity, water temperature, and pressure profiles based on data transmitted through LPWA communication and Iridium communication (salinity values were calculated from these parameters). Despite of merging of data digits, no noticeable deterioration occurred in salinity data. MOF-observed data were consistent with measurements by the MIRAI CTD system in the vicinity of the MOF. Discrepancies are attributable to differences in observation times and locations. Because the maximum significant wave height during the experiments was observed to be approximately 2.7 m, the MOF-LPWA communication is practical even in a condition to the same degree of the wave height; therefore, MOF-LPWA communication was demonstrated to be practicable in sea state 5. The maximum distance which MOF and LPWA were able to communicate was 220 km. The possible communication range is considered to be longer in the direction where signals are less attenuated. Thus, MOF-LPWA communication is practicable over a line-of-sight distance of 220 km or more. MOFs possibly communicate even with satellites in low orbit.

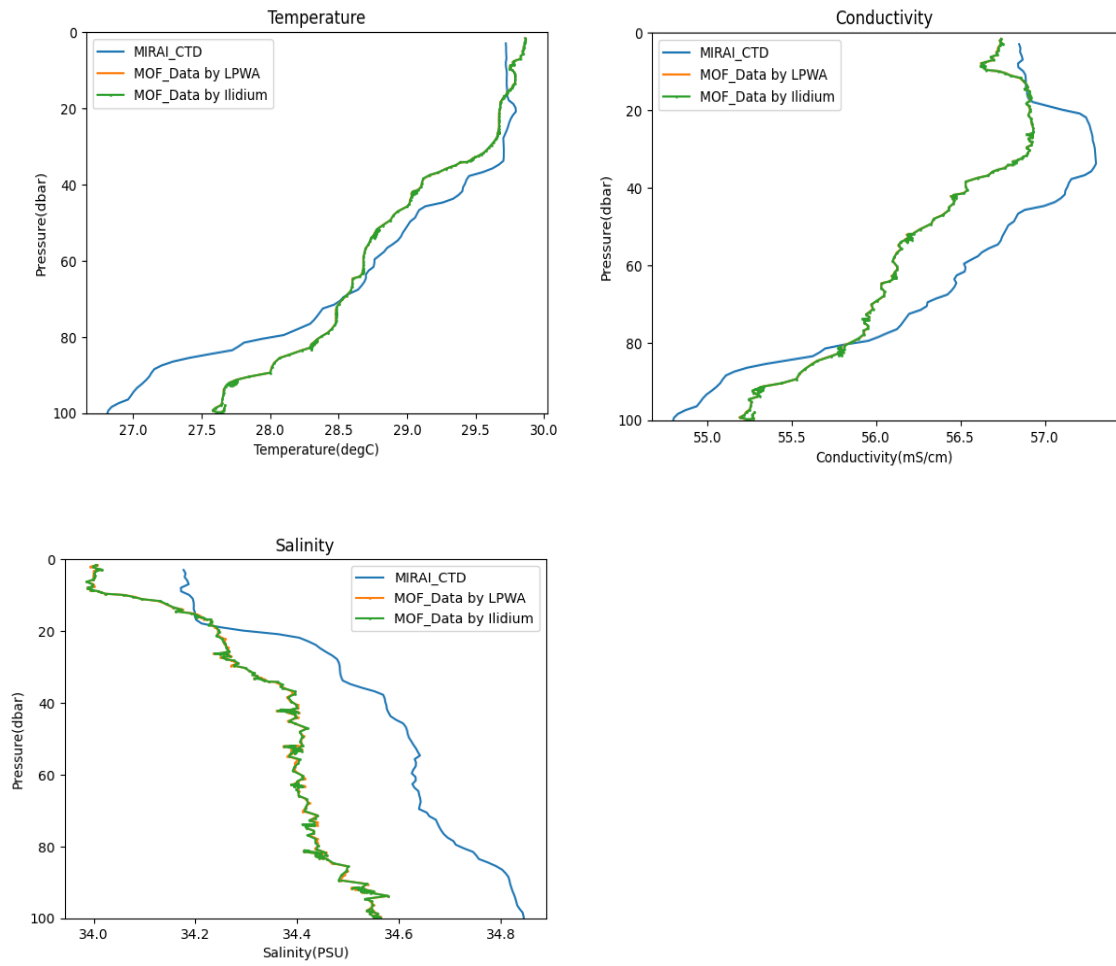


Figure 3.3.4-6 Hydrographic profiles observed by MOF and R/V MIRAI.

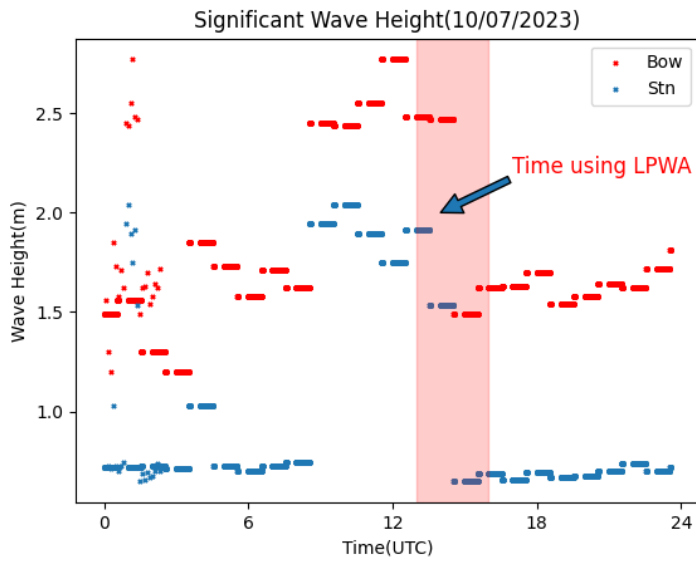


Figure 3.3.4-7 Significant wave height during the LPWA communications

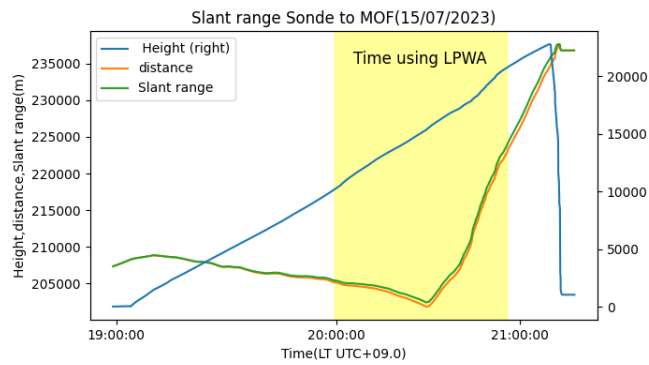


Figure 3.3.4-8 Slant range during the LPWA Communications

### 3.3.5 Virtual mooring drone observation

Kensuke WATARI	(JAMSTEC)
Masahiro KAKU	(JAMSTEC)
Masaki KATSUMATA	(JAMSTEC)
Makito YOKOTA	(MWJ)
Kango FURUYAMA	(MWJ)

#### (1) Background and objectives

For prediction of typhoons, it is important to obtain accurate initial values for data assimilation and to monitor the status of typhoons in real time as much detail as possible. Besides, looking further ahead, the control of typhoons may become reality in the future. The accurate understanding of typhoons is essential to know how the control of typhoons impacts on the surrounding environments after the control will be implemented.

The existing observation systems in the tropical western North Pacific are too weak against typhoons for us to obtain in situ data of atmospheric pressure, wind, temperature, etc. near the center of a typhoon. Researches on typhoons are based largely on satellite observations, which are not sufficient to study the internal structure of the atmospheric and oceanic surface layers, one of the key factors responsible for typhoon development. Uncrewed surface vehicles are potential platforms suitable for typhoon researches. Therefore, we aim to develop a brand-new USV, called a virtual mooring (VM) drone, which autonomously moves using natural energy and efficiently collects data in the unveiled atmospheric and oceanic surface layers. In this cruise, we examined the capability of the prototype drone through collecting data for intercomparison with those by the R/V MIRAI.

#### (2) Instrumentation

A VM drone is a yacht-shaped platform with a total length of 2.2 m, a total height of 2.6 m, a total width of 0.4 m, and a weight of 60 kg. It was equipped with a naca0018 type sail with a total length of 1.6 m, obtaining propulsion from wind power. The prototype drone launched in this cruise was equipped with a CTD sensor at the bottom of the hull to measure SST and sea surface salinity. In addition, a composite weather sensor was installed at the rear of the main unit to measure wind direction/speed, air temperature, atmospheric pressure, and relative humidity. The main body was equipped with a 9-axis gyro to measure the attitude of the main body. Additionally, two-way communication is possible through Wi-Fi and Iridium communications. An iridium beacon, which power unit was separate from the main communication system, was installed to track the drone location in case of trouble.

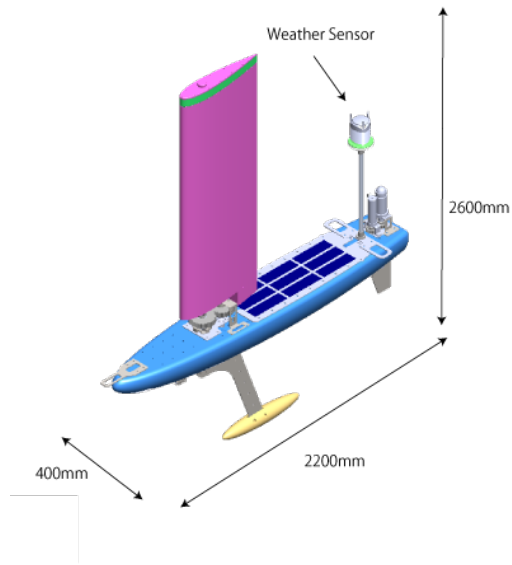


Fig. 3.3.5-1 Diagram of a VM drone.

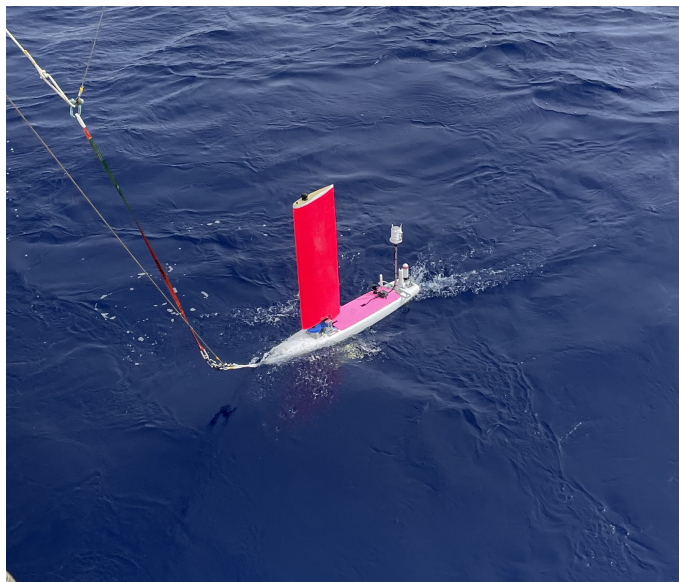


Fig. 3.3.5-2 VM drone deployed from the R/V MIRAI

(3) Deployment and mission details

The VM drone was deployed from and recovery to the R/V MIRAI on July 12 and 15, 2023, respectively.

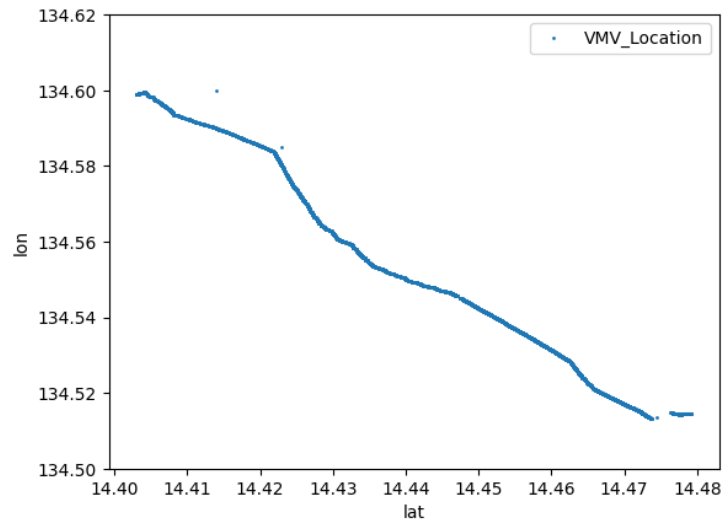


Figure 3.3.5-3 Cruise track of the VM drone during the mission on July 15, 2023.

(4) Preliminary results

Figure 3.3.5-4 shows the time-series plot of data acquired by the VM drone. As shown in this figure, all variables were successfully measured by meteorological and CTD sensors and remarkably exhibit high-frequency wind speed and SST variabilities. These data are acquired in real time via Iridium communications, making it possible to constantly monitor weather events.

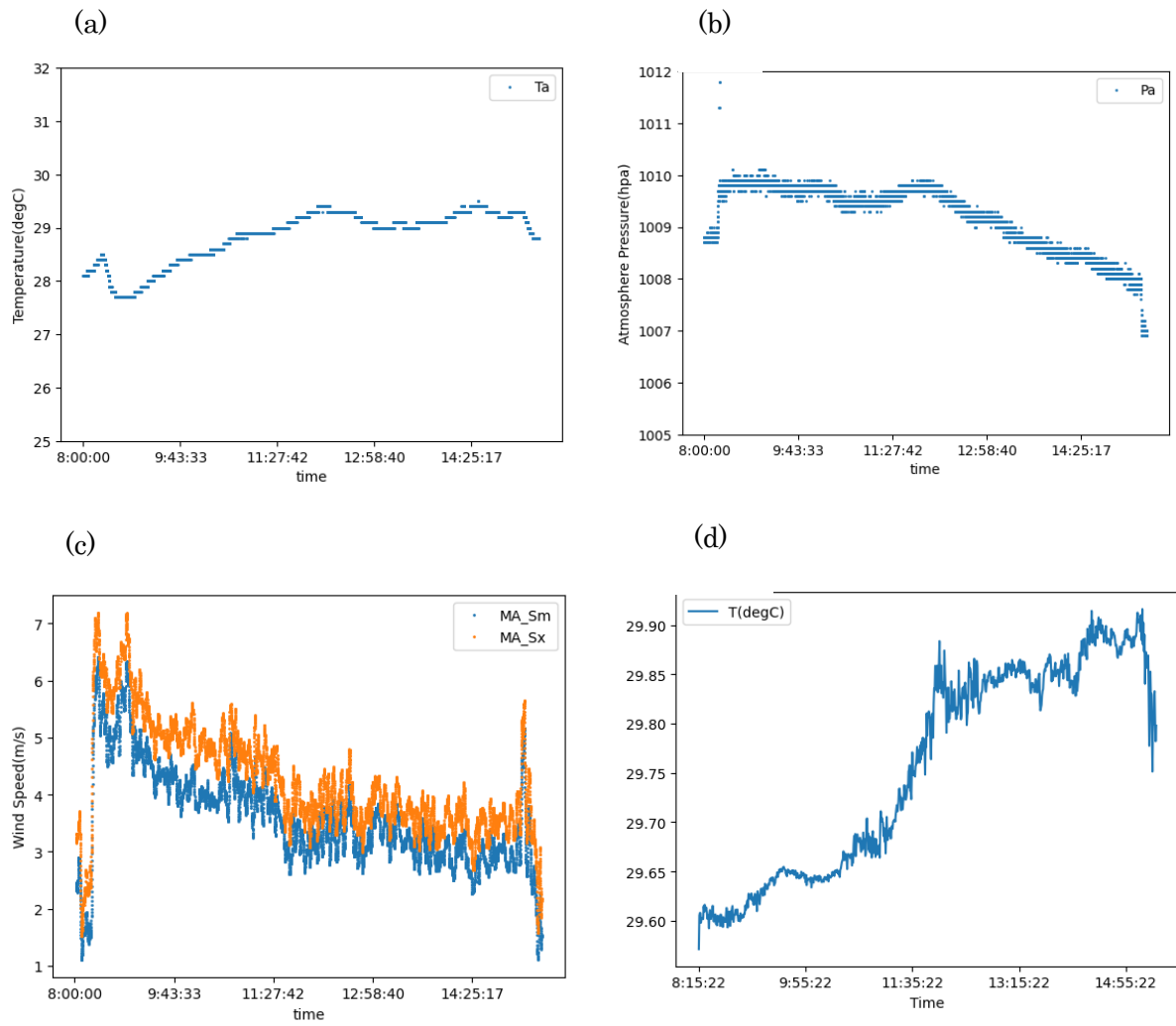


Figure 3.3.5-4 Atmosphere and ocean variables observed by the VM drone. (a) air temperature, (b) atmosphere pressure, (c) wind speed, and (d) SST.

### 3.3.6 Argo float observation (core)

Shigeki HOSODA	(JAMSTEC)	- Principal Investigator (not on board)
Mizue HIRANO	(JAMSTEC)	- Technical Staff (not on board)
Nobuhiro FUJII	(MWJ)	- Technical Staff
Masaki FURUHATA	(MWJ)	- Technical Staff
Aine YODA	(MWJ)	- Technical Staff
Tun Htet Aung	(MWJ)	- Technical Staff

#### (2) Objective

The research objective is to clarify the mechanisms of climate and oceanic environment variability, and to understand changes of earth system through estimations of heat and material transports, improving the Argo observing system in the global ocean. To achieve the objective, three core Argo floats are deployed to carry out automatically measurements of long-term temperature and salinity variations in the western Pacific Ocean where is spatial density of the Argo floats distribution has been constantly sparse due to a lack of float deployment opportunities. The data accumulated from Argo floats also contribute to improve long-term forecasts of climate changes through data assimilation systems.

#### (3) Parameters

- Water temperature, salinity and pressure.

#### (4) Method

We deployed 3APEX floats manufactured by Teledyne Webb Research. APEX is able to equipped with two types of CTD sensors SBE41 CTD SBE41 manufactured by Sea-Bird Scientific and RBRargo<sup>3</sup> C.T.D. manufactured by RBR. The float drifts at a depth of 1000 dbar (called the parking depth) during waiting measurement, then goes upward from a depth of 2000 dbar to the sea surface every 1–10 days. The profile frequency will be finally set to 10 days, which is the frequency of normal core Argo scheme, after the check of float status is done. During the ascent, physical values are measured every 2 dbar in advance following depth table. During surfacing for approximately half an hour, the float sends all measured data to the land via the Iridium RUDICS telecommunication system. The lifetime of floats is expected to be about 4–8 years. The status of float and its launching information is shown in Table 3.3.6-1.

Table 3.3.6-1 Specifications of floats and their launching positions

Float Type	APEX float manufactured by Teledyne Webb Research.
CTD sensor	SBE41 manufactured by Sea-Bird Scientific RBRargo <sup>3</sup> C.T.D. manufactured by RBR
Cycle	Every 1–10 days (approximately 30 minutes at the sea surface)
Iridium transmit type	Router-Based Unrestricted Digital Internetworking Connectivity Solutions (RUDICS)
Target Parking Pressure	1000 dbar
Sampling layers	2-dbar interval from 2000 dbar to surface (approximately 1000 levels)

Launching position

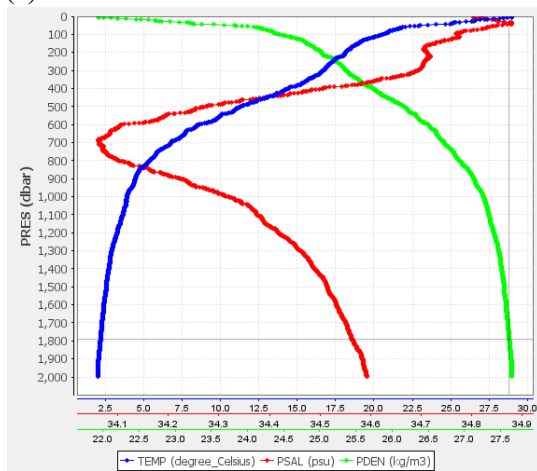
Float S/N	WMO ID	Date and Time of Launch (UTC)	Location of Launch	Station	Remarks (CTD)
9947	5905880	2023/07/02 05:29	24° 59.86'N 144° 59.90' E	002	SBE41
9710	5905883	2023/07/05 07:35	13° 07.61'N 136° 52.97' E	003	RBR
9948	5906384	2023/07/12 00:04	9° 49.93'N 134° 51.60' E	005	SBE41

(5) Data archive

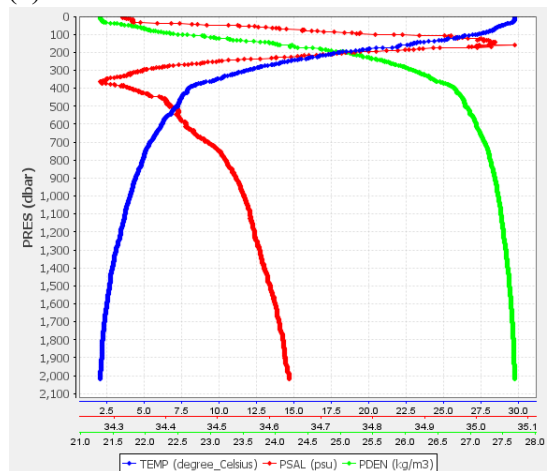
The Argo float data will be provided conducting the real-time quality control within 24 hours following the procedure decided by Argo data management team. Then the delayed mode quality control will be conducted within 6 months ~1 year, to satisfy their data accuracy for climate research use. Those quality-controlled data are freely available via internet and utilized for not only research but also weather forecasts and any other variable use through internet.

Global Data Assembly Center (GDAC: <http://www.usgodae.org/argo/argo.html>, <http://www.coriolis.eu.org/>), Global Telecommunication System (GTS).

(a) S/N 9947



(b) S/N 9710



(c) S/N 9948

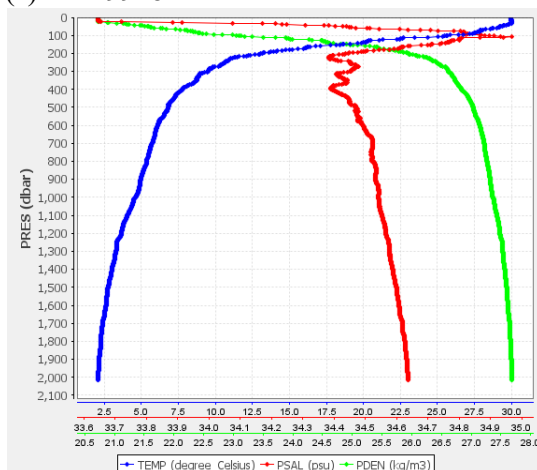


Figure 3.3.6-1 Preliminary results of vertical temperature and salinity profiles from their first measurements by the deployed Argo floats. Blue, red and green lines show temperature, salinity and potential density profiles.

### 3.3.7 Argo float observation for air-sea interaction research

Satoru YOKOI	(JAMSTEC)	- Principal Investigator (not on board)
Ayako SEIKI	(JAMSTEC)	(not on board)
Shigeki HOSODA	(JAMSTEC)	(not on board)
Mizue HIRANO	(JAMSTEC)	(not on board)
Nobuhiro FUJII	(MWJ)	

#### (2) Objectives

The objective of the observation is to measure vertical profiles of sea-water temperature and salinity for investigating oceanic mixed layer structure and air-sea interaction.

#### (3) Methods

Two APEX profiling floats manufactured by Teledyne Webb Research and equipped with RBRargo CTD sensor were deployed on the way from Palau to Shimizu. Information of the deployment is summarized in Table 3.3.7-1. These floats measure vertical profile of sea-water temperature and salinity above 500 dbar at around 1000 UTC (1900 Local Time) every day.

#### (4) Preliminary Results

As an example, Fig. 3.3.7-1 shows observed profiles of temperature and salinity by the two floats on 19 July 2023.

#### (5) Data archive

The ARGO float data with real-time quality control are provided to Global Data Assembly Center (GDAC: <https://argo.ucsd.edu/data/data-from-gdacs/>). Delayed mode quality control is conducted for the float data within 6 months ~1 year, to satisfy their data accuracy for the use of research.

Table 3.3.7-1: Information of the deployment of the floats.

S/N	WMO number	Date and time (UTC)	Latitude	Longitude
<b>10054</b>	5906388	23:35 UTC, 16 July 2023	21°-59.8'N	136°-27.9'E
<b>10055</b>	5906594	05:25 UTC, 17 July 2023	22°-59.9'N	136°-37.4'E

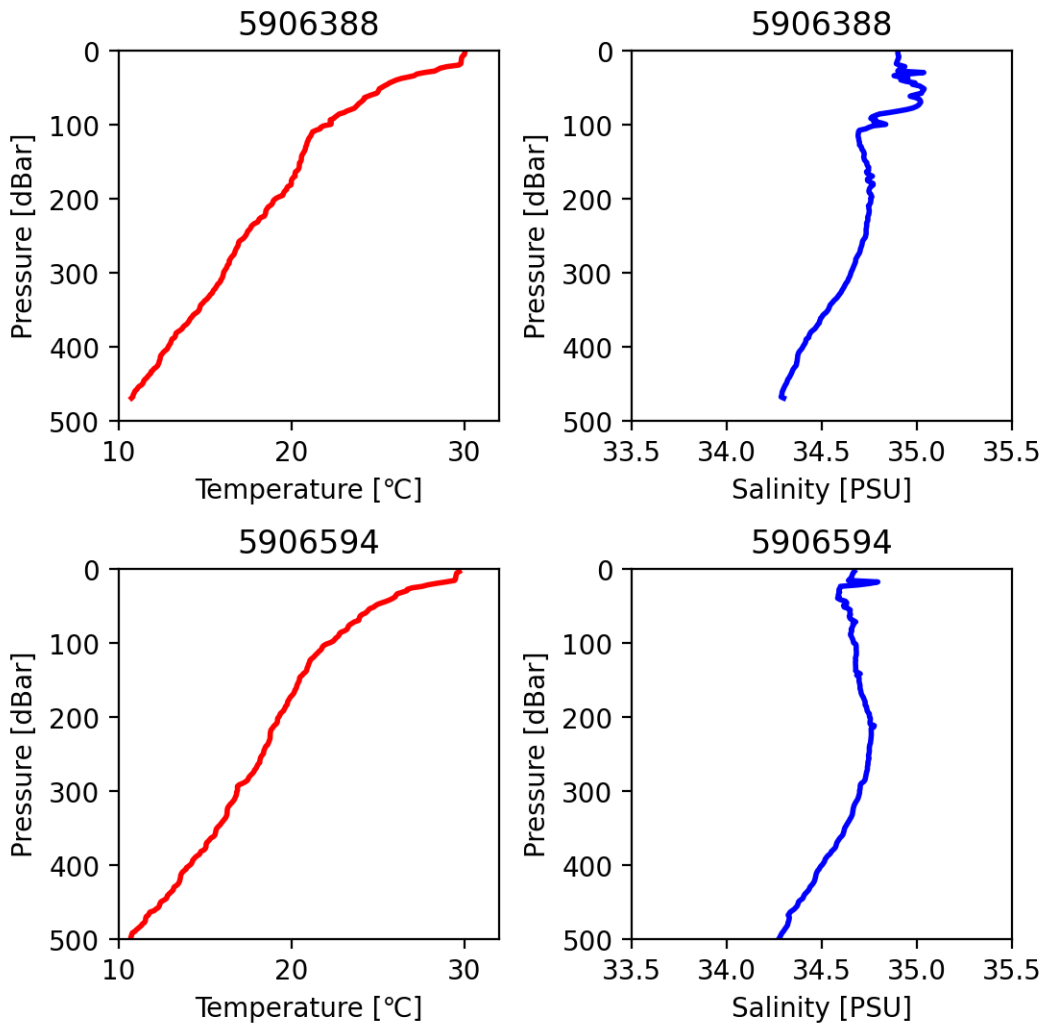


Figure 3.3.7-1: (left) Temperature and (right) salinity profiles observed on 19 July 2023 by the floats with WMO numbers of (top) 5906388 and (bottom) 5906594.

### 3.3.8 Smart CARTHE drifter observation

Yasumasa MIYAZAWA (JASMTEC) - Principal investigator  
Akira NAGANO (JAMSTEC)  
Tun Htet Aung (MWJ)

#### (1) Objectives

Ocean current measurements by tracking the drifter tracks and sensitivity test of water-proofness of the telecommunication unit with or without applying putty.

#### (2) Parameters

GPS positions

#### (3) Instruments and methods

The Smart CARTHE drifter is designed to measure GPS positions accurately and frequently (with 10-minute interval in this version) for capturing the ocean current at approximately 40cm depth for several weeks with relatively low economic and environmental costs (Novelli et al. 2017). The drifter size and dry weight are compact, 38cm x 38cm x 60cm, and 4kg, respectively. Thus, hundred numbers of drifter releases to the ocean are feasible for investigating detailed spatiotemporal variability of meso- to submesoscale eddies (Jacobs et al. 2021). Prior to a planned massive release experiment, to understand basic behaviors of the drifter in a targeted region, south of Japan, we deployed two drifters provided from PacificGyre Inc., in this cruise. In one drifter (0-4694244), putty was applied to waterproof the joints that seal the circuit board. Another one (0-4694242) has no such putty for waterproofing as the default setting. The trial with or without the waterproofing putty was conducted for confirming the validity of the default setting with no additional waterproofing.

#### (4) Preliminary result

On 05:27, 17 July 2023 (UTC), the two drifters were released to the ocean at 22°-59.87'N 136°-37.38'E. On 02:24, 19 July 2023 (UTC), the locations of the two drifters were almost similar to each other and both moved southwestward after the release (Fig. 3.3.8-1).

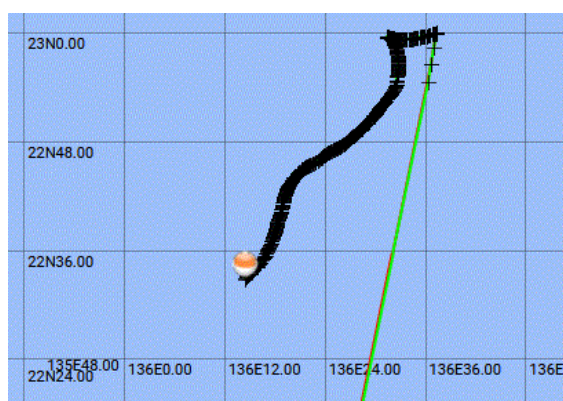


Figure 3.3.8-1. Drifter tracks visualized on 02:24, 19 July 2023 (UTC).  
<https://www.pacificgyre.com/>

#### (5) Data archive

These data obtained in this cruise will be submitted to the Data Management Group (DMG) JAMSTEC, and will be opened to the public via “Data Research System for Whole Cruise Information in JAMSTEC (DARWIN)” in JAMSTEC: <http://www.godac.jamstec.go.jp/darwin/e>

(6) References

Novelli G, Guigand CM, Cousin C, Ryan EH, Laxague NJM, Dai H, Haus BK, Ozgokman TM, 2017: A biodegradable surface drifter for ocean sampling on a massive scale, *Journal of Atmospheric and Oceanic Technology*, 34, 2509-2532.

Jacobs GA, D'Addezio JM, Bartels B, Spence PL, 2021: Constrained scales in ocean forecasting, *Advances in Space Research*, 68, 746-761.

### 3.4 CTD

Akira NAGANO	(JAMSTEC)	- Principal investigator
Kazuhiko MATSUMOTO	(JAMSTEC)	
Aine YODA	(MWJ)	- Operation leader
Tun Htet Aung	(MWJ)	
Nobuhiro FUJII	(MWJ)	

#### (1) Objective

CTDO<sub>2</sub> measurements and water sampling were conducted to obtain vertical profiles of seawater properties by sensors and Niskin bottles.

#### (2) Parameters

Pressure, temperature, salinity, dissolved oxygen concentration, beam transmission, fluorescence, turbidity, photosynthetically active radiation, chromophoric dissolved organic matter (CDOM), altimeter height (100-m range)

#### (3) Instruments and methods

##### Winch and cable

Traction winch system (3.0 ton) (Dynacon, Inc., Bryan, Texas, USA)

Armored cable ( $\phi = 9.53$  mm) (Rochester Wire & Cable, LLC, Culpeper, Virginia, USA)

Compact underwater slip ring swivel (Hanayuu Co., Ltd., Shizuoka, Japan)

##### CTD

SBE911plus CTD system

##### Deck unit

SBE11plus (Sea-Bird Scientific, Washington, USA)  
Serial no. 11P54451-0872

##### Frame and water sampler

Stainless steel frame (460 kg) for 36-position 12-liter water sampling bottles with an aluminum rectangular fin ( $54 \times 90$  cm) to resist rotation of the frame

Thirty six-position carousel water sampler, SBE 32 (Sea-Bird Scientific, Washington, USA).  
Serial no. 3221746-0278

Twelve-liter sampling bottles, model OTE 110 (OceanTest Equipment, Inc., Fort Lauderdale, Florida, USA) (No TEFLON coating). Bottles numbered from 1 to 20 were set with acid-washed Viton O-rings and bottles numbered from 21 to 36 with nitrile rubber O-rings

##### Underwater unit

Pressure sensor, SBE 9plus (Sea-Bird Scientific, Washington, USA)  
Serial no. 09P54451-1027 (117457) (calibration date: Jun 09, 2022)

##### Temperature sensor

Deep standard reference thermometer, SBE 35, (Sea-Bird Scientific, Washington, USA)

Serial no. 22 (calibration date: Jul. 14, 2022)

Primary, SBE 3F (Sea-Bird Scientific, Washington, USA)  
Serial no. 031525 (calibration date: Mar. 22, 2023)  
Secondary, SBE 3Plus (Sea-Bird Scientific, Washington, USA)  
Serial no. 03P2730 (calibration date: Apr. 11, 2023)

Conductivity sensor

Primary, SBE 4C (Sea-Bird Scientific, Washington, USA)  
Serial no. 042435 (calibration date: Sep. 02, 2022)  
Secondary, SBE 4C (Sea-Bird Scientific, Washington, USA)  
Serial no. 041203 (calibration date: Mar. 21, 2023)

Dissolved oxygen sensor

Primary, RINKO III (JFE Advantech Co., Ltd., Hyogo, Japan)  
Serial no. 0287, Sensing foil no. 163011(calibration date: May 11, 2023)  
Secondary, SBE 43 (Sea-Bird Scientific, Washington, USA)  
Serial no. 430949 (calibration date: Mar. 18, 2023)

Chlorophyll Fluorometer (Seapoint Sensors Inc., New Hampshire, USA)  
Serial no. 3618, Gain: 30X (0–5 ug/L)

Transmissometer, C-Star, (WET Labs, Inc., Philomath, Oregon, USA)  
Serial no. 1727DR (calibration date: Jun. 08, 2023)

Deep Ocean Turbidity Meter, ATUD-CAV-S50 (JFE Advantech Co., Ltd., Hyogo, Japan)  
Serial no. 0002 (calibration date: Jun. 21, 2023)

PAR sensor, PAR-Log ICSW (Sea-Bird Scientific, Washington, USA)  
Serial no. 2201 (calibration date: Dec. 16, 2021)

Ultraviolet fluorometer (Seapoint Sensors Inc., New Hampshire, USA)  
Serial no. 6238, Gain setting: 30X (0–50 QSU)

Altimeter, PSA-916T (Teledyne Benthos, Inc.)  
Serial no. 1100

Pump, SBE 5T (Sea-Bird Scientific, Washington, USA)  
Primary serial no. 055816  
Secondary serial no. 054598

Bottom contact switch (Sea-Bird Scientific, Washington, USA)

Other additional sensors

Chlorophyll and turbidity logger, model ACLD70-USB

Software

Data acquisition software, SEASAVE-Win32, version 7.26.7.121

Data processing software, SBEDataProcessing-Win32, version 7.26.7.129 and some original modules

### Data Collection

The CTD system was powered on at least 20 minutes before data acquisition for pressure sensor measurement to be stable. Data were acquired at least 2 minutes before and after CTD casts to collect atmospheric pressure data on the ship deck.

Sensors and Niskin bottles installed to the CTD-frame was lowered into the water from the starboard side and held at 10 m depth below the sea surface to activate the pump. After the pump was activated, the frame was raised to the sea surface and then lowered toward the bottom at a rate of  $1.0 \text{ m s}^{-1}$ . At 200 m depth, the winch was once stopped and the heave compensator of the crane was started to operate. In deep layers where the vertical gradient of water properties was not large, the frame was lowered at a high rate of  $1.2 \text{ m s}^{-1}$ . While up casting, the frame was raised at a rate of  $1.1 \text{ m s}^{-1}$  except for bottle firing stops at sampling depth layers.

Basically, we closed bottles 60 seconds after winch stops and then stayed there for at least 5 seconds for measurement of the SBE 35. When we collected samples of plural bottles at a sampling layer, we closed bottles at intervals of more than 8 seconds to allow SBE35 to process data. When the frame reached 200 m depth, the winch was stopped to terminate the heave compensator of the crane.

#### (4) Problems Encountered

At cast 002M002, an oil leakage and gushing from the winch arm occurred just before the CTD-frame was put into water, and oil droplets were sprayed onto the instruments, sampling bottles, and the frame. They were brought back on the deck and were cleaned. Sampling bottles were thoroughly washed and O-rings of bottles were replaced. The cast was skipped.

In bottle leak checking before water sampling at the next cast (003M001), we found leakage from the bottle end cap of number 20 sampling bottle. The cause of this leakage was due to the removal of the O-ring by mistake when replacing O-rings of the bottle next to it.

In most of the casts during this cruise, the Deep Ocean Turbidity Meter showed negative value of about  $-0.027 \text{ FTU}$  from the sea surface to about 50 dbar during down and up casts. This is considered to be attributed to ambient light interference.

#### (5) Data Processing

The processing of obtained CTD data is described herein. In these processes, a utility software, SBE Data Processing-Win32 (ver.7.26.7.129) and some original modules were used.

##### (The process in order)

DATCNV converted binary raw data to engineering unit data. DATCNV also extracts bottle information where scans were marked with the bottle confirm bit during acquisition. The scan duration to be included in bottle file was set to 4.4 seconds, and the offset was set to 0.0 seconds. The hysteresis correction for the SBE 43 data (voltage) was applied for both profile and bottle information data.

TCORP (original module) corrected the pressure sensitivity of the temperature (SBE3) sensor.  $1.714\text{e-}08 \text{ (degC/dbar)}$  for S/N1525 (t090C)

RINKOCOR (original module) corrected the time dependent, pressure induced effect (hysteresis) of the RINKOIII profile data.

RINKOCORROS (original module) corrected the time dependent, pressure induced effect (hysteresis) of the RINKOIII bottle information data by using the hysteresis corrected profile data.

BOTTLESUM created a summary of the bottle data. The data were averaged over 4.4 seconds.

ALIGNCTD aligned parameter data in time, relative to pressure to ensure that all calculations were made using measurements from the same parcel of water.

For an SBE 9plus with TC-ducted temperature and conductivity sensors and a 3000-rpm pump, the typical lag of temperature to pressure is 0 second and lag of conductivity relative to temperature is 0.073 seconds. The Deck Unit was programmed to advance conductivity relative to pressure so conductivity alignment in ALIGNCTD was not needed. Dissolved oxygen data are systematically delayed with respect to pressure mainly because of the long time constant of the dissolved oxygen sensor and of an additional delay from the transit time of water in the pumped plumbing line. This delay was compensated by 5 seconds advancing dissolved oxygen sensor (SBE43) output (dissolved oxygen voltage) relative to the temperature data. Delay of the RINKOIII data was also compensated by 1 second advancing sensor output (voltage) relative to the temperature data. Delay of the transmissometer data was also compensated by 2 seconds advancing sensor output (voltage) relative to the temperature data.

WILDEDIT marked extreme outliers in the data files. The first pass of WILDEDIT obtained the accurate estimate of the true standard deviation of the data. The data were read in blocks of 1000 scans. Data greater than 10 standard deviations were flagged. The second pass computed a standard deviation over the same 1000 scans excluding the flagged values. Values greater than 20 standard deviations were marked bad. This process was applied to pressure, depth, temperature (primary and secondary), conductivity (primary and secondary), and dissolved oxygen voltage (SBE43).

CELLTM used a recursive filter to remove conductivity cell thermal mass effects from the measured conductivity. Typical values for SBE 9plus with TC duct and 3000 rpm pump which were 0.03 for thermal anomaly amplitude  $\alpha$  and 7.0 for the time constant  $1/\beta$  were used.

FILTER performed a low-pass filter on pressure and depth with a time constant of 0.15 second. In order to produce zero phase lag (no time shift) the filter runs forward first then backward.

WFILTER performed as a median filter to remove spikes in transmissometer data, fluorometer data, deep ocean turbidity meter data, and ultraviolet fluorometer data. A median value was determined by 49 scans of the window. For the ultraviolet fluorometer data, an additional box-car filter with a window of 361 scans was applied to remove noise.

SECTIONU (original module of SECTION) selected a time span of data based on scan number in order to reduce a file size. The minimum number was set to be the starting time when the CTD package was beneath the sea-surface after activation of the pump. The maximum number was set to be the end time when the depth of the package was 1 dbar below the surface. The minimum and maximum numbers were automatically calculated in the module.

LOOPEDIT marked scans where the CTD was moving less than the minimum velocity of 0.0 m/s (traveling backwards due to ship roll).

DESPIKE (original module) removed spikes of the data. A median and mean absolute deviation was calculated in 1-dbar pressure bins for both down and up cast, excluding the flagged values. Values greater than 4 mean absolute deviations from the median were marked bad for each bin. This process was performed twice for temperature, conductivity, SBE 43, and RINKOIII output.

DERIVE was used to compute dissolved oxygen (SBE43), salinity, potential temperature, and sigma-theta.

BINAVG averaged the data into 1 decibar pressure bins and 1 sec time bins.

BOTTOMCUT (original module) deleted the deepest pressure bin when the averaged scan number of the deepest bin was smaller than the average scan number of the bin just above.

SPLIT was used to split data into down cast and up cast.

#### (6) Station list

During the MR23-05 Leg1 cruise, 12 casts of CTD were carried out. Date, time and locations of the CTD casts are listed in Table 3.4-1.

#### (7) Preliminary Results

During the cruise, we judged presence or absence of noise, spike or shift in the obtained hydro-cast data.

Definitions of these problems are as follows.

- 1) noise: not singly but continuously detected outliers.
- 2) spike: one-off outlier which is detected after data processing and is oceanographically impossible.
- 3) shift: continuous data under trend to collect values deviated from accurate ones.

The detailed information above these irregularities is recorded in remarks sheet of data submission.

#### (8) Data archive

These data obtained in this cruise will be submitted to the Data Management Group of JAMSTEC, and will be opened to the public via “Data Research System for Whole Cruise Information in JAMSTEC (DARWIN)” in JAMSTEC web site.

Table 3.4-1 MR23-05 Leg1 CTD cast table

MR23-05 CTD cast table													
Stnno	Castno	Date(UTC)	Time(UTC)		BottomPosition		Depth (m)	Wire Out (m)	HT Above Bottom (m)	Max Depth	Max Pressure	CTD Filename	Remark
		(mmddyy)	Start	End	Latitude	Longitude							
001	001	062923	22:05	23:00	32-27.43N	144-31.96E	5760.0	493.9	-	496.9	501.0	001M001	
001	002	063023	01:34	05:30	32-27.37N	144-31.60E	5770.0	5747.7	9.0	5750.4	5870.0	001M002	
002	001	070123	23:05	00:01	24-59.98N	144-59.98E	5056.0	494.3	-	496.2	500.0	002M001	
002	002	070223	02:03	05:23	24-59.89N	145-00.06E	5058.0	5043.7	9.7	5042.4	5136.0	002M002	
003	001	070523	04:13	07:31	13-07.52N	136-53.11E	5157.0	5135.8	8.9	5136.1	5229.0	003M001	
003	002	070523	23:05	23:58	13-00.00N	136-59.86E	4942.0	495.8	-	496.5	500.0	003M002	
003	003	070723	05:36	05:56	12-53.73N	136-54.70E	5250.0	496.1	-	497.5	501.0	003M003	
003	004	070923	23:05	23:51	13-30.86N	137-03.03E	5098.0	245.9	-	249.4	251.0	003M004	
004	001	071023	23:34	00:36	13-10.23N	135-43.09E	4903.0	495.6	-	498.5	502.0	004M001	
005	001	071123	23:05	23:59	09-49.76N	134-51.64E	4298.0	496.3	-	498.6	502.0	005M001	
006	001	071623	23:07	23:30	21-59.95N	136-27.95E	4692.0	495.8	-	498.3	502.0	006M001	
007	001	071723	05:01	05:22	22-59.92N	136-37.42E	4827.0	498.0	-	498.2	502.0	007M001	

### 3.5 Water sampling

#### 3.5.1. Salinity

Kazuhiko MATSUMOTO (JAMSTEC) - Principal investigator  
Nagisa FUJIKI (MWJ) - Operation leader

##### (1) Objective

To provide calibrations for the measurements of salinity collected from CTD casts, bucket sampling, Marine Snow Catcher and underway surface water monitoring system.

##### (2) Parameters

Salinity

##### (3) Instruments and methods

###### *a. Sampling*

Seawater samples were collected with 12-liter water sampling bottles, Marine Snow Catcher (large and small) and underway surface water monitoring system. The salinity sample bottle of the 250-ml brown glass bottle with screw cap was used for collecting the sample water. Each bottle was rinsed 3 times with the sample water, and was filled with sample water to the bottle shoulder. The salinity sample bottles for underway surface water monitoring system samples were sealed with a plastic septum and screw cap because we took into consideration the possibility of storage for about one month. The caps were rinsed 3 times with the sample seawater before its use. Each bottle was stored for more than 24 hours in the laboratory before the salinity measurement.

The kind and number of samples taken are shown as follows ;

Table 3.5.1-1. Kind and number of samples

Kind of Samples	Number of Samples
Samples for CTD (001M001, 001M002, 002M001, 002M002, 003M001, 003M002, 003M004, 004M001, 005M001)	182
Samples for underway surface water monitoring system	20
Sample for Marine Snow Catcher	6
Total	208

###### *b. Instruments and Method*

The salinity analysis was carried out on the R/V MIRAI during the cruise of MR23-05 Leg1 using the salinometer (Model 8400B “AUTOSAL” ; Guildline Instruments Ltd.: S/N 62556) with an additional peristaltic-type intake pump (Ocean Scientific International, Ltd.). A pair of precision digital thermometers (1502A; FLUKE: S/N B78466 and B81549) were used for monitoring the ambient temperature and the bath temperature of the salinometer.

The specifications of the AUTOSAL salinometer and thermometer are shown as follows:

Salinometer (Model 8400B “AUTOSAL” ; Guildline Instruments Ltd.)

Measurement Range : 0.005 to 42 (PSU)  
 Accuracy : Better than  $\pm 0.002$  (PSU) over 24 hours  
 Maximum Resolution : Better than  $\pm 0.0002$  (PSU) at 35 (PSU)

Thermometer (1502A: FLUKE)

Measurement Range : 16 to 30 deg C (Full accuracy)  
 Resolution : 0.001 degC  
 Accuracy : 0.006 degC (@ 0 degC)

The measurement system was almost the same as Aoyama *et al.* (2002). The salinometer was operated in the air-conditioned ship's laboratory at a bath temperature of 24 degC. The ambient temperature varied from approximately 22 degC to 24 degC, while the bath temperature was very stable and varied within  $\pm 0.002$  degC on rare occasion. The measurement for each sample was done with a double conductivity ratio and defined as the median of 34 readings of the salinometer. (Acquisition of the 34 readings took about 11 seconds when the function dial was turned to the ‘read’ setting) Data were taken after rinsed 5 times with the sample water. The double conductivity ratio of sample was calculated from average value of two measurements. And it was used to calculate the bottle salinity with the algorithm for the practical salinity scale, 1978 (UNESCO, 1981). In the case of the difference between the double conductivity ratio of these two measurements being greater than or equal to 0.00003, continue to be measured up to 3 times. The difference between the double conductivity ratio of these two measurements being smaller than 0.00002 were selected. The measurement was conducted in about 8 hours per day and the cell was cleaned with neutral detergent after the measurement of the day.

#### (4) Preliminary results

##### a. Standard Seawater

Standardization control of the salinometer was set to 600 (July 3). The value of STANDBY was 24+5127 – 5129 and that of ZERO was 0.0 $\pm$ 0000 – –0001. The IAPSO Standard Seawater (SSW) batch P166 was used as the standard for salinity. 11 bottles of P166 were measured.

Figure 3.5.1-1 shows the time series of the double conductivity ratio of the Standard Seawater batch P165. The average of the double conductivity ratio was 1.99971 and the standard deviation was 0.00003 which is equivalent to 0.0002 in salinity.

The specifications of SSW batch P166 used in this cruise are shown as follows:

Batch : P166  
 Conductivity ratio : 0.99987  
 Salinity : 34.995  
 Use by : April 6, 2025

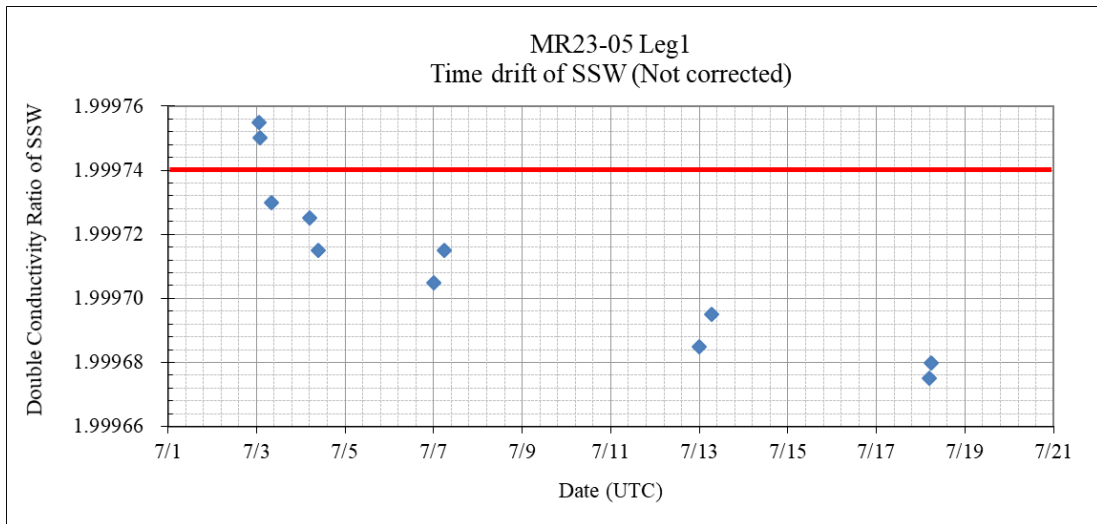


Figure 3.5.1-1: Time series of double conductivity ratio for the Standard Seawater (before correction)

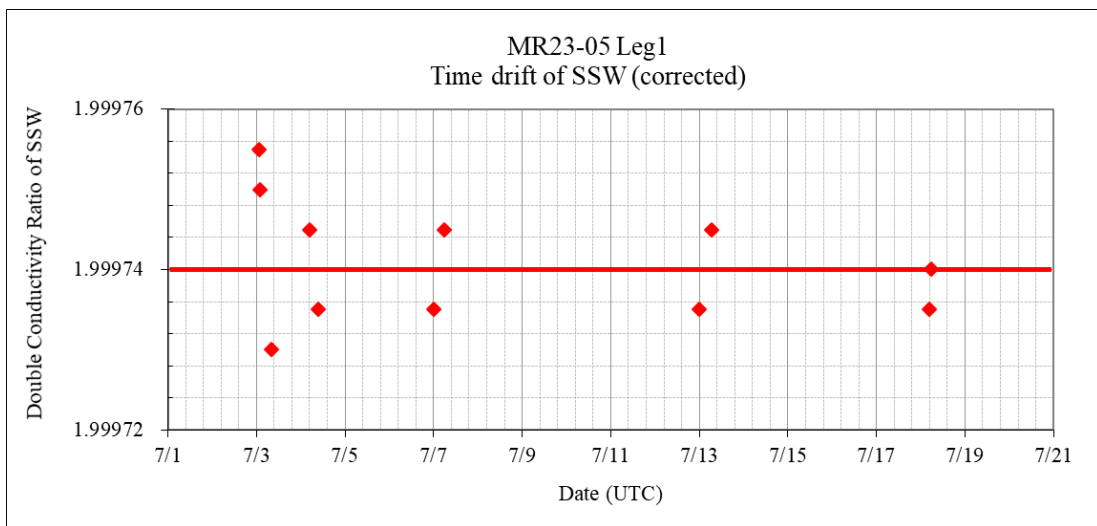


Figure 3.5.1-2: Time series of double conductivity ratio for the Standard Seawater (after correction)

*b. Sub-Standard Seawater*

Sub-standard seawater was made from surface sea water filtered by a pore size of 0.2 micrometer and stored in a 20-liter container made of polyethylene and stirred for at least 24 hours before measuring. It was measured about every about 10 samples in order to check for the possible sudden drifts of the salinometer.

*c. Replicate Samples*

We estimated the precision of this method using 17 pairs of replicate samples taken from the same water sampling bottle. Figure 3.5.1-3 shows the histogram of the absolute difference between each pair of the replicate samples. The average and the standard deviation of absolute difference among 17 pairs of replicate samples were 0.0004 and 0.0004 in salinity, respectively.

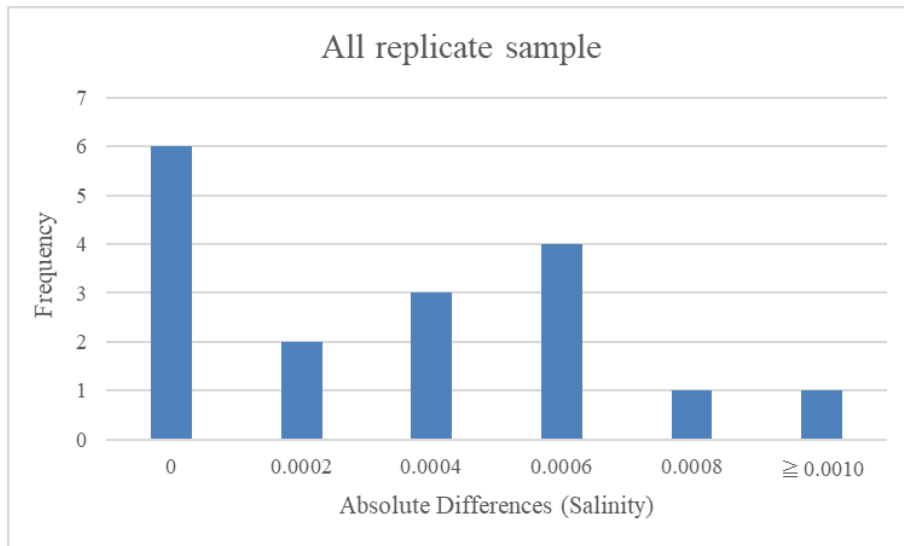


Figure 3.5.1-3 The histogram of the salinity for the absolute difference of all replicate samples

(5) Data archive

These data obtained in this cruise will be submitted to the Data Management Group of JAMSTEC, and will be opened to the public via “Data Research System for Whole Cruise Information in JAMSTEC (DARWIN)” in JAMSTEC web site.

<<http://www.godac.jamstec.go.jp/darwin/e>>

(6) Reference

Aoyama, M., T. Joyce, T. Kawano and Y. Takatsuki: Standard seawater comparison up to P129. Deep-Sea Research, I, Vol. 49, 1103–1114, 2002

UNESCO: Tenth report of the Joint Panel on Oceanographic Tables and Standards. UNESCO Tech. Papers in Mar. Sci., 36, 25 pp., 1981

### 3.5.2 Dissolved oxygen concentration

Kazuhiko MATSUMOTO (JAMSTEC) - Principal Investigator  
Katsunori SAGISHIMA (MWJ) - Operation Leader  
Misato KUWAHARA (MWJ)

#### (1) Objective

Determination of dissolved oxygen in seawater by Winkler titration.

#### (2) Parameters

Dissolved oxygen concentration

#### (3) Instruments and methods

Following procedure is based on Winkler method (Dickson, 1996; Culbertson, 1991).

##### a. Instruments

Burette for sodium thiosulfate and potassium iodate;  
Automatic piston burette (APB-510 / APB-620) manufactured by Kyoto Electronics Manufacturing Co., Ltd. / 10 cm<sup>3</sup> of titration vessel  
Detector;  
Automatic photometric titrator (DOT-15X) manufactured by Kimoto Electric Co., Ltd.  
Software;  
DOT\_Terminal Ver. 1.3.1

##### b. Reagents

Pickling Reagent I: Manganese(II) chloride solution (3 mol dm<sup>-3</sup>)  
Pickling Reagent II:  
Sodium hydroxide (8 mol dm<sup>-3</sup>) / Sodium iodide solution (4 mol dm<sup>-3</sup>)  
Sulfuric acid solution (5 mol dm<sup>-3</sup>)  
Sodium thiosulfate (0.025 mol dm<sup>-3</sup>)  
Potassium iodate (0.001667 mol dm<sup>-3</sup>)

##### c. Sampling

Seawater samples were collected with Niskin bottles attached to the CTD/Carousel Water Sampling System (CTD system). Seawater for oxygen measurement was transferred from a bottle to a volume calibrated flask (ca. 100 cm<sup>3</sup>), and three times volume of the flask was overflowed. Temperature was simultaneously measured by a digital thermometer during the overflowing. After transferring the sample, two reagent solutions (Reagent I and II) of 1 cm<sup>3</sup> each were added immediately and a stopper was inserted carefully into the flask. The sample flask was then shaken vigorously to mix the contents and to disperse the precipitate finely throughout. After the precipitate has settled at least halfway down the flask, the flask was shaken again vigorously to disperse the precipitate. Sample flasks containing pickled samples were stored in a laboratory until they were titrated.

#### d. Sample measurement

For more than 2 hours after re-shaking, pickled samples were measured on board. Sulfuric acid solution with its volume of 1 cm<sup>3</sup> and a magnetic stirrer bar were put into the sample flask and the sample was stirred. The samples were titrated by sodium thiosulfate solution whose morality was determined by potassium iodate solution. Temperature of sodium thiosulfate during titration was recorded by a digital thermometer. Dissolved oxygen concentration (μmol kg<sup>-1</sup>) was calculated by using temperature during seawater sampling, CTD-sensor salinity, flask volume, and titrated volume of sodium thiosulfate solution without the blank. During this cruise, 2 sets of the titration apparatus were used.

#### e. Standardization and determination of the blank

Concentration of sodium thiosulfate titrant was determined by potassium iodate solution. Pure potassium iodate was dried in an oven at 130 °C, and 1.7835 g of it was dissolved in deionized water and diluted to final weight of 5 kg in a flask. After 10 cm<sup>3</sup> of the standard potassium iodate solution was added to another flask using a volume-calibrated dispenser, 90 cm<sup>3</sup> of deionized water, 1 cm<sup>3</sup> of sulfuric acid solution, and 1 cm<sup>3</sup> of pickling reagent solution II and I were added in order. Amount of titrated volume of sodium thiosulfate for this diluted standard potassium iodate solution (usually 5 times measurements average) gave the morality of sodium thiosulfate titrant.

The amount of oxygen in the pickling reagents I (1 cm<sup>3</sup>) and II (1 cm<sup>3</sup>) was assumed to be  $7.6 \times 10^{-8}$  mol (Murray et al., 1968). The blank due to other than oxygen was determined as follows. First, 1 and 2 cm<sup>3</sup> of the standard potassium iodate solution were added to each flask using a calibrated dispenser. Then, 100 cm<sup>3</sup> of deionized water, 1 cm<sup>3</sup> of sulfuric acid solution, 1 cm<sup>3</sup> of pickling II reagent solution, and same volume of pickling I reagent solution were added into the flask in order. The blank was determined by difference between the first (1 cm<sup>3</sup> of potassium iodate) titrated volume of the sodium thiosulfate and the second (2 cm<sup>3</sup> of potassium iodate) one. The titrations were conducted for 3 times and their average was used as the blank value.

#### (4) Observation log

##### a. Standardization and determination of the blank

Table 3.5.2-1 shows results of the standardization and the blank determination during this cruise.

Table 3.5.2-1 Results of the standardization and the blank determinations during cruise

Date (yyyy/mm/ dd)	Potassium iodate ID	Sodium thiosulfate ID	DOT-15X (No.9)		DOT-15X (No.10)		Stations
			E.P. (cm <sup>3</sup> )	Blank (cm <sup>3</sup> )	E.P. (cm <sup>3</sup> )	Blank (cm <sup>3</sup> )	
2023/07/1	K22C06	T-22B	3.992	0.003	3.988	-0.001	C001M001, C001M002, C002M001, C002M002 C003M001, C003M002,
2023/7/7	K22C07	T-22B	3.991	0.000	3.989	-0.001	C003M004 C004M001, C005M001
2023/7/16	K22C08	T-22B	3.992	0.002	3.989	-0.001	

b. Repeatability of sample measurement

Replicate samples were taken at every CTD cast. The standard deviation of the replicate measurement (Dickson et al., 2007) was 0.11  $\mu\text{mol kg}^{-1}$  (n=17).

(5) Data archives

These data obtained in this cruise will be submitted to the Data Management Group (DMG) of JAMSTEC, and will be opened to the public via “Data Research System for Whole Cruise Information in JAMSTEC (DARWIN)” in JAMSTEC web site.

<<http://www.godac.jamstec.go.jp/darwin/e/>>

(6) References

Culberson, C. H. (1991). *Dissolved Oxygen*. WHP O Publication 91-1.

Dickson, A. G. (1996). Determination of dissolved oxygen in sea water by Winkler titration. In *WOCE Operations Manual*, Part 3.1.3 Operations & Methods, WHP Office Report WHP O 91-1.

Dickson, A. G., Sabine, C. L., & Christian, J. R. (Eds.), (2007). *Guide to best practices for ocean CO<sub>2</sub> measurements*, PICES Special Publication 3: North Pacific Marine Science Organization.

Murray, C. N., Riley, J. P., & Wilson, T. R. S. (1968). The solubility of oxygen in Winkler reagents used for the determination of dissolved oxygen. *Deep Sea Res.*, 15, 237-238.

### 3.5.3 Nutrients

Kazuhiko MATSUMOTO	(JAMSTEC)	- Principal investigator
Masahide WAKITA	(JAMSTEC)	
Yuko MIYOSHI	(MWJ)	- Operation leader
Shiori ARIGA	(MWJ)	

#### (1) Objectives

The objective of this document is to show the present status of the nutrient concentrations during the R/V MIRAI MR23-05Leg1 cruise (EXPOCODE: 49NZ20230628) in the Pacific Ocean, and then evaluate the comparability of this obtained data set during this cruise using the certified reference materials of the nutrients in seawater.

#### (2) Parameters

The parameters are nitrate, nitrite, silicate, phosphate and ammonia in seawater.

#### (3) Instruments and methods

##### (3.1) Analytical detail using QuAAtro 39-J systems (BL TEC K.K.)

The analytical platform was replaced from QuAAtro 2-HR to QuAAtro 39 in March 2021. However, since this replacement, the several issues for the QuAAtro 39 system were reported (e.g., unexpected drift issue for the phosphate and the silicate determinations, unusual damage pump cover, see previous cruise report MR21-05C). In July 2022, in order to improve those issue and the analytical precisions, (1) their pumps were replaced from the 13-tube pump (model number: 166+B214-01, BL TEC K.K.) to the 14-tube pump (model number: TRA+B014-02, BL TEC K.K.), (2) their motor brackets were replaced to the new type that is a stainless model (model number: Motor-Bracket-01-Rev-1 and Motor-Bracket-02-Rev-1, BL TEC K.K.), and (3) their light source units were fixed firmly in order to reduce vibration. This modified system now calls “QuAAtro 39-J”.

Nitrate + nitrite and nitrite were analyzed by the following methodology that was modified from the original method of Grasshoff (1976). The flow diagrams were shown in Figure 3.5.3-1 for nitrate + nitrite and Figure 3.5.3-2 for nitrite. For the nitrate + nitrite analysis, the sample were mixed with the alkaline buffer (Imidazole) and then the mixture was pushed through a cadmium coil which was coated with a metallic copper. This step was conducted due to reduce from nitrate to nitrite in the sample, which allowed us to determine nitrate + nitrite in the seawater sample. For the nitrite analysis, the sample was mixed with reagents without this reduction step. In the flow system, seawater sample with or without the reduction step was mixed with an acidic sulfanilamide reagent through a mixing coil to produce a diazonium ion. And then, the mixture was mixed with the N-1-naphthylethylenediamine dihydrochloride (NED) to produce a red azo dye. The azo dye compound was injected into the spectrophotometric detection to monitor the signal at 545 nm. Thus, for the nitrite analysis, sample was determined without passing through the Cd coil. Nitrate was computed by the difference between nitrate+nitrite concentration and nitrite concentration.

The silicate method is analogous to that described for phosphate (see below). The method is essentially that of Grasshoff et al. (1999). The flow diagrams were shown in Figure 3.5.3-3. Silicomolybdic acid compound was first formed by mixing silicate in the sample with the molybdic acid. The silicomolybdic acid compound was then reduced to silicomolybdous acid,

"molybdenum blue," using L-ascorbic acid as the reductant. And then the signal was monitored at 630 nm.

The methodology for the phosphate analysis is a modified procedure of Murphy and Riley (1962). The flow diagrams were shown in Figure 3.5.3-4. Molybdic acid was added to the seawater sample to form the phosphomolybdic acid compound, and then it was reduced to phosphomolybdous acid compound using L-ascorbic acid as the reductant. And then the signal was monitored at 880 nm.

The ammonia in seawater was determined using the flow diagrams shown in Fig. 3.5.3-5. Sample was mixed with an alkaline solution containing EDTA, which ammonia as gas state was formed from seawater. The ammonia (gas) is absorbed in a sulfuric acid by way of 0.5  $\mu\text{m}$  pore size membrane filter (ADVANTEC PTFE) at the dialyzer attached to the analytical system. And then the ammonia absorbed in sulfuric acid was determined by coupling with phenol and hypochlorite to form indophenols blue, and the signal was determined at 630 nm.

The details of a modification of analytical methods for four parameters, nitrate, nitrite, silicate and phosphate, are also compatible with the methods described in nutrients section in the new GO-SHIP repeat hydrography nutrients manual (Becker et al., 2019). This manual is a revised version of the GO-SHIP repeat hydrography nutrients manual (Hydes et al., 2010). The analytical method of ammonium is compatible with the determination of ammonia in seawater using a vaporization membrane permeability method (Kimura, 2000).

### (3.2) Nitrate + Nitrite reagents

#### 50 % Triton solution

50 mL of Triton<sup>TM</sup> X-100 (CAS No. 9002-93-1) were mixed with 50 mL of ethanol (99.5 %).

#### Imidazole (buffer), 0.06 M (0.4 % w/v)

Dissolved 4 g of the imidazole (CAS No. 288-32-4) in 1000 mL ultra-pure water, and then added 2 mL of the hydrogen chloride (CAS No. 7647-01-0). After mixing, 1 mL of the 50 % triton solution was added.

#### Sulfanilamide, 0.06 M (1 % w/v) in 1.2 M HCl

Dissolved 10 g of 4-aminobenzenesulfonamide (CAS No. 63-74-1) in 900 mL of ultra-pure water, and then add 100 mL of the hydrogen chloride (CAS No. 7647-01-0). After mixing, 2 mL of the 50 % triton solution was added.

#### NED, 0.004 M (0.1 % w/v)

Dissolved 1 g of N-(1-naphthalenyl)-1,2-ethanediamine dihydrochloride (CAS No. 1465-25-4) in 1000 mL of ultra-pure water and then added 10 mL of hydrogen chloride (CAS No. 7647-01-0). After mixing, 1 mL 50 % of the Triton solution was added. This reagent was stored in a dark bottle.

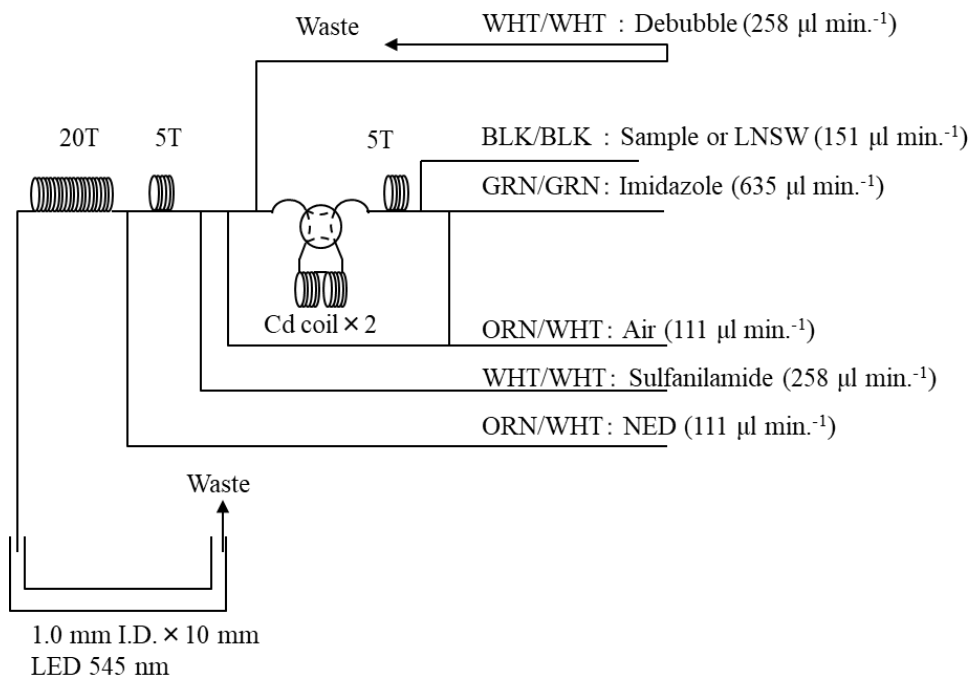


Figure 3.5.3-1 NO<sub>3</sub>+NO<sub>2</sub> (1ch.) flow diagram.

### (3.3) Nitrite reagents

#### 50 % Triton solution

50 mL of the Triton™ X-100 (CAS No. 9002-93-1) were mixed with 50 mL ethanol (99.5 %).

#### Sulfanilamide, 0.06 M (1 % w/v) in 1.2 M HCl

Dissolved 10 g of 4-aminobenzenesulfonamide (CAS No. 63-74-1) in 900 mL of ultra-pure water, and then added 100 mL of hydrogen chloride (CAS No. 7647-01-0). After mixing, 2 mL of the 50 % triton solution were added.

#### NED, 0.004 M (0.1 % w/v)

Dissolved 1 g of N-(1-naphthalenyl)-1,2-ethanediamine dihydrochloride (CAS No. 1465-25-4) in 1000 mL of ultra-pure water and then added 10 mL of hydrogen chloride (CAS No. 7647-01-0). After mixing, 1 mL of the 50 % triton solution was added. This reagent was stored in a dark bottle.



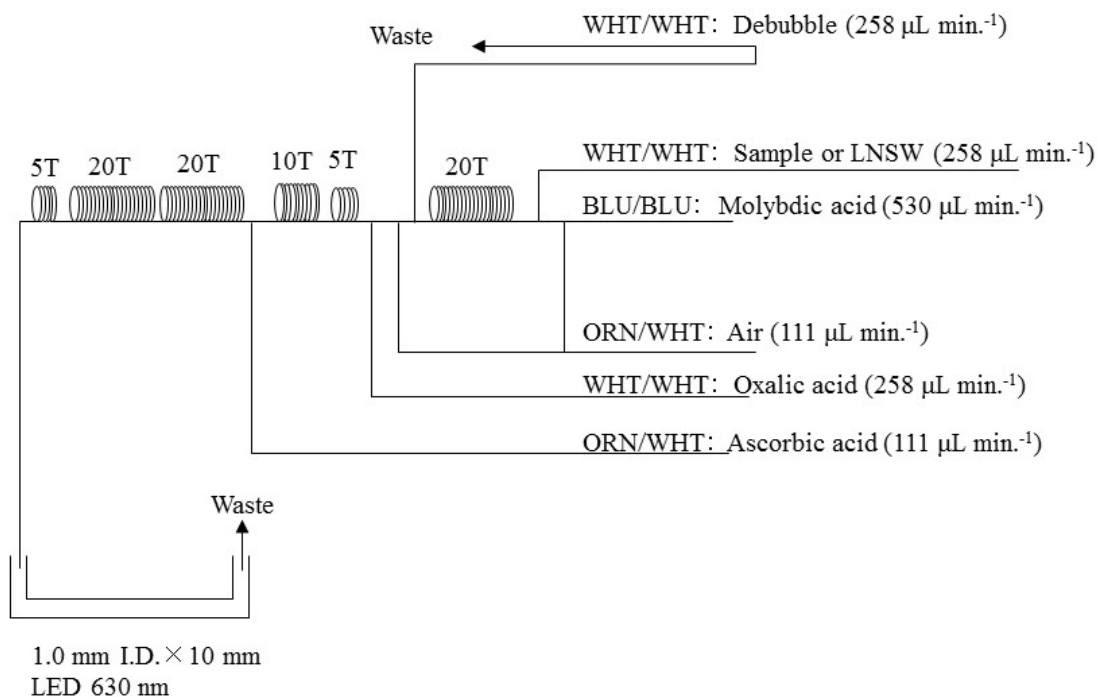


Figure 3.5.3-3  $\text{SiO}_2$  (3ch.) flow diagram.

### (3.5) Phosphate reagents

#### 15 % Sodium dodecyl sulfate solution

Seventy-five grams of sodium dodecyl sulfate (CAS No. 151-21-3) were mixed with 425 mL of ultra-pure water.

#### Stock molybdate solution, 0.03 M (0.8 % w/v)

Dissolved 8 g of sodium molybdate dihydrate (CAS No. 10102-40-6) and 0.17 g of antimony potassium tartrate trihydrate (CAS No. 28300-74-5) in 950 mL of ultra-pure water, and then added 50 mL of sulfuric acid (CAS No. 7664-93-9).

#### $\text{PO}_4$ color reagent

Dissolved 1.2 g of L-ascorbic acid (CAS No. 50-81-7) in 150 mL of the stock molybdate solution. After mixing, 3 mL of the 15 % sodium dodecyl sulfate solution was added. This reagent was freshly prepared before every measurement.

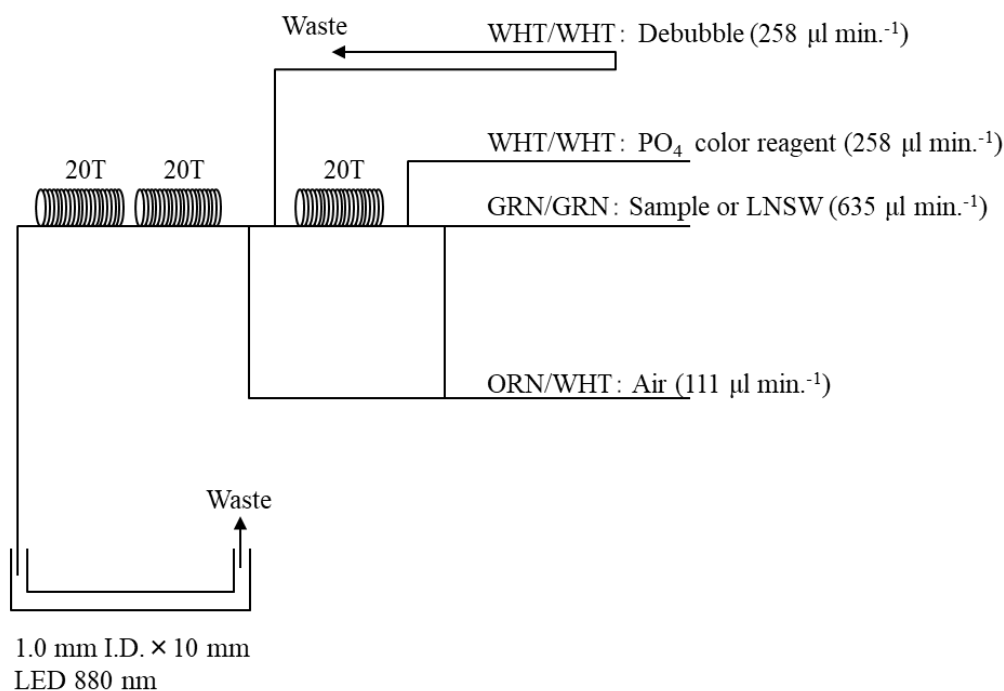


Figure 3.5.3-4 PO<sub>4</sub> (4ch.) flow diagram.

### (3.6) Ammonia reagents

#### 30 % Triton solution

Thirty milli-liters of a Triton™ X-100 (CAS No. 9002-93-1) were mixed with 70 mL ultra-pure water.

#### EDTA

Dissolved 41 g of a tetrasodium; 2-[2-[bis(carboxylatomethyl)amino]ethyl-(carboxylatomethyl)amino]acetate;tetrahydrate (CAS No. 13235-36-4) and 2 g of a boric acid (CAS No. 10043-35-3) in 200 mL of ultra-pure water. After mixing, a 1 mL of the 30 % triton solution was added. This reagent is prepared every week.

#### NaOH liquid

Dissolved 1.5 g of a sodium hydroxide (CAS No. 1310-73-2) and 16 g of a tetrasodium; 2-[2-[bis(carboxylatomethyl) amino]ethyl - (carboxylatomethyl) amino]acetate; tetrahydrate (CAS No. 13235-36-4) in 100 mL of ultra-pure water. This reagent was prepared every week. Note that we reduced the amount of a sodium hydroxide from 5 g to 1.5 g because pH of C standard solutions has been lowered 1 pH unit due to the change of recipe of B standards solution (the detailed of those standard solution, see 7.2.4).

#### Stock nitroprusside

Dissolved 0.25 g of a sodium nitroferricyanide dihydrate (CAS No. 13755-38-9) in 100 mL of ultra-pure water, and then added 0.2 mL of a 1M sulfuric acid. Stored in a dark bottle and prepared every month.

### Nitroprusside solution

Added 4 mL of the stock nitroprusside and 4 mL of a 1M sulfuric acid in 500 mL of ultra-pure water. After mixing, 2 mL of the 30 % triton solution was added. This reagent was stored in a dark bottle and prepared every 2 or 3 days.

### Alkaline phenol

Dissolved 10 g of a phenol (CAS No. 108-95-2), 5 g of a sodium hydroxide (CAS No. 1310-73-2) and 2 g of a sodium citrate dihydrate (CAS No. 6132-04-3) in 200 mL of ultra-pure water. Stored in a dark bottle and prepared every week.

### NaClO solution

Mixed 3 mL of a sodium hypochlorite (CAS No. 7681-52-9) in 47 mL of ultra-pure water. Stored in a dark bottle and freshly prepared before every measurement. This reagent need be 0.3 % available chlorine.

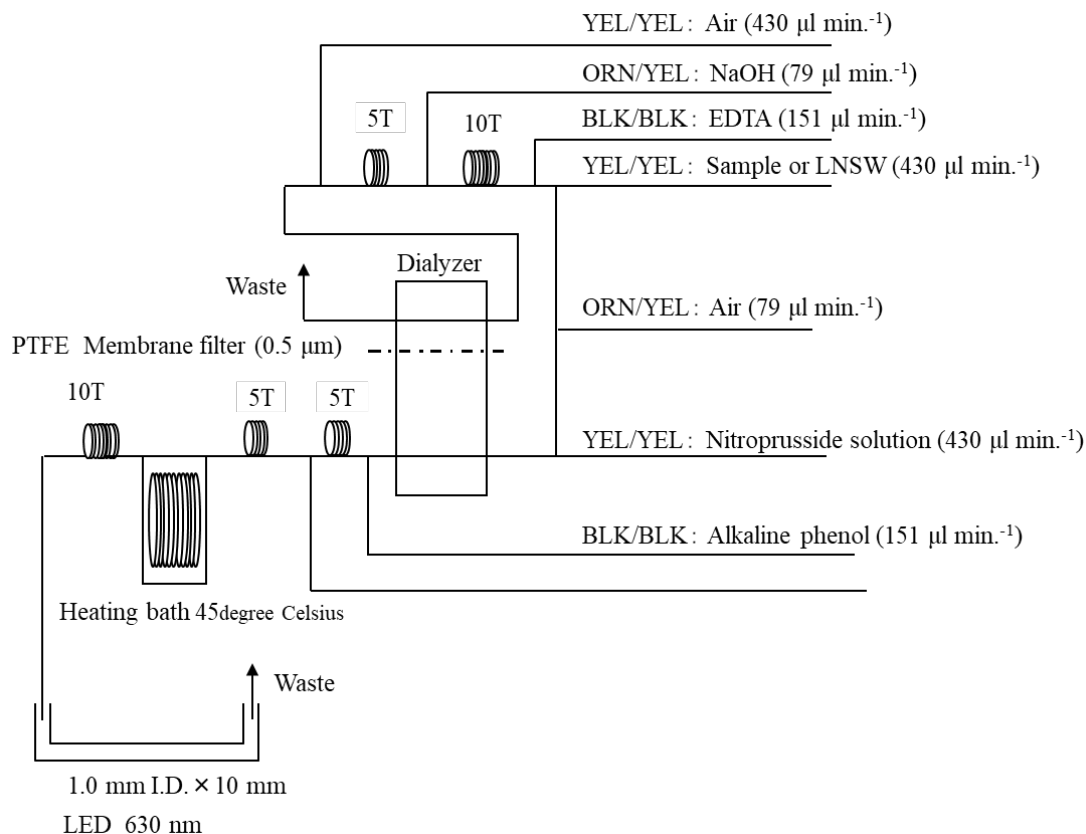


Figure 3.5.3-5 NH<sub>4</sub> (5ch.) flow diagram.

### (3.7) Sampling procedures

Sampling for the nutrient samples was conducted right after the sampling for other parameters (oxygen, trace gases and salinity). Samples were collected into two new 10 mL polyacrylates vials without any sample drawing tube that usually used for the oxygen samples. Each vial was rinsed three times before filling and then was sealed without any head-space immediately after the

collection. The vials were put into a water bath that was adjusted to the ambient temperature at  $19.8 \pm 0.2$  degree Celsius, for more than 30 minutes to keep the constant temperature of samples before measuring.

No transfer from the vial to another container was made and the vials were placed on an autosampler tray directly. Samples were analyzed within 24 hours after collection.

### (3.8) Data processing

Raw data from QuAAtro 39-J were treated as follows:

- Checked if there were any baseline shift.
- Checked the shape of each peak and positions of peak values. If necessary, a change was made for the positions of peak values.
- Conducted carry-over correction and baseline drift correction followed by sensitivity correction to apply to the peak height of each sample.
- Conducted baseline correction and sensitivity correction using the linear regression.
- Using the salinity (determined on the ship) and the laboratory room temperature (20 degree Celsius), the density of each sample was calculated. The obtained density was used to calculate the final nutrient concentration with the unit of  $\mu\text{mol kg}^{-1}$ .
- Calibration curves to obtain the nutrients concentrations were assumed second order equations.

### (3.9) Summary of nutrients analysis

Total of the 9 runs were conducted to obtain the values for the samples that collected by 9 casts at 5 stations during this cruise. The total number of the seawater samples were 165. For each sample depth, the duplicate of each were collected. The sampling locations for the nutrients was shown in Fig. 3.5.3-6.

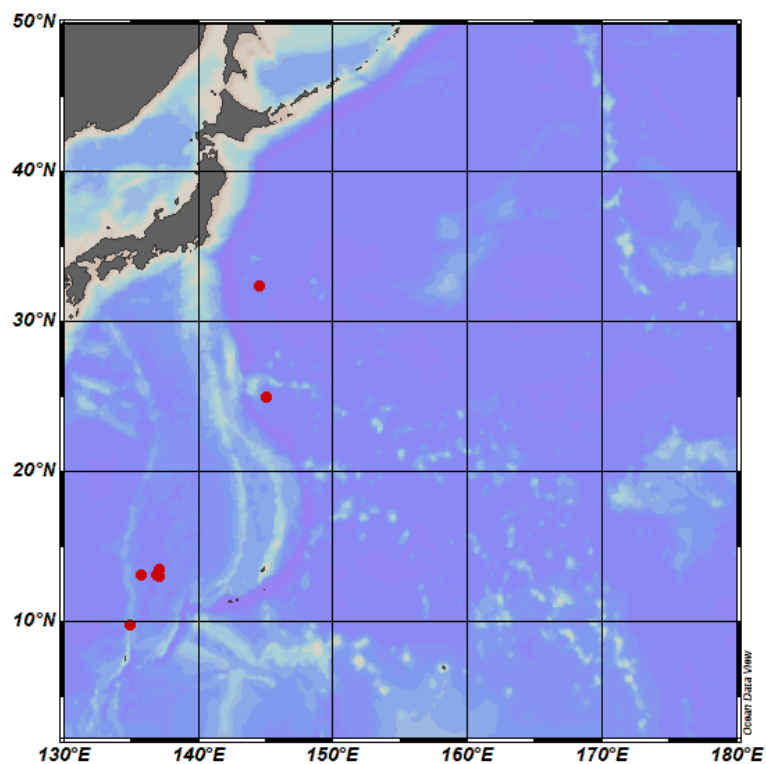


Figure 3.5.3-6 Sampling positions of nutrients sample.

(4) Station list

The sampling stations were listed as shown in Table 3.5.3-1.

Table 3.5.3-1 List of stations

Station	Cast	Date (UTC) (mmddyy)	Position*		Depth (m)
			Latitude	Longitude	
001	1	062923	32-27.44N	144-31.97E	5760
001	2	063023	32-27.37N	144-31.60E	5770
002	1	070123	24-59.98N	144-59.99E	5056
002	2	070223	24-59.90N	145-00.00E	5058
003	1	070523	13-07.52N	136-53.11E	5157
003	2	070523	13-00.08N	136-59.87E	4942
003	4	070923	13-30.87N	137-03.03E	5098
004	1	071023	13-10.24N	135-43.10E	4903
005	1	071123	9.-49.76N	134-51.65E	4298

\* Position indicates latitude and longitude where CTD reached maximum depth at the cast.

#### (5) Certified Reference Material of nutrients in seawater

KANSO certified reference materials (CRMs, Lot: CQ, CR, CO, CM, CN) were used to ensure the comparability and traceability of nutrient measurements during this cruise. The details of CRMs are shown below.

#### Production

KANSO CRMs for inorganic nutrients in seawater were produced by KANSO Co.,Ltd. This CRM has been produced using autoclaved natural seawater based on the quality control system under ISO Guide 34 (JIS Q 0034).

KANSO Co.,Ltd. has been accredited under the Accreditation System of National Institute of Technology and Evaluation (ASNITE) as a CRM producer since 2011. (Accreditation No.: ASNITE 0052 R)

#### Property value assignment

The certified values were the arithmetic means of the results of 30 bottles from each batch (measured in duplicates) analyzed by both KANSO Co.,Ltd. and Japan Agency for Marine-Earth Science and Technology (JAMSTEC) using the colorimetric method (continuous flow analysis, CFA, method). The salinity of the calibration standards solution to obtain each calibration curve was adjusted to the salinity of the used CRMs within  $\pm 0.5$ .

#### Metrological Traceability

Each certified value of nitrate, nitrite, and phosphate of KANSO CRMs were calibrated using one of Japan Calibration Service System (JCSS) standard solutions for each nitrate ions, nitrite ions, and phosphate ions. JCSS standard solutions were calibrated using the secondary solution of JCSS for each of these ions. The secondary solution of JCSS was calibrated using the specified primary solution produced by Chemicals Evaluation and Research Institute (CERI), Japan. CERI specified primary solutions were calibrated using the National Metrology Institute of Japan (NMIJ) primary standards solution of nitrate ions, nitrite ions and phosphate ions, respectively.

For the certified value of silicate of KANSO CRM was calibrated using a newly established silicon standards solution Lot.AA produced by KANSO. This silicon standard solution was produced by a dissolution technique with an alkaline solution. The mass fraction of Si in the produced solution was calibrated based on NMIJ CRM 3645-a03 Si standard solution by a technology consulting system of National Institute of Advanced Industrial Science and Technology (AIST), and this value is traceable to the International System of Units (SI).

The certified values of nitrate, nitrite, and phosphate of KANSO CRM are thus traceable to the SI through the unbroken chain of calibrations, JCSS, CERI and NMIJ solutions as stated above, each having stated uncertainties. The certified values of silicate of KANSO CRM are traceable to the SI through the unbroken chain of calibrations, NMIJ CRM 3645-a03 Si standard solution, having stated uncertainties.

As stated in the certificate of NMIJ CRMs, each certified value of dissolved silica, nitrate ions, and nitrite ions was determined by more than one method using one of NIST SRM of silicon standard solution and NMIJ primary standards solution of nitrate ions and nitrite ions. The concentration of phosphate ions as stated information value in the certificate was determined

NMIJ primary standards solution of phosphate ions. Those values in the certificate of NMIJ CRMs are traceable to the SI.

One of the analytical methods used for certification of NMIJ CRM for nitrate ions, nitrite ions, phosphate ions and dissolved silica was a colorimetric method (continuous mode and batch mode). The colorimetric method is the same as the analytical method (continuous mode only) used for certification of KANSO CRM. For certification of dissolved silica, exclusion chromatography/isotope dilution-inductively coupled plasma mass spectrometry and ion exclusion chromatography with post-column detection was used. For certification of nitrate ions, ion chromatography by direct analysis and ion chromatography after halogen-ion separation was used. For certification of nitrite ions, ion chromatography by direct analysis was used.

NMIJ CRMs were analyzed at the time of certification process for CRM and the results were confirmed within expanded uncertainty stated in the certificate of NMIJ CRMs.

#### (5.1) CRM for this cruise

Ten sets of CRM lots CQ, CR, CO, CM and CN were used, which almost cover a range of nutrients concentrations in the Pacific Ocean.

Each CRM's serial number was randomly selected. The CRM bottles were stored at a room named "BIOCHEMICAL LABORATORY" on the ship, where the temperature was maintained around 17.60 degree Celsius – 22.83 deg C.

#### (5.2) CRM concentration

Nutrients concentrations for the CRM lots CQ, CR, CO, CM and CN were shown in Table 3.5.3-2.

Table 3.5.3-2 Certified concentration and the uncertainty (k=2) of CRMs.

Lot	unit: $\mu\text{mol kg}^{-1}$				
	Nitrate	Nitrite**	Silicate	Phosphate	Ammonia***
CQ	$0.06 \pm 0.03$	$0.074 \pm 0.07$	$2.20 \pm 0.07$	$0.030 \pm 0.009$	$1.76 \pm 0.07$
CR	$5.46 \pm 0.16$	$0.975 \pm 0.07$	$14.0 \pm 0.3$	$0.394 \pm 0.014$	$0.95 \pm 0.15$
CO	$15.86 \pm 0.15$	$0.056 \pm 0.04$	$34.72 \pm 0.16$	$1.177 \pm 0.014$	0.54
CM	$33.2 \pm 0.3$	$0.028 \pm 0.006$	$100.5 \pm 0.5$	$2.38 \pm 0.03$	0.59
CN*	$43.6 \pm 0.4$	$0.020 \pm 0.004$	$152.7 \pm 0.8$	$2.94 \pm 0.03$	0.46

\*Nitrite values of CRM lot CN are below quantifiable detection limit and shown as only reference values.

\*\* For Nitrite concentration, there is a trend that the value has been increased  $0.004 \pm 0.002 \mu\text{mol kg}^{-1}$  per year. Nitrite concentration values were determined by JAMSTEC in June 2023.

\*\*\*Ammonia values are all reference value. The value of CRM lot CQ and CR was reported by KANSO. The other reported values were determined by JAMSTEC.

#### (6) Nutrients standards

##### (6.1) Volumetric laboratory-ware of in-house standards

All volumetric glassware and polymethylpentene (PMP)-ware used were gravimetrically calibrated. Plastic volumetric flasks were gravimetrically calibrated at the water temperature of use within 0.9 K at around 20.6 deg C.

#### (6.1.1) Volumetric flasks

Volumetric flasks of Class quality (Class A) are used because their nominal tolerances are 0.05 % or less over the size ranges likely to be used in this work. Since Class A flasks are made of borosilicate glass, the standard solutions were transferred to plastic bottles as quickly as possible after the solutions were made up to volume and well mixed in order to prevent the excessive dissolution of silicate from the glass. PMP volumetric flasks were gravimetrically calibrated and used only within 1.3 K of the calibration temperature.

The computation of volume contained by the glass flasks at various temperatures other than the calibration temperatures were conducted by using the coefficient of linear expansion of borosilicate crown glass.

The coefficients of cubical expansion of each glass and PMP volumetric flask was determined by actual measurement in 2023. The coefficient of cubical expansion of glass volumetric flask (SHIBATA HARIO) was  $0.0000110 \text{ K}^{-1}$  and that of PMP volumetric flask (NALGEN PMP) was  $0.00038$  to  $0.00042 \text{ K}^{-1}$ . The weights obtained in the calibration weightings were corrected for the density of water and air buoyancy.

#### (6.1.2) Pipettes

All glass pipettes have nominal calibration tolerances of 0.1% or better. These were gravimetrically calibrated to verify and improve upon this nominal tolerance.

### (6.2) Reagents, general considerations

#### (6.2.1) Specifications

For nitrate standard, “potassium nitrate 99.995 suprapur®” provided by Merck, Batch B1983565, CAS No. 7757-79-1, was used.

For nitrite standard solution, we used a nitrite ion standard solution ( $\text{NO}_2^-$  1000) provided by Wako, Lot DLJ3947 and TPH2043, Code. No. 146-06453. This standard solution was certified by Wako using the ion chromatography method. Calibration result is 1002 and 1004  $\text{mg L}^{-1}$  respectively at 20 deg C. Expanded uncertainty of calibration ( $k=2$ ) is 0.8 % for the calibration result.

For the silicate standard solution, we used Si standard solution Lot.AA which was produced by alkali fusion technique from 5N  $\text{SiO}_2$  powder produced by KANSO. The mass fraction of Si in the Lot.AA solution was calibrated based on NMIJ CRM 3645-a03 Si standard solution.

For phosphate standard, we used a potassium dihydrogen phosphate anhydrous 99.995 suprapur®” provided by Merck, Batch B2015508, CAS No.: 7778-77-0, was used.

For ammonia standard, ammonium chloride (CRM 3011-a) provided by NMIJ, CAS No. 12125-02-9 was used. The purity of this standard was reported as > 99.9 % by the manufacture. Expanded uncertainty of calibration ( $k=2$ ) was 0.026 %.

#### (6.2.2) Ultra-pure water

Ultra-pure water (Milli-Q water) freshly drawn was used for the preparation of reagents, standard solutions and for measurements of the reagent and the system blanks.

#### (6.2.3) Low nutrients seawater (LNSW)

Surface water having low nutrient concentration was taken and filtered using 0.20  $\mu\text{m}$  pore

capsule cartridge filter around 17S and 100E during MR19-04 cruise in February 2020. This water was drained into 20 L cubitainers and stored in a cardboard box.

Nutrients concentrations in LNSW were measured on June 2022. The averaged nutrient concentrations in the LNSW were 0.00  $\mu\text{mol L}^{-1}$  for nitrate, 0.00  $\mu\text{mol L}^{-1}$  for nitrite, 1.93  $\mu\text{mol L}^{-1}$  for silicate, 0.076  $\mu\text{mol L}^{-1}$  for phosphate and 0.00  $\mu\text{mol L}^{-1}$  for ammonia. We observed phosphate concentration values were different in each cardboard box, so we measured the values for each box. The phosphate concentration value in the LNSW we used in this cruise was 0.069 to 0.082  $\mu\text{mol L}^{-1}$ . The concentrations of nitrate, nitrite and ammonia were lower than detection limit as stated in section (7.5).

#### (6.2.4) Concentrations of nutrients for A, D, B, and C standards

Concentrations of nutrients for A, D, B and C standards were adjusted as shown in Table 3.5.3-3.

We used KANSO Si standard solution for A standard of silicate, which doesn't need to neutralize by the hydrochloric acid. B standard was diluted from A standard with the following recipes shown in Table 3.5.3-4. In order to match the salinity and the density of the stock solution (B standard) to the LNSW, during this dilution step, 15.30 g of a sodium chloride powder was dissolved in B standard, and then the final volume was adjusted to 500 mL.

The C standard solution was prepared in the LNSW following the recipes shown in Table 3.5.3-5. All volumetric laboratory tools were calibrated prior the cruise as stated in chapter (7.1). Then the actual concentrations of nutrients in each fresh standard solution were calculated based on the solution temperature, together with the determined factors of volumetric laboratory wares.

The calibration curves for each run for nitrate, nitrite, silicate and phosphate were obtained using 6 levels, C-2, C-3, C-4, C-5, C-6 and C-7. For ammonia, that was obtained using 3 levels, C-1, C-5, C-7. C-1 was LNSW, C-2, C-3, C-4 and C-6 were the CRM of nutrients in seawater and C-5 and C-7 were diluting using the B standard solution.

The D standard solutions were made to calculate the reduction rate of Cd coil. The D standard was diluted from the A standard solution into the pure water.

Table 3.5.3-3 Nominal concentrations of nutrients for A, D, B and C standards.

	A	B	D	C-1	C-2	C-3	C-4	C-5	C-6	C-7
$\text{NO}_3$	45000	900	900	-	CQ	CR	CO	27.7	CM	55.5
$\text{NO}_2$	21800	26	870	-	CQ	CR	CO	0.79	CM	1.57
$\text{SiO}_2$	35500	2840		-	CQ	CR	CO	86.2	CM	171
$\text{PO}_4$	6000	60		-	CQ	CR	CO	1.87	CM	3.66
$\text{NH}_4$	4000	40		LNSW	-	-	-	1.21	-	2.41

Table 3.5.3-4 B standard recipes. Final volume was 500 mL.

A Std.	
NO <sub>3</sub>	10 mL
NO <sub>2</sub> *	15 mL
SiO <sub>2</sub>	40 mL
PO <sub>4</sub>	5 mL
NH <sub>4</sub>	5 mL

\*NO<sub>2</sub> was D standard solution which was diluted from A standard.

Table 3.5.3-5 Working calibration standard recipes. Final volume was 500 mL.

C Std.	B Std.
C-5	15 mL
C-7	30 mL

(6.2.5) Renewal of in-house standard solutions

Standard solutions as stated in paragraph (7.2.4) were remade by each “renewal time” shown in Table 3.5.3-6(a) to (c).

Table 3.5.3-6(a) Timing of renewal of standards.

NO <sub>3</sub> , NO <sub>2</sub> , SiO <sub>2</sub> , PO <sub>4</sub> , NH <sub>4</sub>	Renewal time
A-1 Std. (NO <sub>3</sub> )	maximum a month
A-2 Std. (NO <sub>2</sub> )	commercial prepared solution
A-3 Std. (SiO <sub>2</sub> )	commercial prepared solution
A-4 Std. (PO <sub>4</sub> )	maximum a month
A-5 Std. (NH <sub>4</sub> )	maximum a month
D-1 Std.	maximum 8 days
D-2 Std.	maximum 8 days
B Std. (mixture of A-1, D-2, A-3, A-4 and A-5 std.)	maximum 8 days

Table 3.5.3-6(b) Timing of renewal of working calibration standards.

Working standards	Renewal time
C Std. (diluted from B Std.)	every 24 hours

Table 3.5.3-6(c) Timing of renewal of in-house standards for reduction estimation.

Reduction estimation	Renewal time
36 µM NO <sub>3</sub> (diluted D-1 Std.)	when C Std. renewed
35 µM NO <sub>2</sub> (diluted D-2 Std.)	when C Std. renewed

(7) Quality control

(7.1) The precision of the nutrient analyses during the cruise

The highest standard solution (C-7) was repeatedly determined every 4 to 12 samples to obtain

the analytical precision of the nutrient analyses during this cruise. During each run, the total number of the C-7 determination was 8-13 times depending on the run. Each run, we obtained the analytical precision based on this C-7 results. In this cruise, there was total 10 runs. Except for a few runs, the analytical precisions were less than 0.2 % for nitrate, silicate, and phosphate.

The overall precisions throughout this cruise were calculated based on the analytical precisions obtained from all of the runs, and shown in Table 3.5.3-7. During this cruise, overall median precisions were 0.12 % for nitrate, 0.23 % for nitrite, 0.14 % for silicate, 0.17 % for phosphate and 0.48 % for ammonia, respectively. The overall median precision for each parameter during this cruise was comparable to the previously published the precisions during the R/V Mirai cruises conducted in 2009 - 2022.

Table 3.5.3-7 Summary of overall precision based on the replicate analyses ( $k=1$ )

	Nitrate	Nitrite	Silicate	Phosphate	Ammonia
	CV %	CV %	CV %	CV %	CV %
Median	0.12	0.23	0.14	0.17	0.48
Mean	0.12	0.23	0.14	0.17	0.48
Maximum	0.21	0.31	0.18	0.20	0.62
Minimum	0.07	0.10	0.09	0.10	0.31
N	10	10	10	10	10

#### (7.2) CRM lot. CN measurement during this cruise

CRM lot. CN was measured every run to evaluate the comparability throughout the cruise. All of the measured concentrations of CRM lot. CN was within the uncertainty of certified values for nitrate, nitrite, silicate and phosphate shown in Table 3.5.3-8. The reported CRM values were shown in Table 3.5.3-2.

Table 3.5.3-8 Summary of CRM lot. CN measurement

	Nitrate	Nitrite	Silicate	Phosphate	Ammonia
					Unit: $\mu\text{mol kg}^{-1}$
Median	43.62	0.02	152.64	2.932	1.05
Mean	43.60	0.02	152.65	2.931	1.01
STDEV	0.12	0.00	0.32	0.012	0.27
N	10	10	10	10	10

#### (7.3) Carryover

We also summarized the magnitudes of carry over throughout the cruise. In order to evaluate carryover in each run, we conducted determinations of C-7 followed by determination of LNSW twice. The difference from LNSW-1 to LNSW-2 was obtained and used for this “carryover” evaluation. The Carryover (%) was obtained from the following equation.

$$\text{Carryover (\%)} = (\text{LNSW-1} - \text{LNSW-2}) / (\text{C-7} - \text{LNSW-2}) * 100 (\%)$$

The summary of the carryover (%) was shown in Table 3.5.3-9. The results were low % (<0.2 % for nitrate, nitrite and silicate; < 0.3 % for phosphate; < 1 % for ammonia). The low % indicates that there is no significant issue during this cruise.

Table 3.5.3-9 Summary of carryover throughout this cruise.

	Nitrate %	Nitrite %	Silicate %	Phosphate %	Ammonia %
Median	0.19	0.12	0.19	0.20	0.97
Mean	0.19	0.16	0.19	0.20	1.03
Maximum	0.24	0.39	0.22	0.33	1.55
Minimum	0.16	0.00	0.16	0.05	0.65
N	10	10	10	10	10

(7.4) Estimation of uncertainty of nitrate, silicate, phosphate, nitrite and ammonia concentrations

Empirical equations, Eq. (1), (2) and (3) to estimate the uncertainty of measurement of nitrate, silicate and phosphate were obtained based on 22 measurements of 22 sets of CRMs (Table 3.5.3-2) in MR23-05Leg1 and MR23-05Leg2. These empirical equations are as follows, respectively.

Nitrate Concentration  $C_{\text{NO}_3}$  in  $\mu\text{mol kg}^{-1}$ :

$$\text{Uncertainty of measurement of nitrate (\%)} = 0.18966 + 1.3458 * (1 / C_{\text{NO}_3}) \quad \text{--- (1)}$$

where  $C_{\text{NO}_3}$  is nitrate concentration of sample.

Silicate Concentration  $C_{\text{SiO}_2}$  in  $\mu\text{mol kg}^{-1}$ :

$$\text{Uncertainty of measurement of silicate (\%)} = 0.16944 + 3.0370 * (1 / C_{\text{SiO}_2}) \quad \text{--- (2)}$$

where  $C_{\text{SiO}_2}$  is silicate concentration of sample.

Phosphate Concentration  $C_{\text{PO}_4}$  in  $\mu\text{mol kg}^{-1}$ :

$$\text{Uncertainty of measurement of phosphate (\%)} = 0.31322 + 0.18374 * (1 / C_{\text{PO}_4}) + 0.0078893 * (1 / C_{\text{PO}_4}) * (1 / C_{\text{PO}_4}) \quad \text{--- (3)}$$

where  $C_{\text{PO}_4}$  is phosphate concentration of sample.

Empirical equations, Eq. (4) and (5) to estimate the uncertainty of measurement of nitrite and ammonia were obtained based on duplicate measurements of the samples in MR23-05Leg1 and MR23-05Leg2.

Nitrite Concentration  $C_{\text{NO}_2}$  in  $\mu\text{mol kg}^{-1}$ :

$$\text{Uncertainty of measurement of nitrite (\%)} = 3.6616 + 0.16622 * (1 / C_{\text{NO}_2}) \quad \text{--- (4)}$$

where  $C_{\text{NO}_2}$  is nitrite concentration of sample.

Ammonia Concentration  $C_{\text{NH}_4}$  in  $\mu\text{mol kg}^{-1}$ :

$$\text{Uncertainty of measurement of ammonia (\%)} =$$

$$2.0942 + 1.3244 * (1 / C_{\text{NH}_4}) + 0.0018044 * (1 / C_{\text{NH}_4}) * (1 / C_{\text{NH}_4}) \quad \text{--- (5)}$$

where  $C_{\text{NH}_4}$  is ammonia concentration of sample.

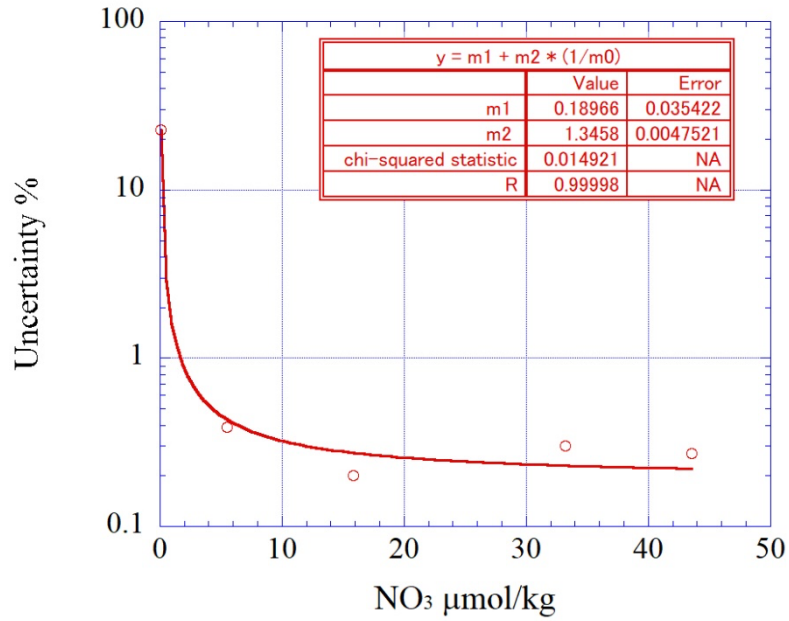


Figure 3.5.3-7 Estimation of uncertainty for nitrate.

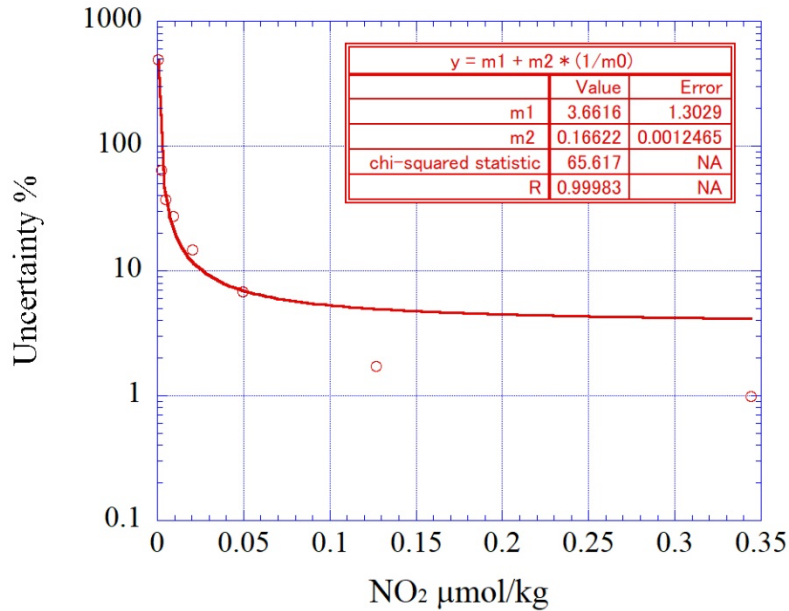


Figure 3.5.3-8 Estimation of uncertainty for nitrite.

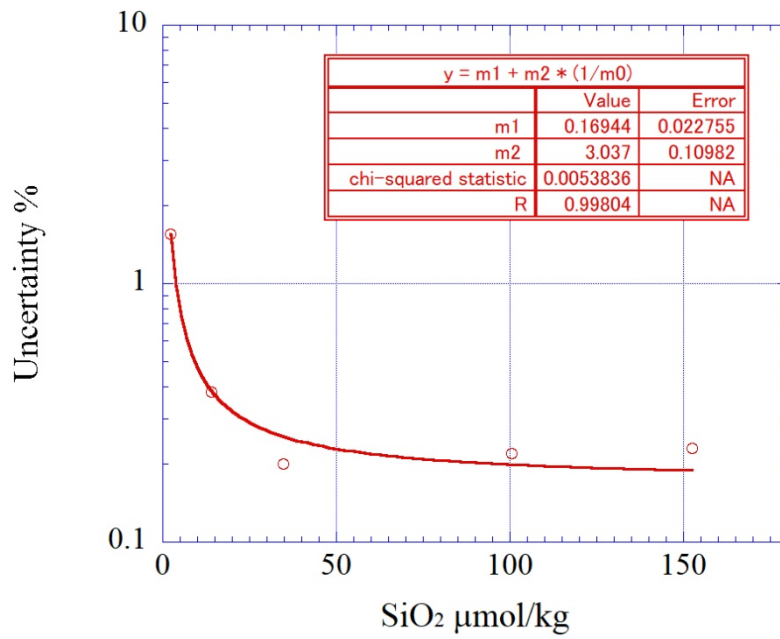


Figure 3.5.3-9 Estimation of uncertainty for silicate.

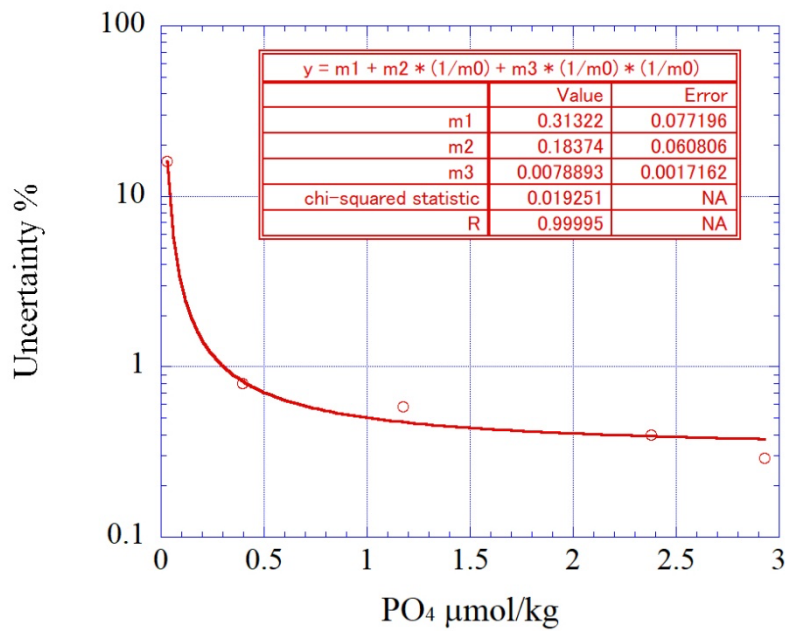


Figure 3.5.3-10 Estimation of uncertainty for phosphate.

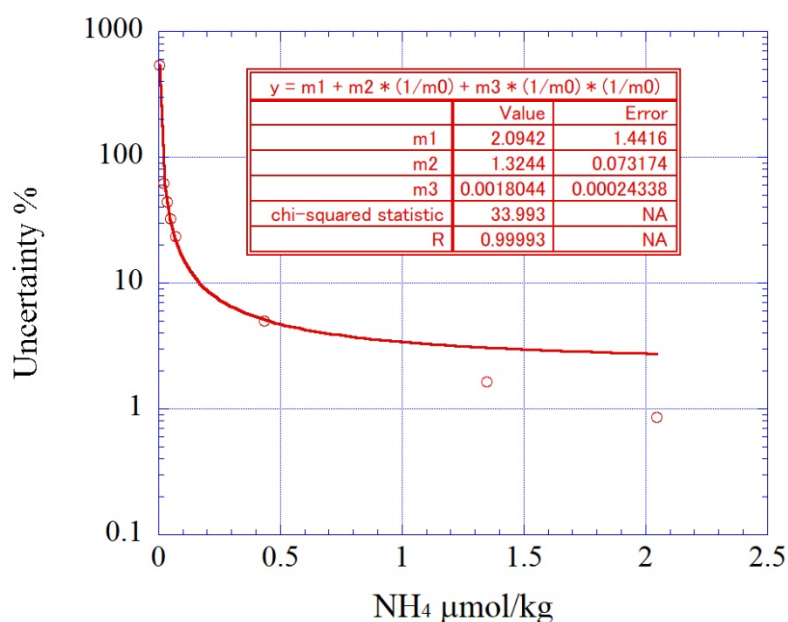


Figure 3.5.3-11 Estimation of uncertainty for ammonia.

#### (7.5) Detection limit and quantitative determination of nutrients analyses during the cruise

The LNSW was determined every 4 to 12 samples to obtain detection limit of the nutrient analyses during this cruise. During each run, the total number of the LNSW determination was 7–12 times depending on the run. The detection limit was calculated based on the LNSW results obtained from all the runs by the following equation.

$$\text{Detection limit} = 3 * \text{standard deviation of repeated measurement of LNSW}$$

The summary of detection limit is shown in Table 3.5.3-10. During in this cruise, detection limit is 0.02  $\mu\text{mol kg}^{-1}$  for nitrate, 0.003  $\mu\text{mol kg}^{-1}$  for nitrite, 0.07  $\mu\text{mol kg}^{-1}$  for silicate, 0.005  $\mu\text{mol kg}^{-1}$  for phosphate and 0.02  $\mu\text{mol kg}^{-1}$  for ammonia, respectively.

The quantitative determination of nutrient analyses is the concentration of which uncertainty is 33 % in the empirical equations, eq. (1) to (5) in chapter (8.4). The summary of quantitative determination is shown in Table 3.5.3-10. During in this cruise, the quantitative determination was 0.04  $\mu\text{mol kg}^{-1}$  for nitrate, 0.010  $\mu\text{mol kg}^{-1}$  for nitrite, 0.09  $\mu\text{mol kg}^{-1}$  for silicate, 0.019  $\mu\text{mol kg}^{-1}$  for phosphate and 0.04  $\mu\text{mol kg}^{-1}$  for ammonia, respectively.

Replicate samples were taken at most of the layers. The summary of average and standard deviation of the difference between each pair of analysis was shown in Table 3.5.3-11. During this cruise, average of the difference between each pair of analyses were 0.03  $\mu\text{mol kg}^{-1}$  for nitrate, 0.003  $\mu\text{mol kg}^{-1}$  for nitrite, 0.12  $\mu\text{mol kg}^{-1}$  for silicate, 0.005  $\mu\text{mol kg}^{-1}$  for phosphate and 0.02  $\mu\text{mol kg}^{-1}$  for ammonia, respectively. Standard deviation of the difference between each pair of analyses were 0.03  $\mu\text{mol kg}^{-1}$  for nitrate, 0.003  $\mu\text{mol kg}^{-1}$  for nitrite, 0.12  $\mu\text{mol kg}^{-1}$  for silicate, 0.004  $\mu\text{mol kg}^{-1}$  for phosphate and 0.01  $\mu\text{mol kg}^{-1}$  for ammonia, respectively.

Table 3.5.3-10 Summary of detection limit and quantitative determination.

	Nitrate $\mu\text{mol kg}^{-1}$	Nitrite $\mu\text{mol kg}^{-1}$	Silicate $\mu\text{mol kg}^{-1}$	Phosphate $\mu\text{mol kg}^{-1}$	Ammonia $\mu\text{mol kg}^{-1}$
Detection limit	0.02	0.003	0.07	0.005	0.02
Quantitative determination	0.04	0.010	0.09	0.019	0.04

Table 3.5.3-11 Summary of average and standard deviation of the difference between each pair of analysis.

	Nitrate $\mu\text{mol kg}^{-1}$	Nitrite $\mu\text{mol kg}^{-1}$	Silicate $\mu\text{mol kg}^{-1}$	Phosphate $\mu\text{mol kg}^{-1}$	Ammonia $\mu\text{mol kg}^{-1}$
Mean	0.03	0.003	0.12	0.005	0.02
STDEV	0.03	0.003	0.12	0.004	0.01
N	160	163	164	156	150

(8) Problems and our actions/solutions

There is no significant issue for this data set.

(9) List of reagents

List of reagents is shown in Table 3.5.3-12.

Table 3.5.3-12 List of reagent used in this cruise.

IUPAC name	CAS Number	Formula	Compound Name	Manufacture	Grade
4-Aminobenzenesulfonamide	63-74-1	C <sub>6</sub> H <sub>8</sub> N <sub>2</sub> O <sub>2</sub> S	Sulfanilamide	FUJIFILM Wako Pure Chemical Corporation	JIS Special Grade
Ammonium chloride	12125-02-9	NH <sub>4</sub> Cl	Ammonium Chloride	FUJIFILM Wako Pure Chemical Corporation	JIS Special Grade
Antimony potassium tartrate trihydrate	28300-74-5	K <sub>2</sub> (SbC <sub>4</sub> H <sub>2</sub> O <sub>6</sub> ) <sub>2</sub> ·3H <sub>2</sub> O	Bis[(+)-tartrato]diantimonate(III) Dipotassium Trihydrate	FUJIFILM Wako Pure Chemical Corporation	JIS Special Grade
Boric acid	10043-35-3	H <sub>3</sub> BO <sub>3</sub>	Boric Acid	FUJIFILM Wako Pure Chemical Corporation	JIS Special Grade
Hydrogen chloride	7647-01-0	HCl	Hydrochloric Acid	FUJIFILM Wako Pure Chemical Corporation	JIS Special Grade
Imidazole	288-32-4	C <sub>3</sub> H <sub>4</sub> N <sub>2</sub>	Imidazole	FUJIFILM Wako Pure Chemical Corporation	JIS Special Grade
L-Ascorbic acid	50-81-7	C <sub>6</sub> H <sub>8</sub> O <sub>6</sub>	L-Ascorbic Acid	FUJIFILM Wako Pure Chemical Corporation	JIS Special Grade
N-(1-Naphthalenyl)-1,2-ethanediamine, dihydrochloride	1465-25-4	C <sub>12</sub> H <sub>16</sub> Cl <sub>2</sub> N <sub>2</sub>	N-1-Naphthylethylenediamine Dihydrochloride	FUJIFILM Wako Pure Chemical Corporation	for Nitrogen Oxides Analysis
Oxalic acid	144-62-7	C <sub>2</sub> H <sub>2</sub> O <sub>4</sub>	Oxalic Acid	FUJIFILM Wako Pure Chemical Corporation	Wako Special Grade
Phenol	108-95-2	C <sub>6</sub> H <sub>6</sub> O	Phenol	FUJIFILM Wako Pure Chemical Corporation	JIS Special Grade
Potassium nitrate	7757-79-1	KNO <sub>3</sub>	Potassium Nitrate	Merck KGaA	Suprapur®
Potassium dihydrogen phosphate	7778-77-0	KH <sub>2</sub> PO <sub>4</sub>	Potassium dihydrogen phosphate anhydrous	Merck KGaA	Suprapur®
Sodium chloride	7647-14-5	NaCl	Sodium Chloride	FUJIFILM Wako Pure Chemical Corporation	TraceSure®
Sodium citrate dihydrate	6132-04-3	Na <sub>3</sub> C <sub>6</sub> H <sub>5</sub> O <sub>7</sub> ·2H <sub>2</sub> O	Trisodium Citrate Dihydrate	FUJIFILM Wako Pure Chemical Corporation	JIS Special Grade
Sodium dodecyl sulfate	151-21-3	C <sub>12</sub> H <sub>25</sub> NaO <sub>4</sub> S	Sodium Dodecyl Sulfate	FUJIFILM Wako Pure Chemical Corporation	for Biochemistry
Sodium hydroxide	1310-73-2	NaOH	Sodium Hydroxide for Nitrogen Compounds Analysis	FUJIFILM Wako Pure Chemical Corporation	for Nitrogen Analysis
Sodium hypochlorite	7681-52-9	NaClO	Sodium Hypochlorite Solution	Kanto Chemical co., Inc.	Extra pure
Sodium molybdate dihydrate	10102-40-6	Na <sub>2</sub> MoO <sub>4</sub> ·2H <sub>2</sub> O	Disodium Molybdate(VI) Dihydrate	FUJIFILM Wako Pure Chemical Corporation	JIS Special Grade
Sodium nitroferrocyanide dihydrate	13755-38-9	Na <sub>2</sub> [Fe(CN) <sub>5</sub> NO]·2H <sub>2</sub> O	Sodium Pentacyanonitrosylferrate(III) Dihydrate	FUJIFILM Wako Pure Chemical Corporation	JIS Special Grade
Sulfuric acid	7664-93-9	H <sub>2</sub> SO <sub>4</sub>	Sulfuric Acid	FUJIFILM Wako Pure Chemical Corporation	JIS Special Grade
tetrasodium,2-[2-[bis(carboxylatomethyl)amino]ethyl-(carboxylatomethyl)amino]acetate;tetrahydrate	13235-36-4	C <sub>10</sub> H <sub>12</sub> N <sub>2</sub> Na <sub>4</sub> O <sub>8</sub> ·4H <sub>2</sub> O	Ethylenediamine-N,N,N',N'-tetraacetic Acid Tetrasodium Salt Tetrahydrate (4NA)	Dojindo Molecular Technologies, Inc.	-
Synonyms: t-Octylphenoxy polyoxyethanol 4-(1,1,3,3-Tetramethylbutyl)phenyl- polyethylene glycol Polyethylene glycol tert-octylphenyl ether	9002-93-1	(C <sub>2</sub> H <sub>4</sub> O) <sub>n</sub> C <sub>14</sub> H <sub>22</sub> O	Triton® X-100	MP Biomedicals, Inc.	-

## (10) Data archives

These data obtained in this cruise will be submitted to the Data Management Group (DMG) of JAMSTEC, and will open to the public via “Data Research System for Whole Cruise Information in JAMSTEC (DARWIN)” in JAMSTEC web site.

<<http://www.godac.jamstec.go.jp/darwin/e>>

## (11) References

- Susan Becker, Michio Aoyama E. Malcolm S. Woodward, Karel Bakker, Stephen Coverly, Claire Mahaffey, Toste Tanhua, (2019) The precise and accurate determination of dissolved inorganic nutrients in seawater, using Continuous Flow Analysis methods, n: The GO-SHIP Repeat Hydrography Manual: A Collection of Expert Reports and Guidelines. Available online at: <http://www.go-ship.org/HydroMan.html>. DOI: <http://dx.doi.org/10.25607/OBP-555>
- Grasshoff, K. 1976. Automated chemical analysis (Chapter 13) in *Methods of Seawater Analysis*. With contribution by Almgreen T., Dawson R., Ehrhardt M., Fonselius S. H., Josefsson B., Koroleff F., Kremling K. Weinheim, New York: Verlag Chemie.
- Grasshoff, K., Kremling K., Ehrhardt, M. et al. 1999. *Methods of Seawater Analysis*. Third, Completely Revised and Extended Edition. WILEY-VCH Verlag GmbH, D-69469 Weinheim (Federal Republic of Germany).
- Hydes, D.J., Aoyama, M., Aminot, A., Bakker, K., Becker, S., Coverly, S., Daniel, A., Dickson, A.G., Grosso, O., Kerouel, R., Ooijen, J. van, Sato, K., Tanhua, T., Woodward, E.M.S., Zhang, J.Z., 2010. Determination of Dissolved Nutrients (N, P, Si) in Seawater with High Precision and Inter-Comparability Using Gas-Segmented Continuous Flow Analysers, In: *GO-SHIP Repeat Hydrography Manual: A Collection of Expert Reports and Guidelines*. IOCCP Report No. 14, ICPO Publication Series No 134.
- Kimura, 2000. Determination of ammonia in seawater using a vaporization membrane permeability method. 7th auto analyzer Study Group, 39-41.
- Murphy, J., and Riley, J.P. 1962. *Analytica Chimica Acta* 27, 31-36.

### 3.5.4 Dissolved inorganic carbon

Kazuhiko MATSUMOTO	(JAMSTEC)	- Principal investigator
Masahiro ORUI	(MWJ)	- Operation leader
Nagisa FUJIKI	(MWJ)	

#### (1) Objective

To discuss CO<sub>2</sub> dynamics in seawater of the western subtropical Pacific, total dissolved inorganic carbon was measured on board during the MR23-05 Leg1 cruise.

#### (2) Methods, Apparatus and Performance

##### (2)-1 Seawater sampling

Seawater samples were collected by 12-liter sampling bottles mounted on the CTD/Carousel Water Sampling System and a bucket at 5 stations. Seawater was sampled in a 250 mL glass bottle (SCHOTT DURAN) that was previously soaked in 5 % alkaline detergent solution (decon 90, Decon Laboratories Limited) at least 3 hours and was cleaned by fresh water for 5 times and Milli-Q deionized water for 3 times. A sampling silicone rubber tube with PFA tip was connected to the sampling bottle when sampling was carried out. The glass bottles were filled from its bottom gently, without rinsing, and were overflowed for 20 seconds. They were sealed using the polyethylene inner lids with its diameter of 29 mm with care not to leave any bubbles in the bottle. Within about one hour after collecting the samples on the deck, the glass bottles were carried to the laboratory to be poisoned. Small volume (3 mL) of the sample (1 % of the bottle volume) was removed from the bottle and 100  $\mu$ L of over saturated solution of mercury (II) chloride was added. Then the samples were sealed by the polyethylene inner lids with its diameter of 31.9 mm and stored in a refrigerator at approximately 5 °C. About one hour before the analysis, the samples were taken from refrigerator and put in the water bath kept about 25 °C.

##### (2)-2 Seawater analysis

Measurements of DIC were made with total CO<sub>2</sub> measuring system (Nihon ANS Inc.). The system comprises of seawater dispensing unit, a CO<sub>2</sub> extraction unit, and a coulometer (Model 3000, Nihon ANS Inc.).

The seawater dispensing unit has an auto-sampler (10 ports), which dispenses the seawater from a glass bottle to a pipette of nominal 15 mL volume. The pipette was kept at 25.00 °C  $\pm$  0.05 °C by a water jacket, in which water circulated through a thermostatic water bath (NESLAB RTE10, Thermo Fisher Scientific).

The CO<sub>2</sub> dissolved in a seawater sample is extracted in a stripping chamber of the CO<sub>2</sub> extraction unit by adding 10 % phosphoric acid solution. The stripping chamber is made approx. 25 cm long and has a fine frit at the bottom. First, a constant volume of acid is added to the stripping chamber from its bottom by pressurizing an acid bottle with nitrogen gas (99.9999 %). Second, a seawater sample kept in a pipette is introduced to the stripping chamber by the same method. The seawater and phosphoric acid are stirred by the nitrogen bubbles through a fine frit at the bottom of the stripping chamber. The stripped CO<sub>2</sub> is carried to the coulometer through two electric dehumidifiers (kept at 2 °C) and a chemical desiccant (magnesium perchlorate) by the nitrogen gas (flow rate of 140 mL min<sup>-1</sup>).

Measurements of system blank (phosphoric acid blank) and seawater samples (6 samples) were programmed to repeat. The variation of our own made JAMSTEC DIC reference material was used to correct the signal drift results from chemical alternation of coulometer solutions.

(3) Preliminary result

A few replicate samples were taken at most of the stations and difference between each pair of analyses was plotted on a range control chart (Fig. 3.5.4-1). The average of the differences was  $1.1 \mu\text{mol kg}^{-1}$ , with its standard deviation of  $1.0 \mu\text{mol kg}^{-1}$  ( $n = 15$ ).

(4) Data archive

These data obtained in this cruise will be submitted to the Data Management Group (DMG) of JAMSTEC, and will open to the public via “Data Research System for Whole Cruise Information in JAMSTEC (DARWIN)” in JAMSTEC web site.

<<http://www.godac.jamstec.go.jp/darwin/e>>

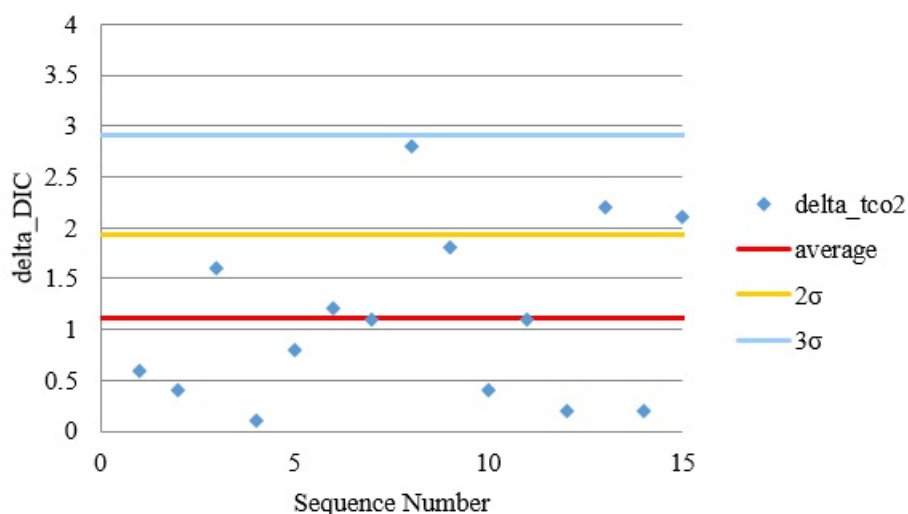


Figure 3.5.4-1 Range control chart of the absolute differences of replicate measurements of DIC carried out during this cruise. AVE represents the average of absolute difference,  $3\sigma$  the upper control limit (standard deviation of  $AVE \times 3$ ), and  $2\sigma$  upper warning limit (standard deviation of  $AVE \times 2$ ).

### 3.5.5 Total alkalinity

Kazuhiko MATSUMOTO	(JAMSTEC)	- Principal Investigator
Nagisa FUJIKI	(MWJ)	- Operation Leader
Masahiro ORUI	(MWJ)	

#### (1) Objective

Concentration of CO<sub>2</sub>, one of the greenhouse gasses, in the atmosphere is now increasing owing to human activities such as burning of fossil fuels. Because the ocean is thought to be a key player to absorb the increased atmospheric CO<sub>2</sub>, to clarify the mechanism of CO<sub>2</sub> absorption and to estimate absorption capacity are important and urgent tasks. Increasing of the CO<sub>2</sub> absorption also causes ocean acidification. When CO<sub>2</sub> dissolves into seawater, chemical reaction takes place and CO<sub>2</sub> alters its appearance into several species. Unfortunately, the concentrations of the individual species of the CO<sub>2</sub> system in seawater cannot be measured directly. There are, however, four parameters that can be measured (i.e., total dissolved inorganic carbon, total alkalinity, pH, and pCO<sub>2</sub>), these are used to obtain description of the CO<sub>2</sub> system in sea water (Dickson et al., 2007). In the MR23-05 Leg1 cruise, total dissolved inorganic carbon and total alkalinity were measured on board. We here report the latter parameter in this section.

#### (2) Methods, Apparatus and Performance

##### (2)-1 Seawater sampling

Seawater samples were collected by 12-liter sampling bottles mounted on the CTD/Carousel Water Sampling System and a bucket at 5 stations. The seawater from the sampling bottle was filled into the 250 mL borosilicate glass bottles (SCHOTT DURAN) using a sampling silicone rubber tube with PFA tip. The water was filled into the bottle from the bottom smoothly, without rinsing, and overflowed for 2 times bottle volume (20 seconds). These bottles were pre-washed in advance by soaking in 5 % alkaline detergent (decon90, Decon Laboratories Limited) for more than 3 hours, and then rinsed 5 times with tap water and 3 times with Milli-Q deionized water. The samples were stored in a refrigerator at approximately 5 °C before the analysis, and were put in the water bath with its temperature of about 25 °C for one hour just before analysis.

##### (2)-2 Seawater analyses

The total alkalinity was measured using a spectrophotometric system (Nihon ANS, Inc.) using a scheme of Yao and Byrne (1998). The calibrated volume of sample seawater (ca. 42 mL) was transferred from a sample bottle into the titration cell with its light path length of 4 cm long via dispensing unit. The TA is calculated by measuring two sets of absorbance at three wavelengths (730, 616, and 444) nm applied by the spectrometer (TM-UV/VIS C10082CAH, Hamamatsu Photonics). One is the absorbance of seawater sample before injecting an acid with indicator solution (bromocresol green sodium salt) and another the one after the injection. For mixing the acid with indicator solution and the seawater sufficiently, they are circulated through the line by a peristaltic pump equipped with periodically renewed TYGON tube 5 minutes before the measurement. Nitrogen bubble were introduced into the titration cell for degassing CO<sub>2</sub> from the mixed solution sufficiently.

The TA is calculated based on the following equation:

$$\begin{aligned} \text{pH}_T = & 4.2699 + 0.002578 \times (35 - S) \\ & + \log ((R(25) - 0.00131) / (2.3148 - 0.1299 \times R(25))) \\ & - \log (1 - 0.001005 \times S), \end{aligned} \quad (1)$$

$$\begin{aligned} A_T = & (N_A \times V_A - 10^{\text{pHT}} \times \text{DensSW} (T, S) \times (V_S + V_A)) \\ & \times (\text{DensSW} (T, S) \times V_S)^{-1}, \end{aligned} \quad (2)$$

where R(25) represents the difference of absorbance at 616 nm and 444 nm between before and after the injection. The absorbance of wavelength at 730 nm is used to subtract the variation of absorbance caused by the system. DensSW (T, S) is the density of seawater at temperature (T) and salinity (S),  $N_A$  the concentration of the added acid,  $V_A$  and  $V_S$  the volume of added acid and seawater, respectively.

### (3) Preliminary result

The repeatability of this system was  $2.9 \mu\text{mol kg}^{-1}$  ( $n = 12$ ) which was estimated from standard deviation of measured KRM value during this cruise. A few replicate samples were taken at most of stations and the difference between each pair of analyses was plotted on a range control chart (see Fig. 3.5.5-1). The average of the difference was provisionally  $0.8 \mu\text{mol kg}^{-1}$  ( $n = 15$ ) with its standard deviation of  $0.7 \mu\text{mol kg}^{-1}$ .

### (4) Data archive

Obtained data will be submitted to the Data Management Group (DMG) of JAMSTEC.

### (5) References

- Dickson, A. G., Sabine, C. L. & Christian, J. R. (Eds.). (2007). *Guide to best practices for ocean CO<sub>2</sub> measurements, PICES Special Publication 3*: North Pacific Marine Science Organization.
- Yao, W. and Byrne, R. H. (1998). Simplified seawater alkalinity analysis: Use of linear array spectrometers. *Deep-Sea Research I*, 45, 1383-1392.

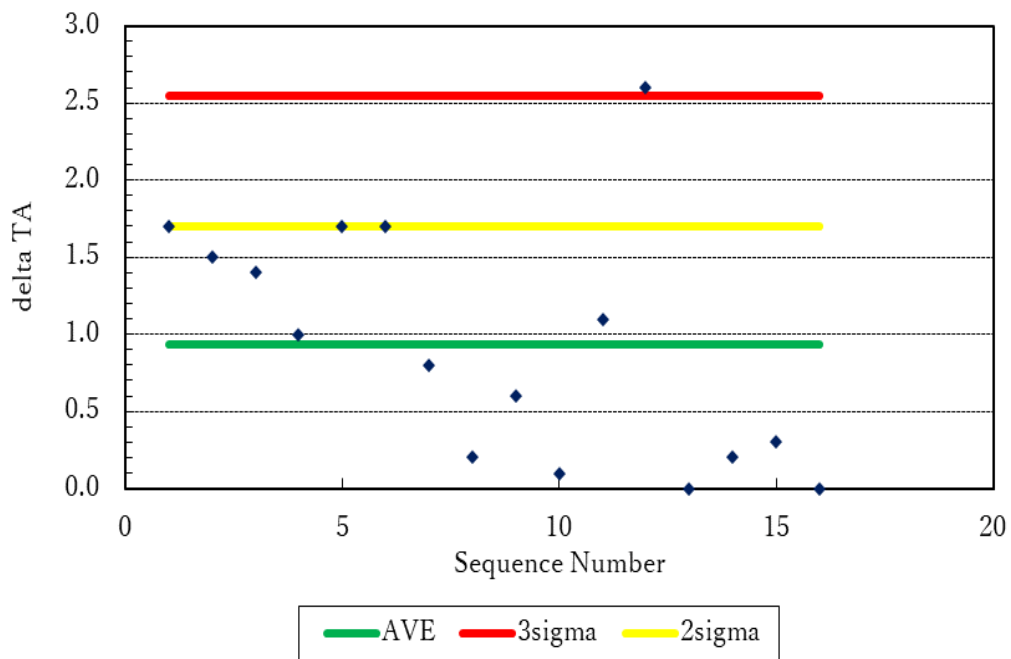


Figure 3.5.5-1 Range control chart of the absolute differences of replicate measurements of TA carried out during this cruise. AVE represents the average of absolute difference,  $3\sigma$  the upper control limit (standard deviation of AVE  $\times$  3), and  $2\sigma$  upper warning limit (standard deviation of AVE  $\times$  2).

### 3.5.6 Inorganic iodine

Yoko IWAMOTO	(Hiroshima University)	- not on board
Kazuhiko TAKEDA	(Hiroshima University)	- not on board
Fumikazu TAKETANI	(JAMSTEC)	- on board
Takashi SEKIYA	(JAMSTEC)	- on board
Yugo KANAYA	(JAMSTEC)	- not on board

Seawater sampling was supported by Marine work Japan, Ltd.

#### (1) Objectives

Iodine in seawater exists mainly as iodide and iodate ions, with a total reported to be approximately 0.4–0.5  $\mu\text{M}$ . Iodine is present as iodate ion ( $\text{IO}_3^-$ ) below 200 m, and approximately half of the iodine in the surface layer exists as iodide ion ( $\text{I}^-$ ) reduced by organisms. The presence of organic iodine in the surface layer has also been reported. It is well known that iodine in the atmosphere is oceanic origin and involved in various chemical reactions in the atmosphere such as particle formation and ozone depletion. In order to understand the iodine cycle in the oceans and evaluate its impact on the atmospheric environment, it is essential to use methods for quantifying iodine in seawater according to its state. The objective of this study is to obtain the vertical profile and spatial distribution of iodine by its state in the western North Pacific.

#### (2) Instruments and methods

##### i) Seawater collection

Seawater samples for halogen species are listed in Table 3.5.6-1. For the vertical profiles of halogen species including iodine, the water samples were collected using Niskin-X bottles on a CTD-rosette system at stations 001–005. For the spatial distribution of halogen species in surface seawater, the water samples were collected using a plastic bucket at every station. Surface seawater samples from the faucet on board were also collected (Table 3.5.6-2). All of the seawater samples were collected in 125-mL HDPE bottles after filtering. The bottles were stored at  $\sim 4^\circ\text{C}$  on board.

##### ii) Ion chromatography

An ion chromatography combining a high ion exchange capacity column and a UV detector which was originally developed (Yamane et al., 2015; Takeda et al., 2017; Ito et al., 2018) will be used for determination of iodine. Iodate ( $\text{IO}_3^-$ ), iodide ( $\text{I}^-$ ), nitrite ( $\text{NO}_2^-$ ), nitrate ( $\text{NO}_3^-$ ) and bromide ( $\text{Br}^-$ ) in seawater can be separated and analyzed using a dodecylammonium-coated octadecylsilyl column (TSKgel ODS-120H; Tosoh) with a mobile phase containing 0.3 M NaCl, 0.5 mM n-dodecylamine hydrochloride, and 5 mM phosphate buffer (pH=4.5). Organic iodine will be measured after decomposition of organic iodine to inorganic iodine by UV-light irradiation (500-W Xe lamp).

(3) References

- Ito, K., Takeda, K. and Hirokawa, T (2019) Determination of Trace Iodine in Seawater –Use of Ion Chromatography and Capillary Zone Electrophoresis–. *Bunseki Kagaku*, 68, 227–239.
- Takeda, K., Yamane, K., Horioka, Y. and Ito, K (2017) The iodide and iodate distribution in the Seto Inland Sea, Japan. *Aquatic Geochemistry*, 23, 315-330.
- Yamane K, Horioka Y, Fujino M, Ito K (2015) Anion chromatography using reversed-phase C18 columns coated with dodecylammonium cation and its application to simultaneous determination of inorganic anions in seawater. *Bunseki Kagaku* 64, 601–608.

(4) Data archives

All data obtained during this cruise will be submitted to Data Management Group (DMG) of JAMSTEC after the sample analysis and validation. The data will be opened to the public via “Data Research System for Whole Cruise Information (DARWIN)” in JAMSTEC web site.

Table 3.5.6-1 List of sea water sampling for halogen species.

On board ID	Depth [m]	Date Collected					Latitude			Longitude		
		YYYY	MM	DD	hh:mm	UTC	Deg.	Min.	N/S	Deg.	Min.	E/W
Stn001_shallow	0	2023	06	30	0:13	UTC	32	27.28	N	144	31.85	E
Stn001_shallow	5	2023	06	30	0:13	UTC	32	27.28	N	144	31.85	E
Stn001_shallow	10	2023	06	30	0:13	UTC	32	27.28	N	144	31.85	E
Stn001_shallow	20	2023	06	30	0:13	UTC	32	27.28	N	144	31.85	E
Stn001_shallow	60	2023	06	30	0:13	UTC	32	27.28	N	144	31.85	E
Stn001_shallow	100	2023	06	30	0:13	UTC	32	27.28	N	144	31.85	E
Stn001_shallow	Chl-max	2023	06	30	0:13	UTC	32	27.28	N	144	31.85	E
Stn001_shallow	140	2023	06	30	0:13	UTC	32	27.28	N	144	31.85	E
Stn001_shallow	200	2023	06	30	0:13	UTC	32	27.28	N	144	31.85	E
Stn001_shallow	300	2023	06	30	0:13	UTC	32	27.28	N	144	31.85	E
Stn001_Deep	500	2023	06	30	5:37	UTC	32	27.28	N	144	31.35	E
Stn001_Deep	1000	2023	06	30	5:37	UTC	32	27.28	N	144	31.35	E
Stn001_Deep	1600	2023	06	30	5:37	UTC	32	27.28	N	144	31.35	E
Stn001_Deep	2000	2023	06	30	5:37	UTC	32	27.28	N	144	31.35	E
Stn001_Deep	3000	2023	06	30	5:37	UTC	32	27.28	N	144	31.35	E
Stn001_Deep	4000	2023	06	30	5:37	UTC	32	27.28	N	144	31.35	E
Stn001_Deep	5000	2023	06	30	5:37	UTC	32	27.28	N	144	31.35	E
Stn001_Deep	5500	2023	06	30	5:37	UTC	32	27.28	N	144	31.35	E
Stn001_Deep	B-10	2023	06	30	5:37	UTC	32	27.28	N	144	31.35	E
Stn002_shallow	0	2023	07	02	0:08	UTC	25	0.02	N	145	0.13	E
Stn002_shallow	5	2023	07	02	0:08	UTC	25	0.02	N	145	0.13	E
Stn002_shallow	10	2023	07	02	0:08	UTC	25	0.02	N	145	0.13	E
Stn002_shallow	20	2023	07	02	0:08	UTC	25	0.02	N	145	0.13	E
Stn002_shallow	60	2023	07	02	0:08	UTC	25	0.02	N	145	0.13	E
Stn002_shallow	100	2023	07	02	0:08	UTC	25	0.02	N	145	0.13	E
Stn002_shallow	Chl-max	2023	07	02	0:08	UTC	25	0.02	N	145	0.13	E
Stn002_shallow	140	2023	07	02	0:08	UTC	25	0.02	N	145	0.13	E
Stn002_shallow	200	2023	07	02	0:08	UTC	25	0.02	N	145	0.13	E
Stn002_shallow	300	2023	07	02	0:08	UTC	25	0.02	N	145	0.13	E

Table 3.5.6-1 (continue)

On board ID	Depth [m]	Date Collected					Latitude			Longitude		
		YYYY	MM	DD	hh:mm	UTC	Deg.	Min.	N/S	Deg.	Min.	E/W
Stn002_Deep	500	2023	07	02	10:58	UTC	25	0.02	N	145	0.13	E
Stn002_Deep	1000	2023	07	02		UTC	25	0.02	N	145	0.13	E
Stn002_Deep	1600	2023	07	02		UTC	25	0.02	N	145	0.13	E
Stn002_Deep	2000	2023	07	02		UTC	25	0.02	N	145	0.13	E
Stn002_Deep	3000	2023	07	02		UTC	25	0.02	N	145	0.13	E
Stn002_Deep	4000	2023	07	02		UTC	25	0.02	N	145	0.13	E
Stn002_Deep	5000	2023	07	02		UTC	25	0.02	N	145	0.13	E
Stn002_Deep	B-10	2023	07	02		UTC	25	0.02	N	145	0.13	E
Stn003_Deep	500	2023	07	05	8:32	UTC	12	58.24	N	136	52.33	E
Stn003_Deep	1000	2023	07	05	8:32	UTC	12	58.24	N	136	52.33	E
Stn003_Deep	1600	2023	07	05	8:32	UTC	12	58.24	N	136	52.33	E
Stn003_Deep	2000	2023	07	05	8:32	UTC	12	58.24	N	136	52.33	E
Stn003_Deep	3000	2023	07	05	8:32	UTC	12	58.24	N	136	52.33	E
Stn003_Deep	4000	2023	07	05	8:32	UTC	12	58.24	N	136	52.33	E
Stn003_Deep	5000	2023	07	05	8:32	UTC	12	58.24	N	136	52.33	E
Stn003_Deep	B-10	2023	07	05	8:32	UTC	12	58.24	N	136	52.33	E
Stn003_Shallow	0	2023	07	06	1:24	UTC	12	60.00	N	136	59.87	E
Stn003_Shallow	5	2023	07	06	1:24	UTC	12	60.00	N	136	59.87	E
Stn003_Shallow	10	2023	07	06	1:24	UTC	12	60.00	N	136	59.87	E
Stn003_Shallow	20	2023	07	06	1:24	UTC	12	60.00	N	136	59.87	E
Stn003_Shallow	40	2023	07	06	1:24	UTC	12	60.00	N	136	59.87	E
Stn003_Shallow	60	2023	07	06	1:24	UTC	12	60.00	N	136	59.87	E
Stn003_Shallow	80	2023	07	06	1:24	UTC	12	60.00	N	136	59.87	E
Stn003_Shallow	100	2023	07	06	1:24	UTC	12	60.00	N	136	59.87	E
Stn003_Shallow	Chl.amax.	2023	07	06	1:24	UTC	12	60.00	N	136	59.87	E
Stn003_Shallow	120	2023	07	06	1:24	UTC	12	60.00	N	136	59.87	E
Stn003_Shallow	140	2023	07	06	1:24	UTC	12	60.00	N	136	59.87	E
Stn003_Shallow	160	2023	07	06	1:24	UTC	12	60.00	N	136	59.87	E
Stn003_Shallow	180	2023	07	06	1:24	UTC	12	60.00	N	136	59.87	E
Stn003_Shallow	200	2023	07	06	1:24	UTC	12	60.00	N	136	59.87	E
Stn003_Shallow	300	2023	07	06	1:24	UTC	12	60.00	N	136	59.87	E
Stn003_Shallow	400	2023	07	06	1:24	UTC	12	60.00	N	136	59.87	E
Stn003_Shallow	500	2023	07	06	1:24	UTC	12	60.00	N	136	59.87	E
Stn003_Shallow2	5	2023	07	09	23:55	UTC	13	30.76	N	137	3.26	E
Stn003_Shallow2	Chl.amax.	2023	07	09	23:55	UTC	13	30.76	N	137	3.26	E
Stn004_shallow	0	2023	07	11	0:43	UTC	13	9.95	N	135	43.33	E
Stn004_shallow	5	2023	07	11	0:43	UTC	13	9.95	N	135	43.33	E
Stn004_shallow	10	2023	07	11	0:43	UTC	13	9.95	N	135	43.33	E
Stn004_shallow	20	2023	07	11	0:43	UTC	13	9.95	N	135	43.33	E
Stn004_shallow	60	2023	07	11	0:43	UTC	13	9.95	N	135	43.33	E
Stn004_shallow	100	2023	07	11	0:43	UTC	13	9.95	N	135	43.33	E
Stn004_shallow	Chl-max	2023	07	11	0:43	UTC	13	9.95	N	135	43.33	E
Stn004_shallow	140	2023	07	11	0:43	UTC	13	9.95	N	135	43.33	E
Stn004_shallow	200	2023	07	11	0:43	UTC	13	9.95	N	135	43.33	E
Stn004_shallow	300	2023	07	11	0:43	UTC	13	9.95	N	135	43.33	E
Stn005_Shallow	0	2023	07	12	0:06	UTC	9	49.91	N	134	51.62	E
Stn005_Shallow	5	2023	07	12	0:06	UTC	9	49.91	N	134	51.62	E
Stn005_Shallow	10	2023	07	12	0:06	UTC	9	49.91	N	134	51.62	E
Stn005_Shallow	20	2023	07	12	0:06	UTC	9	49.91	N	134	51.62	E
Stn005_Shallow	40	2023	07	12	0:06	UTC	9	49.91	N	134	51.62	E
Stn005_Shallow	60	2023	07	12	0:06	UTC	9	49.91	N	134	51.62	E
Stn005_Shallow	80	2023	07	12	0:06	UTC	9	49.91	N	134	51.62	E
Stn005_Shallow	100	2023	07	12	0:06	UTC	9	49.91	N	134	51.62	E
Stn005_Shallow	Chl.amax.	2023	07	12	0:06	UTC	9	49.91	N	134	51.62	E
Stn005_Shallow	120	2023	07	12	0:06	UTC	9	49.91	N	134	51.62	E
Stn005_Shallow	140	2023	07	12	0:06	UTC	9	49.91	N	134	51.62	E
Stn005_Shallow	160	2023	07	12	0:06	UTC	9	49.91	N	134	51.62	E
Stn005_Shallow	180	2023	07	12	0:06	UTC	9	49.91	N	134	51.62	E
Stn005_Shallow	200	2023	07	12	0:06	UTC	9	49.91	N	134	51.62	E
Stn005_Shallow	300	2023	07	12	0:06	UTC	9	49.91	N	134	51.62	E
Stn005_Shallow	400	2023	07	12	0:06	UTC	9	49.91	N	134	51.62	E
Stn005_Shallow	500	2023	07	12	0:06	UTC	9	49.91	N	134	51.62	E

Table 3.5.6-2 List of surface seawater samples from the faucet.

On board ID	Depth	Date Collected					Latitude			Longitude		
	[m]	YYYY	MM	DD	hh:mm	UTC	Deg.	Min.	N/S	Deg.	Min.	E/W
Surf-001	6	2023	07	13	22:50	UTC	10	36.12	N	134	42.39	E
Surf-002	6	2023	07	14	7:40	UTC	12	31.28	N	134	55.02	E
Surf-003	6	2023	07	14	22:11	UTC	14	39.55	N	134	59.65	E
Surf-004	6	2023	07	15	7:35	UTC	14	59.81	N	134	51.36	E
Surf-005	6	2023	07	15	22:25	UTC	18	6.53	N	135	33.21	E
Surf-006	6	2023	07	16	7:21	UTC	19	59.37	N	135	56.52	E
Surf-007	6	2023	07	16	22:25	UTC	21	57.6	N	136	27.3	E
Surf-008	6	2023	07	17	8:40	UTC	23	38.1	N	136	43.5	E
Surf-009	6	2023	07	17	22:21	UTC	26	47.1	N	137	10.93	E
Surf-010	6	2023	07	18	7:20	UTC	28	38.71	N	137	29.85	E
Surf-011	6	2023	07	18	21:45	UTC	32	4.53	N	137	56.16	E

### 3.5.7 Volatile organic iodine

Atsushi OOKI	(Hokkaido University)	- not on board
Cui TIANCHANG	(Hokkaido University)	- on board
Fumikazu TAKETANI	(JAMSTEC)	- on board
Takashi SEKIYA	(JAMSTEC)	- on board
Yugo KANAYA	(JAMSTEC)	- not on board

Sampling was supported by Marine work Japan, Ltd.

#### (1) Objectives

Volatile organic iodine (VOI) in seawater consists of mainly iodomethane ( $\text{CH}_3\text{I}$ ), iodoethane ( $\text{C}_2\text{H}_5\text{I}$ ), chloro-iodomethane ( $\text{CH}_2\text{ClI}$ ) and diiodomethane ( $\text{CH}_2\text{I}_2$ ). These concentrations are from  $0.1 \text{ pmol L}^{-1}$  to  $1000 \text{ pmol L}^{-1}$ . High concentrations of  $\text{CH}_3\text{I}$  have been found in the surface of oligotrophic subtropical North Pacific Ocean in summer, whereas concentrations of the other VOIs are low (Ooki et al., 2015). Objectives of this study is to obtain vertical distributions of VOIs in water column in the subtropical and tropical Pacific Ocean to understand reasons to form their distributions.

#### (2) Instruments and methods

##### i) Seawater collection

Seawater samples for VOIs are listed in Table 3.5.7-1. For the vertical profiles of VOIs, the water samples were collected using Niskin-X bottles on a CTD-rosette system. Seawater samples were collected in 125-mL glass bottles.  $100 \mu\text{L}$  of saturated  $\text{HgCl}_2$  solution was added to the bottle to stop biological activity. The bottle was sealed with a butyl rubber septum and aluminum cap. The bottles were stored at  $\sim 4 \text{ }^\circ\text{C}$  on board.

##### ii) Gas chromatography mass spectrometry analysis

Analysis will be performed in the laboratory after the cruise using a purge & trap /preconcentration/capillary gas chromatography-mass spectrometry (GC-MS) system developed for automated measurement of atmospheric halocarbons. VOIs will be measured by the analytical system (Ooki et al., 2011).

#### (3) References

- Ooki, A., Nomura, D., Nishino, S., Kikuchi, T., and Yokouchi, Y.: A global-scale map of isoprene and volatile organic iodine in surface seawater of the Arctic, Northwest Pacific, Indian, and Southern Oceans, *Journal of Geophysical Research-Oceans*, 120, 4108-4128, 10.1002/2014jc010519, 2015.
- Ooki, A. and Yokouchi, Y.: Determination of Henry's law constant of halocarbons in seawater and analysis of sea-to-air flux of iodoethane ( $\text{C}_2\text{H}_5\text{I}$ ) in the Indian and Southern oceans based on partial pressure measurements, *Geochemical Journal*, 45, E1-E7, 2011.

#### (4) Data archives

All data obtained during this cruise will be submitted to Data Management Group (DMG) of JAMSTEC after the sample analysis and validation. The data will be opened to the public via

“Data Research System for Whole Cruise Information (DARWIN)” in JAMSTEC web site.

Table 3.5.7-1 List of sea water sampling for VOIs.

On board ID		Date Collected					Latitude			Longitude		
		YYYY	MM	DD	hh:mm:ss	UTC/JST	Deg.	Min.	N/S	Deg.	Min.	E/W
Station ID	Depth (m)	Date Collected					Latitude			Longitude		
Stn001_shallow	5	2023	06	30	0:13	UTC	32	27.2777	N	144	31.85197	E
Stn001_shallow	10	2023	06	30	0:13	UTC	32	27.2777	N	144	31.85197	E
Stn001_shallow	20	2023	06	30	0:13	UTC	32	27.2777	N	144	31.85197	E
Stn001_shallow	60	2023	06	30	0:13	UTC	32	27.2777	N	144	31.85197	E
Stn001_shallow	100	2023	06	30	0:13	UTC	32	27.2777	N	144	31.85197	E
Stn001_shallow	Chl-max	2023	06	30	0:13	UTC	32	27.2777	N	144	31.85197	E
Stn001_shallow	140	2023	06	30	0:13	UTC	32	27.2777	N	144	31.85197	E
Stn001_shallow	200	2023	06	30	0:13	UTC	32	27.2777	N	144	31.85197	E
Stn001_shallow	300	2023	06	30	0:13	UTC	32	27.2777	N	144	31.85197	E
Stn001_Deep	500	2023	06	30	5:37	UTC	32	27.2781	N	144	31.35363	E
Stn001_Deep	1000	2023	06	30	5:37	UTC	32	27.2781	N	144	31.35363	E
Stn001_Deep	2000	2023	06	30	5:37	UTC	32	27.2781	N	144	31.35363	E
Stn001_Deep	bottom10	2023	06	30	5:37	UTC	32	27.2781	N	144	31.35363	E
Stn002_shallow	0	2023	07	02	0:08	UTC	25	0.0180	N	145	0.13221	E
Stn002_shallow	5	2023	07	02	0:08	UTC	25	0.0180	N	145	0.13221	E
Stn002_shallow	10	2023	07	02	0:08	UTC	25	0.0180	N	145	0.13221	E
Stn002_shallow	20	2023	07	02	0:08	UTC	25	0.0180	N	145	0.13221	E
Stn002_shallow	60	2023	07	02	0:08	UTC	25	0.0180	N	145	0.13221	E
Stn002_shallow	100	2023	07	02	0:08	UTC	25	0.0180	N	145	0.13221	E
Stn002_shallow	Chl-max	2023	07	02	0:08	UTC	25	0.0180	N	145	0.13221	E
Stn002_shallow	140	2023	07	02	0:08	UTC	25	0.0180	N	145	0.13221	E
Stn002_shallow	200	2023	07	02	0:08	UTC	25	0.0180	N	145	0.13221	E
Stn002_shallow	300	2023	07	02	0:08	UTC	25	0.0180	N	145	0.13221	E
Stn002_Deep	500	2023	07	02	10:58	UTC	25	0.0180	N	145	0.13221	E
Stn002_Deep	1000	2023	07	02	10:58	UTC	25	0.0180	N	145	0.13221	E
Stn002_Deep	2000	2023	07	02	10:58	UTC	25	0.0180	N	145	0.13221	E
Stn002_Deep	bottom10	2023	07	02	10:58	UTC	25	0.0180	N	145	0.13221	E
Stn003_Shallow	0	2023	07	06	1:24	UTC	12	59.9956	N	136	59.87325	E
Stn003_Shallow	5	2023	07	06	1:24	UTC	12	59.9956	N	136	59.87325	E
Stn003_Shallow	10	2023	07	06	1:24	UTC	12	59.9956	N	136	59.87325	E
Stn003_Shallow	20	2023	07	06	1:24	UTC	12	59.9956	N	136	59.87325	E
Stn003_Shallow	40	2023	07	06	1:24	UTC	12	59.9956	N	136	59.87325	E
Stn003_Shallow	60	2023	07	06	1:24	UTC	12	59.9956	N	136	59.87325	E
Stn003_Shallow	80	2023	07	06	1:24	UTC	12	59.9956	N	136	59.87325	E
Stn003_Shallow	100	2023	07	06	1:24	UTC	12	59.9956	N	136	59.87325	E
Stn003_Shallow	Chl.amax.	2023	07	06	1:24	UTC	12	59.9956	N	136	59.87325	E
Stn003_Shallow	120	2023	07	06	1:24	UTC	12	59.9956	N	136	59.87325	E
Stn003_Shallow	140	2023	07	06	1:24	UTC	12	59.9956	N	136	59.87325	E
Stn003_Shallow	160	2023	07	06	1:24	UTC	12	59.9956	N	136	59.87325	E
Stn003_Shallow	180	2023	07	06	1:24	UTC	12	59.9956	N	136	59.87325	E
Stn003_Shallow	200	2023	07	06	1:24	UTC	12	59.9956	N	136	59.87325	E
Stn003_Shallow	300	2023	07	06	1:24	UTC	12	59.9956	N	136	59.87325	E

Table 3.5.7 (Continued)

On board ID		Date Collected					Latitude			Longitude		
		YYYY	MM	DD	hh:mm:ss	UTC/IST	Deg.	Min.	N/S	Deg.	Min.	E/W
Station ID	Depth (m)	Date Collected					Latitude			Longitude		
Stn005_Shallow	0	2023	07	12	0:06	UTC	9	49.9120	N	134	51.61692	E
Stn005_Shallow	5	2023	07	12	0:06	UTC	9	49.9120	N	134	51.61692	E
Stn005_Shallow	10	2023	07	12	0:06	UTC	9	49.9120	N	134	51.61692	E
Stn005_Shallow	20	2023	07	12	0:06	UTC	9	49.9120	N	134	51.61692	E
Stn005_Shallow	40	2023	07	12	0:06	UTC	9	49.9120	N	134	51.61692	E
Stn005_Shallow	60	2023	07	12	0:06	UTC	9	49.9120	N	134	51.61692	E
Stn005_Shallow	80	2023	07	12	0:06	UTC	9	49.9120	N	134	51.61692	E
Stn005_Shallow	100	2023	07	12	0:06	UTC	9	49.9120	N	134	51.61692	E
Stn005_Shallow	Chl.amax.	2023	07	12	0:06	UTC	9	49.9120	N	134	51.61692	E
Stn005_Shallow	120	2023	07	12	0:06	UTC	9	49.9120	N	134	51.61692	E
Stn005_Shallow	140	2023	07	12	0:06	UTC	9	49.9120	N	134	51.61692	E
Stn005_Shallow	160	2023	07	12	0:06	UTC	9	49.9120	N	134	51.61692	E
Stn005_Shallow	180	2023	07	12	0:06	UTC	9	49.9120	N	134	51.61692	E
Stn005_Shallow	200	2023	07	12	0:06	UTC	9	49.9120	N	134	51.61692	E
Stn005_Shallow	300	2023	07	12	0:06	UTC	9	49.9120	N	134	51.61692	E

### 3.5.8 Phytoplankton pigments

Kazuhiko MATSUMOTO	(JAMSTEC)	- Principal investigator
Katsunori SAGISHIMA	(MWJ)	
Misato KUWAHARA	(MWJ)	- Operation leader

#### (1) Objective

Phytoplankton biomass can estimate as the concentration of chlorophyll *a*, because all oxygenic photosynthetic plankton contain chlorophyll *a*. The objective of this study is to investigate the vertical distribution of phytoplankton as chlorophyll *a* by using the fluorometric determination.

Furthermore, the chemotaxonomic assessment of phytoplankton populations present in natural seawater requires taxon-specific algal pigments as good biochemical markers. In this cruise, we collect samples to investigate the marine phytoplankton community structure by the marine phytoplankton pigments measured by using the high-performance liquid chromatography (HPLC).

#### (2) Parameters

Total chlorophyll *a*

Marine phytoplankton pigments

#### (3) Instruments and Methods

We collected 500ml seawater samples for total chlorophyll *a* from 2 to 15 depths between the surface and 300 dbar depth including a chlorophyll *a* maximum layer. The chlorophyll *a* maximum layer was determined by a Chlorophyll Fluorometer (Seapoint Sensors, Inc.) attached to the CTD system.

Seawater samples for total chlorophyll *a* were vacuum-filtrated (< 0.02 MPa) through glass microfiber filter (ADVANTEC GF-75, 25mm-in diameter). Phytoplankton pigments retained on the filters were immediately extracted in a polypropylene tube with 7 ml of N,N-dimethylformamide (FUJIFILM Wako Pure Chemical Corporation Ltd.) (Suzuki and Ishimaru, 1990). The tubes were stored at -20 °C under the dark condition to extract chlorophyll *a* at least for 24 hours.

Chlorophyll *a* concentration was measured by the fluorometer (10-AU, TURNER DESIGNS), which was previously calibrated against a pure chlorophyll *a* (Sigma-Aldrich Co., LLC). To estimate chlorophyll *a* concentration, we applied to the fluorometric “Non-acidification method” (Welschmeyer, 1994).

For HPLC measurements of marine phytoplankton pigments, 2.4-L seawater samples were filtered onto a 47 mm GF/F filter. The filters with moisture wiped off and vacuum dried at 0 °C within a few hours are stored in a deep-freezer (-80 °C) until analysis on land. Samples will be analyzed according to the method of Van Heukelem and Thomas (2001).

#### (4) Station list

The number of samples, stations and the sampling positions were shown in Table 3.5.8-1 and Fig. 3.5.8-1.

(5) Preliminary Results

The results of total chlorophyll *a* at station were shown in Fig. 3.5.8-2. At each station, Triplicate samples were collected from water of surface, 5m, 40m depth and chlorophyll *a* maximum layer. Results of triplicate sample measurements were shown in Table 3.5.8-1.

(6) Data archives

These data obtained in this cruise will be submitted to the Data Management Group of JAMSTEC, and will be opened to the public via “Data Research System for Whole Cruise Information in JAMSTEC (DARWIN)” in JAMSTEC web site.

<http://www.godac.jamstec.go.jp/darwin/e>

(7) Reference

- Suzuki, R., and T. Ishimaru (1990), An improved method for the determination of phytoplankton chlorophyll using N, N-dimethylformamide, *J. Oceanogr. Soc. Japan*, 46, 190-194.
- Welschmeyer, N. A. (1994), Fluorometric analysis of chlorophyll *a* in the presence of chlorophyll *b* and pheopigments. *Limnol. Oceanogr.* 39, 1985-1992.
- Van Heukelem, L., and C. S. Thomas (2001), Computer-assisted high-performance liquid chromatography method development with applications to the isolation and analysis of phytoplankton pigments, *J. Chromatogr. A*, 910(1), 31-49.

Table 3.5.8-1 Number of samples and casts.

	Number of samples	Number of casts
Total chlorophyll <i>a</i>	105	06

Table 3.5.8-2 Results of the triplicate sample measurements

	All samples
Number of triplicate sample pairs	14
Standard deviation ( $\mu\text{g L}^{-1}$ )	0.01

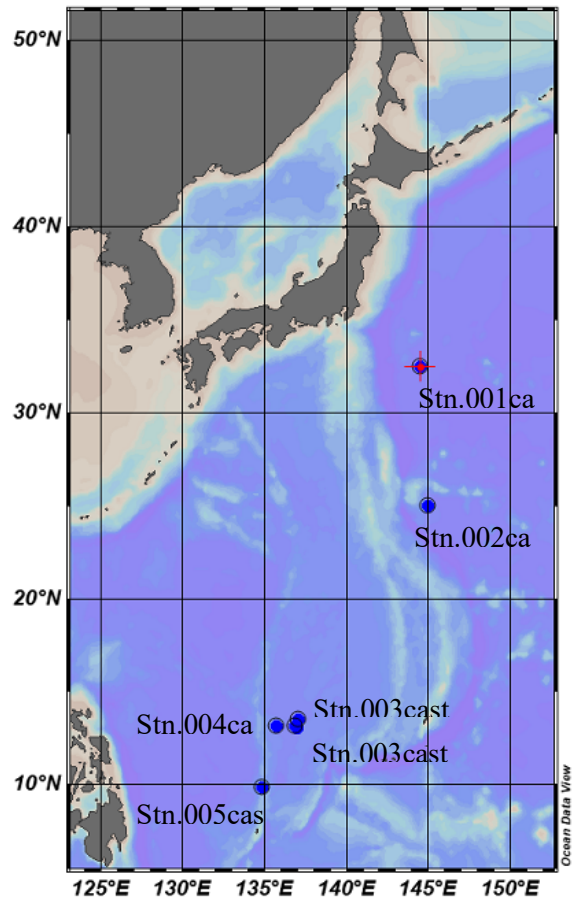


Figure 3.5.8-1 Sampling positions of chlorophyll *a* in MR23-05 Leg1

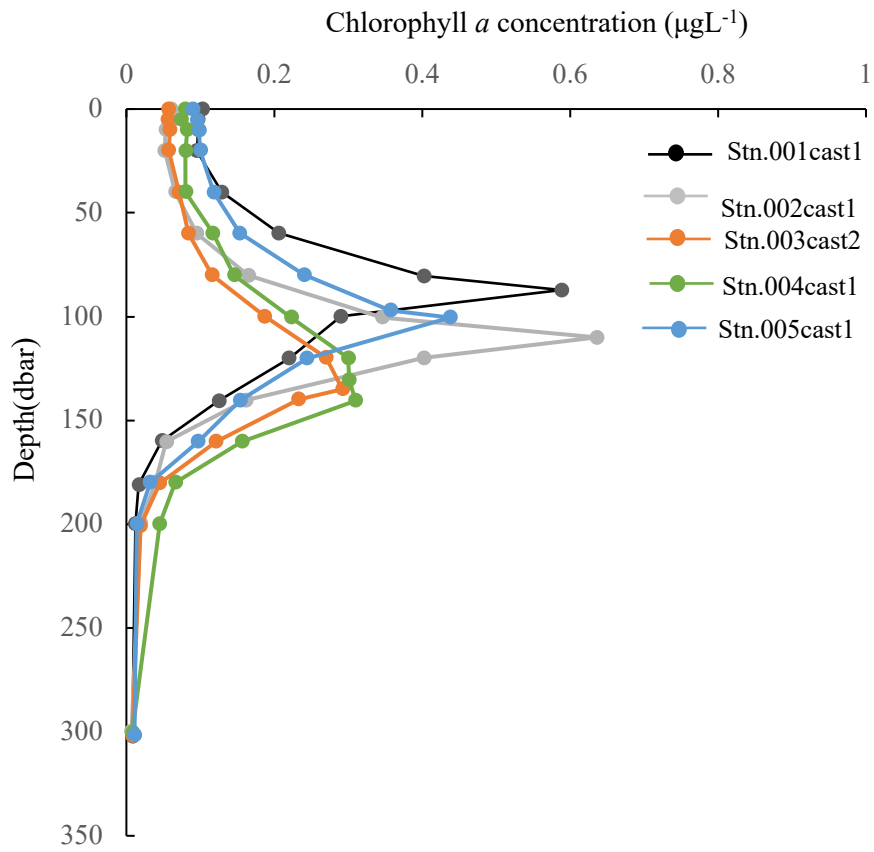


Figure 3.5.8-2 Vertical distribution of chlorophyll *a* at Stn.001 to stn.005.

### 3.5.9 Photosynthesis–irradiance parameters of phytoplankton

Kazuhiko MATSUMOTO	(JAMSTEC)
Fumikazu TAKETANI	(JAMSTEC)
Takashi SEKIYA	(JAMSTEC)

#### (1) Objectives

Atmospheric deposition is expected to be an important source of limiting nutrients to the ocean, potentially stimulating marine primary productivity. To investigate the impact of atmospheric deposition, photosynthetic characteristics of marine phytoplankton are estimated by the photosynthesis–irradiance (P–E) experiment.

#### (2) Methods and Instruments

##### (2-1) Sampling

Seawater samples were collected using Niskin-X bottles installed acid-cleaned O-ring and a bucket. Sampling logs are listed in Table 3.5.9-1.

##### (2-2) Incubation

Seawater samples were transferred into the acid-cleaned, transparent bottles. Nutrients, rainwater, and copper were added into the sample bottles and phytoplankton were incubated under natural light conditions in a temperature-controlled, on-deck water tank until the subsequent P–E experiments. Just before the P–E experiments in laboratory,  $\text{NaH}^{13}\text{CO}_3$  was added to each bottle at a final concentration of 0.2 mM, sufficient to enrich the bicarbonate concentration by about 10%. The time-zero samples were filtered immediately after the addition of  $^{13}\text{C}$  solution. Four incubators were filled with water, and their water temperature were controlled appropriately by water chillers. Each incubator was illuminated at one end by a 500W halogen lamp attached infrared cut-off filter, and eight bottles were arranged linearly against the lamp and controlled light intensity by shielding with a neutral density filter on lamp side. Incubations were conducted for 3 h during daytime.

##### (2-3) Measurement

After the incubation, water samples were immediately filtered through a pre-combusted GF/F filter, then the filters were dehydrated in a dry oven (40 °C), and the remained inorganic carbon in the filter was removed by fuming HCl. The incorporation of inorganic  $^{13}\text{C}$  content of the particulate fraction will be measured with an automatic nitrogen and carbon analyzer mass spectrometer (SerCon, Ltd., UK) based on the method of Hama et al. (1983) on land. The analytical function and parameter values used to describe the relationship between the photosynthetic rate (P) and scalar irradiance (E) are best determined using a least-squares procedure from the following equation (Platt et al., 1980).

$$P = P_{\max}(1 - e^{-\alpha E/P_{\max}})e^{-b\alpha E/P_{\max}}$$

where,  $P_{max}$  is the light-saturated maximum photosynthetic rate,  $\alpha$  is the initial slope of the P vs. E curve,  $b$  is a dimensionless photoinhibition parameter. The chl  $a$ -specific, light absorption coefficient spectrum of phytoplankton were measured using a quantitative filter technique (QFT) method (Kishino et al., 1985), then the P–E data have been corrected for the spectrum of the lamp source following the method of Kyewalyanga et al. (1997). In addition, HPLC and flow cytometry samples were taken concurrently with the P–E experiment to investigate the effect of phytoplankton composition.

### (3) References

- Hama T, Miyazaki T, Ogawa Y, Iwakuma T, Takahashi M, Otsuki A, Ichimura S (1983), Measurement of photosynthetic production of a marine phytoplankton population using a stable  $^{13}C$  isotope. *Marine Biology* 73: 31-36.
- Platt T, Gallegos CL, Harrison WG (1980), Photoinhibition of photosynthesis in natural assemblages of marine phytoplankton. *Journal of Marine Research* 38: 687-701.
- Kishino, M., M. Takahashi, N. Okami, and S. Ichimura (1985), Estimation of the spectral absorption coefficients of phytoplankton in the sea, *Bulletin of Marine Science*, 37, 634-642.
- Kyewalyanga, M. N., T. Platt, and S. Sathyendranath (1997), Estimation of the photosynthetic action spectrum: implication for primary production models, *Marine Ecology Progress Series*, 146: 207-223.

Table 3.5-9 Sampling list for P–E experiment

Station/cast	Date Collected					Latitude			Longitude			Depth [m]
	YYYY	MM	DD	time		Deg.	Min.	N/S	Deg.	Min.	E/W	
Stn001_shallow	2023	06	29	22:17	UTC	32	27.44	N	144	31.97	E	0
Stn001_shallow	2023	06	29	22:17	UTC	32	27.44	N	144	31.97	E	5
Stn001_shallow	2023	06	29	22:17	UTC	32	27.44	N	144	31.97	E	40
Stn001_shallow	2023	06	29	22:17	UTC	32	27.44	N	144	31.97	E	87
Stn002_shallow	2023	07	01	23:16	UTC	24	59.98	N	144	59.99	E	0
Stn002_shallow	2023	07	01	23:16	UTC	24	59.98	N	144	59.99	E	5
Stn002_shallow	2023	07	01	23:16	UTC	24	59.98	N	144	59.99	E	40
Stn002_shallow	2023	07	01	23:16	UTC	24	59.98	N	144	59.99	E	109
Stn003_shallow1	2023	07	05	23:16	UTC	13	0	N	136	59.87	E	5
Stn003_shallow2	2023	07	09	23:11	UTC	13	30.87	N	137	3.03	E	5
Stn003_shallow2	2023	07	09	23:11	UTC	13	30.87	N	137	3.03	E	124
Stn004_shallow	2023	07	10	23:45	UTC	13	10.24	N	135	43.1	E	5
Stn004_shallow	2023	07	10	23:45	UTC	13	10.24	N	135	43.1	E	40
Stn005_shallow	2023	07	11	23:16	UTC	9	49.76	N	134	51.65	E	5

### 3.5.10 Transparent exopolymer particles

Kazuhiko MATSUMOTO

(JAMSTEC)

#### (1) Objectives

Transparent exopolymer particles (TEP), i.e., polysaccharide-rich microgels that are produced primarily by the abiotic coagulation of phytoplankton exudates, are identifying as organic gels in the ocean interior. TEP is very sticky, and it aggregates with other suspended particles, resulting in the formation of sinking marine snow. In addition, TEP becomes enriched in the surface microlayer and expected to produce marine organic aerosol directly at the sea surface due to the interaction between wind and waves. To understand the processes of settling particles and organic aerosol formation, the concentrations of TEP are measured.

#### (2) Sampling and measurement procedure

Seawater samples were collected with Niskin-X bottles and a bucket vertically at Stations 001 and 002, and at the depths where P-E experiments were conducted. Samples were fixed with 1% (v/v) formalin and stored in refrigerator. The analyses will be conducted after the cruise on land as follows. The water samples of 200 mL are filtered onto 0.4- $\mu\text{m}$  polycarbonate filters, and the filters are stained with 1 mL alcian blue solution which adjusted to pH 2.5 and rinsed thrice with 1 mL of Milli-Q water. Stained filter samples are stored in freezer until analysis. Filter samples are soaked for 2 - 5 h in 80% sulfuric acid ( $\text{H}_2\text{SO}_4$ ) to elute the dye and then the absorbance of the solution is measured at 787 nm in a 1 cm cuvette. The calibration curve is produced by using a xanthan gum solution (XG, Sigma-Aldrich), and the TEP concentrations are represented as XG equivalent (Passow and Alldredge, 1995).

#### (3) Data archive

The data obtained during this cruise will be submitted to the JAMSTEC Data Management Group (DMG).

#### (4) Reference

Passow, U., and A. L. Alldredge (1995), A dye-binding assay for the spectrophotometric measurement of transparent exopolymer particles (TEP) in the ocean, *Limnol. Oceanogr.*, 40(7): 1326-1335.

### 3.6 Marine snow catcher observation

Takuhei SHIOZAKI

(Atmosphere and Ocean Research Institute, The University of Tokyo) - not on board

Qin HONG-WEI

(Atmosphere and Ocean Research Institute, The University of Tokyo) - on board

#### (1) Purpose and background

Sinking particles are playing important role in the process of the biological carbon pump. So far, the research focused on the sinking particles are collected by Niskin bottle or sediment trap, however, these kinds of sampling methods have a problem. They could not collect suspended particles and sinking particles separately. During my research, sinking particles and suspended particles were collected by Marine Snow Catcher (MSC) to examine the microbial community structures and check the similarities and differences between sinking particles and suspended particles' microbial community structures.

#### (2) Activities

Water samples have been collected in five depths based on 100, 25,10,1, and 0.1% of surface light intensity at target station. The water samples would be used for size fractionated DNA (>3  $\mu\text{m}$  and 0.2–3  $\mu\text{m}$ ), particulate organic carbon / nitrogen (POC/N), size fractionated chlorophyll *a* (>3  $\mu\text{m}$  and 0.2–3  $\mu\text{m}$ ), salinity, nutrients analysis and primary production. For marine snow catcher, samples were collected from subsurface chlorophyll maximum (SCM) and 1000 m depth using Normal and Giant MSC at target station.

#### (3) Methods, instruments

During this cruise, two kinds of MSC were used (Normal and Giant) to collect sinking and suspended particles. Normal and giant MSC can collect 120 and 370 L seawater, respectively. The MSC deployment was performed using the ship's A-frame. The speed of wire out is set to be 1.0  $\text{m s}^{-1}$ . After reaching the desired depth, the MSC was closed using a messenger. After collecting the water sample, winch wire was wound up at 1.0  $\text{m s}^{-1}$ . Both Normal and giant MSC were kept on the deck for 2 hours to make the suspended and sinking particles separated, after 2 hours, samples would be collected. For the suspended samples (Both Normal one and Giant one) would be filtered onto 3- and 0.2-3  $\mu\text{m}$  filters, for fast-sinking samples, in Normal MSC, samples would be collected by a tray setting at the bottom of MSC and then be filtered onto 3- $\mu\text{m}$  polycarbonate filters, in Giant MSC, samples would be collected by tubes controlled by hand which could get the particles on the bottom accurately, and then filtered onto 3- $\mu\text{m}$  polycarbonate filters. The samples would be stored at a freezer (-20°C) until onshore analysis.

Samples for POC/N were collected from the sinking fraction. From the suspended fraction, samples for chlorophyll *a*, POC/N, salinity, and nutrients were collected. The chlorophyll *a* in the suspended fraction were sequentially filtered onto 3- and 0.2- $\mu\text{m}$  filters. Seawater samples for salinity and nutrients analysis were collected in 250 ml brown glass bottles and 10 mL acrylic tubes, respectively, and were immediately measured on board.

Samples for primary production were collected duplicate by using 1.2L polycarbonate bottles.

They were then added <sup>13</sup>C-labeled sodium bicarbonate at a final concentration of 200 μmol L<sup>-1</sup>. The bottles would be covered with different neutral-density screens to adjust the light intensity and incubated for 24 h in an on-deck incubator which filled with flowing surface seawater. Incubations were terminated by filtration onto pre-combusted (450°C, 6h) GF/F filters. Samples for POC/N (2 L) were also filtered onto pre-combusted GF/F filters. Samples for size fractionated DNA (2.3 L) and chlorophyll a (0.5 L) were sequentially filtered onto 3- and 0.2-μm filters. The filters for DNA were stored at a freezer until onshore analysis. The chlorophyll a concentrations were measured fluorometrically using a Turner Design 10-AU fluorometer after extraction with N,N-dimethylformamide on board.

(4) Station list

St.KEO; St.KEOS; St.PHSMO; St.4

(5) Data archives

These data obtained in this cruise will be submitted to the Data Management Group of JAMSTEC when ready.

### 3.7 GPS radiosonde observation

Masaki KATSUMATA	(JAMSTEC)	- Principal investigator
Kyoko TANIGUCHI	(JAMSTEC)	- not on board
Yutaro MURAKAMI	(NME)	- Operation leader
Ryo OYAMA	(NME)	

#### (1) Objectives

To obtain atmospheric profile of temperature, humidity, and wind speed/direction, and their temporal variations

#### (2) Methods

Atmospheric sounding by radiosonde by using system by Vaisala Oyj was carried out. The GPS radiosonde sensor RS-41SGP was utilized. The on-board system to calibrate, to launch, to log the data and to process the data is MW41, which consists of processor (Vaisala, SPS-311), processing and recording software (MW41, ver.2.11.0), GPS antenna (GA20), UHF antenna (RB21), ground check kit for RS41 (RI41), pressure sensor for ground check (Vaisala PTB-330), and balloon launcher (ASAP). The sensor was launched with balloon (Totex TA-200). When the relative wind to the ship (launcher) is not appropriate to use the ASAP, the handy launch was selected.

The radiosondes were launched every 6 hours from 06UTC on Jun. 28 to 12UTC on Jul. 1 when the vessel was at or around the station KEO, and from 00UTC on Jul. 5 to 00UTC on Jul. 12 when the vessel was at or around the station PHSMO. In addition, the launch at 12UTC was made from Jul. 2 to Jul. 4 and from Jul. 14 to Jul. XX. In total, XX launches were carried out as listed in Table 3.7-1.

#### (3) Preliminary Results

The results are shown in the figures. Figure 3.7-1 is the time-height cross sections during the stationary observation period at around the station PHSMO for the potential temperature, relative humidity, zonal and meridional wind components. Several vertically-integrated parameters are derived from sounding data as in Fig. 3.7-2, including convective available potential energy (CAPE), convective inhibition (CIN) and total precipitable water vapor (TPW).

#### (4) Data archive

Data were sent to the world meteorological community via Global Telecommunication System (GTS) through the Japan Meteorological Agency, immediately after each observation. The ASCII data, corrected by MW41 software is available for every launch during ascent. Raw data, in the Vaisala original binary format, is also available for every launch during ascent and descent. These datasets will be submitted to JAMSTEC Data Management Group (DMG).

#### (5) Acknowledgments

The observations are greatly helped by Dr. Iwao Ueki and Dr. Akira Nagano of JAMSTEC.

Table 3.7-1 Radiosonde launch log, with the surface conditions and the reached maximum height.

ID	Nominal Time YYYYMMDDhh	Launched Location		Surface Values					Max Height	Clouds	
		Lat.	Lon.	P	T	RH	WD	WS		Amount	Types
		deg.N	deg.E	hPa	deg.C	%	deg.	m/s	m		
RS001	2023062806	34.096	139.063	1008.9	25.6	92	228	13.2	23779	9	St,As
RS002	2023062812	33.437	140.424	1010.0	25.4	91	231	11.6	27932	3	Ci, St
RS003	2023062818	33.012	141.961	1009.2	24.1	96	202	10.7	23987	2	N/A
RS004	2023062900	32.649	143.456	1009.9	24.3	95	206	10.3	26058	5	As,Ci,St
RS005	2023062906	32.367	144.416	1010.4	25.1	89	224	7.6	25674	7	Ac, St, Sc
RS006	2023062912	32.600	144.760	1010.8	24.4	96	198	7.5	26000	4	Ci, St, Sc,Cu
RS007	2023062918	32.538	144.618	1010.0	24.4	94	213	10.4	27148	3	N/A
RS008	2023063000	32.456	144.532	1011.0	24.9	93	218	8.5	25808	5	St,As,Ac,Sc,Cu
RS009	2023063006	32.455	144.524	1010.3	25.4	90	237	9.1	26678	5	As,St
RS010	2023063012	32.367	144.419	1011.6	25.0	92	208	10.2	24825	2	Ci,Cs
RS011	2023063018	31.275	144.499	1012.1	24.6	91	225	8.2	25832	2	Ci, Sc
RS012	2023070100	30.067	144.604	1013.5	25.7	86	198	7.0	26729	7	As,Cs,Sc
RS013	2023070106	28.759	144.719	1013.4	27.2	84	229	3.5	24841	4	St, Sc, As
RS014	2023070112	27.383	144.838	1014.4	27.0	87	143	0.8	26864	2	Ci, Sc, As
RS015	2023070212	24.177	144.150	1013.7	27.8	85	204	2.6	24160	2	Cu,Sc, Ci
RS016	2023070312	20.079	140.565	1010.6	29.2	76	130	4.5	26095	4	Cu, Sc, Cs, Ci
RS017	2023070412	15.681	138.274	1009.6	30.0	70	104	2.0	24605	2	Cu, Sc, Ci
RS018	2023070500	13.367	137.144	1008.8	29.1	77	97	4.7	25504	7	As,Ci,Cu,Sc
RS019	2023070506	13.125	136.885	1007.1	29.3	77	75	2.9	26447	2	Cu, As, Sc
RS020	2023070512	12.905	136.896	1009.0	29.1	83	44	6.1	25753	1	Cu, Sc
RS021	2023070518	12.952	136.910	1008.7	28.4	80	47	5.1	24884	8	Cu, Sc, As, Ci
RS022	2023070600	13.000	136.998	1009.3	29.4	79	57	6.8	26009	3	Nb,Ns,Sc,As,Cu
RS023	2023070606	13.000	137.004	1006.8	29.5	78	60	7.3	26071	4	Sc, As
RS024	2023070612	12.965	137.052	1008.6	29.5	80	64	9.1	26059	1	Sc, Cu
RS025	2023070618	12.896	137.094	1007.8	29.3	82	76	6.6	26682	2	Cu, Sc
RS026	2023070700	12.866	136.774	1008.5	29.1	82	70	5.8	23763	4	As,St,Cu,Ac
RS027	2023070706	12.895	126.911	1007.3	29.4	77	80	6.5	25472	8	Cu, Cs, Sc, As
RS028	2023070712	13.201	136.601	1009.9	29.2	80	72	5.0	25245	2	Sc
RS029	2023070718	13.161	136.744	1008.1	28.8	81	64	3.4	24878	3	Cu, Sc, As
RS030	2023070800	13.106	136.893	1008.4	29.3	79	51	5.4	26795	7	Cu,Sc,St,As
RS031	2023070806	13.013	136.781	1006.6	29.4	79	87	4.2	26333	7	Sc, St, Cu, As
RS032	2023070812	12.902	136.757	1008.0	28.3	88	133	1.8	24971	6	Cu, Sc, Ci
RS033	2023070818	12.946	136.920	1006.3	27.4	87	174	6.4	24857	9	Cu, Sc, Ci
RS034	2023070900	12.990	137.128	1007.1	27.9	83	176	4.2	25545	8	Ns,As,Sc
RS035	2023070906	12.989	137.119	1006.1	27.5	86	65	3.2	24706	9	Ns,Cu,Sc,As
RS036	2023070912	13.737	136.726	1007.3	27.6	85	103	7.9	24922	10	As, etc.
RS037	2023070918	13.650	136.833	1005.4	26.7	90	100	9.0	24126	7	Cu,, Sc, As, Ci
RS038	2023071000	13.514	137.050	1006.5	28.3	82	118	8.5	25496	8	Ns,Sc,Cu,As
RS039	2023071006	13.537	136.989	1004.5	29.1	83	89	7.3	27886	8	Cu, Ns, St, As
RS040	2023071012	13.407	136.323	1006.2	27.8	86	126	10.3	25018	10	N/A
RS041	2023071018	13.250	135.669	1004.1	28.5	82	118	6.6	24617	4	Sc, Cs, Ci
RS042	2023071100	13.176	135.718	1007.0	29.0	82	155	5.3	26313	7	Cu,St,Sc,As,Cc
RS043	2023071106	13.123	135.787	1004.4	28.9	82	113	4.2	26328	9	Cu, St,Sc
RS044	2023071112	12.172	135.519	1006.5	29.2	77	117	4.7	23816	2	N/A
RS045	2023071118	11.016	135.149	1004.2	28.7	81	148	7.0	24743	2	Cu, Sc, Ci
RS046	2023071200	9.830	134.861	1007.9	25.6	94	237	6.1	23350	10	Ns,Cu,St
RS047	2023071412	13.218	134.936	1008.3	27.3	83	68	6.6	22404	7	Sc, Ci, Cu
RS048	2023071512	15.749	135.003	1006.8	28.6	82	76	10.2	23717	10	N/A
RS049	2023071612	20.524	136.141	1010.1	29.4	83	96	9.6	24199	1	St, Ci
RS050	2023071712	24.153	136.808	1012.4	29.4	78	87	8.3	24789	0+	N/A
RS051	2023071718	25.493	137.039	1012.1	28.6	82	75	5.2	25108	0+	N/A
RS052	2023071800	26.971	137.213	1013.4	28.3	78	67	6.6	26372	4	Cu,St

RS053	2023071806	28.202	137.425	1012.3	28.6	76	70	2.1	26037	1	Sc
RS054	2023071812	29.474	137.626	1011.6	28.4	78	228	0.9	26159	0+	N/A
RS055	2023071818	30.893	137.891	1009.5	28.0	85	270	6.8	26472	2	Sc, St
RS056	2023071900	32.426	138.002	1008.4	29.5	74	269	11.2	26377	5	Sc,Cu,As

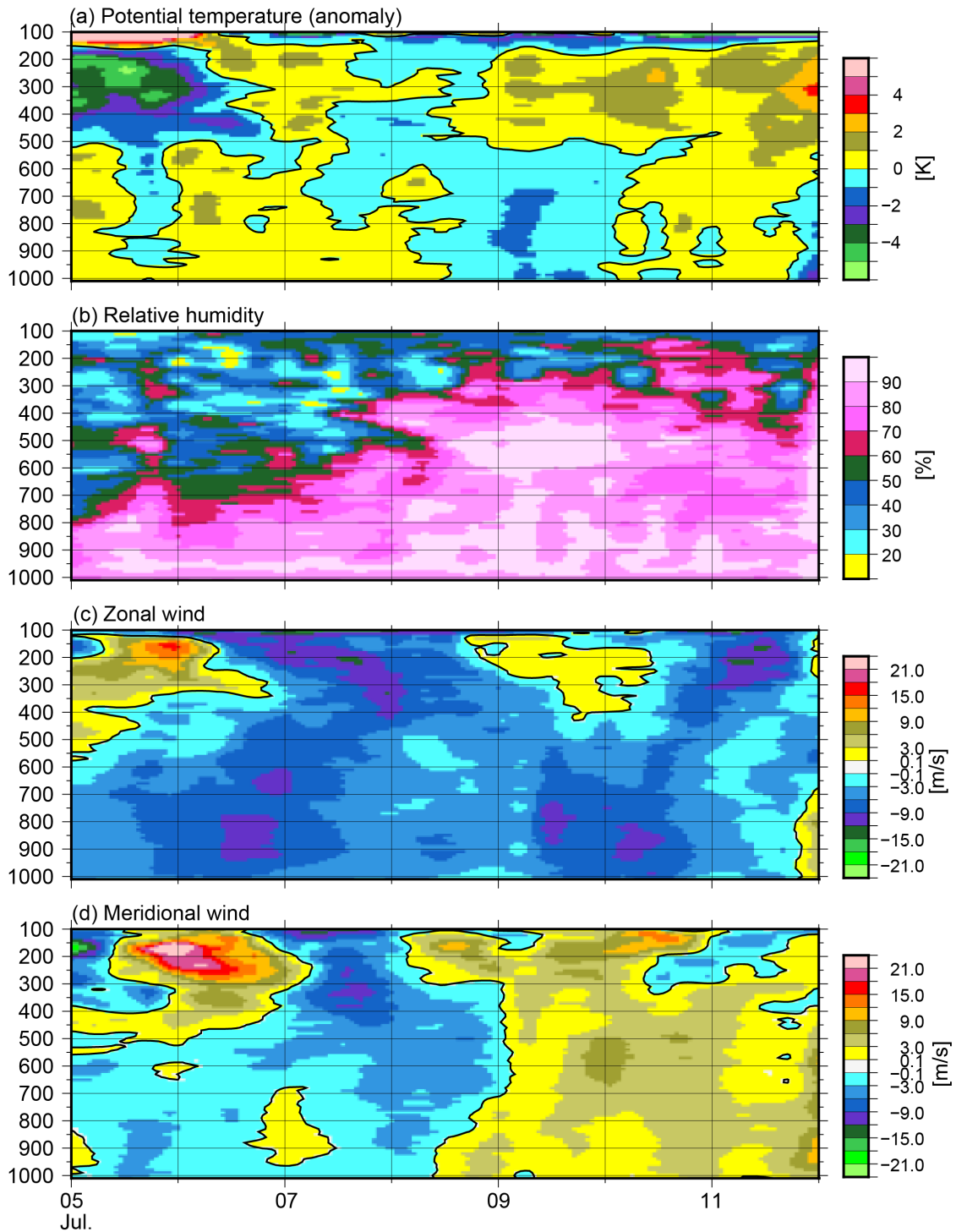


Figure 3.7-1 Time-height cross sections of observed parameters at and near the station PHSMO, from 00Z on Jul.05 to 00Z on Jul.12; (top) temperature, in anomaly to the period-averaged value at each pressure level, (second top) relative humidity, (third top) zonal wind (absolute value), and (bottom) meridional wind (absolute value).

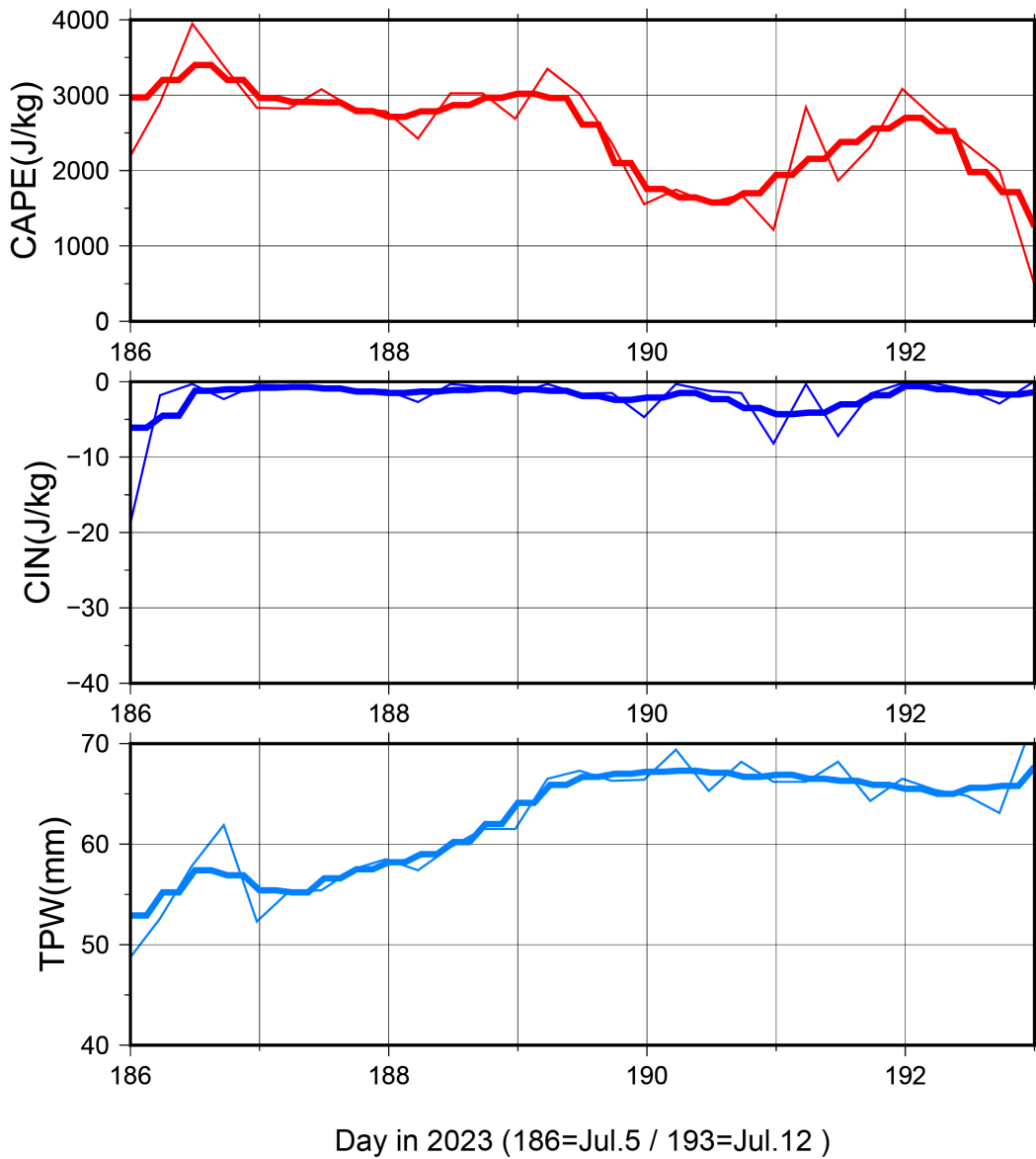


Figure 3.7-2 Time series of the parameters derived from the radiosonde observations near the station PHSMO; (top) convective available potential energy (CAPE), (middle) convective inhibition (CIN), and (bottom) total precipitable water vapor (TPW). The thin lines are the values from each 6-hourly sounding, while the thick lines are the running mean for 25 hours.

### 3.8 C-band weather radar observation

Masaki KATSUMATA	(JAMSTEC)	- Principal Investigator
Biao GENG	(JAMSTEC)	- not on board
Yutaro MURAKAMI	(NME)	- Operation Leader
Ryo OYAMA	(NME)	

#### (1) Objective

Weather radar observations in this cruise aim to investigate the structure and evolution of precipitating systems over the tropical ocean.

#### (2) Radar specifications

The C-band weather radar on board the R/V MIRAI is used. The basic specifications of the radar are as follows:

Frequency:	5370 MHz (C-band)
Polarimetry:	Horizontal and vertical (simultaneously transmitted and received)
Transmitter:	Solid-state transmitter
Pulse configuration:	Using pulse-compression
Output power:	6 kW (H) + 6 kW (V)
Antenna diameter:	4 meters
Beam width:	1.0 degrees
Inertial navigation unit:	PHINS (IXBLUE SAS France)

#### (3) Available radar variables

Radar variables, which are converted from the power and phase of the backscattered signal at vertically- and horizontally-polarized channels, are as follows:

Radar reflectivity:	Z
Doppler velocity:	V <sub>r</sub>
Spectrum width of Doppler velocity:	SW
Differential reflectivity:	ZDR
Differential propagation phase:	ΦDP
Specific differential phase:	KDP
Co-polar correlation coefficients:	ρ <sub>HV</sub>

#### (4) Operational methodology

The antenna is controlled to point the commanded ground-relative direction, by controlling the azimuth and elevation to cancel the ship attitude (roll, pitch, and yaw) detected by the navigation unit. The Doppler velocity is also corrected by subtracting the ship movement in the beam direction.

For maintenance, internal signals of the radar are checked and calibrated at the beginning and the end of the cruise. Meanwhile, the peak output power and the radar's pulse width are checked daily.

During the cruise, the radar is operated in modes shown in Table 3.8-1. A dual PRF mode is

used for volume scans. For RHI and surveillance PPI scans, a single PRF mode is used.

(5) Data

The C-band weather radar observations were conducted continuously during the cruise, except nearby the main islands of Japan and Palau. The observation periods were as follows:

1500UTC on June 28 – 0659UTC on July 12

0800UTC on July 13 – 2159UTC on July 18

An example of the obtained snapshots is shown in Fig. 3.8-1. Some precipitation features in the meso-beta-scale can be found in the surveillance PPI (upper panel). Among them, one in the east of the R/V MIRAI and another in the southwest of the R/V MIRAI were found to be approaching the R/V MIRAI. Both of them are found to have strong negative Doppler velocity inside, which indicates the approaching wind. These two features collided nearby the R/V MIRAI after 30–60 minutes of the scene shown.

Detailed analyses of the data observed by the radar will be performed after the cruise.

(6) Data archive

The obtained data will be submitted to the Data Management Group of JAMSTEC.

Table 3.8-1 Scan modes of C-band weather radar

	Surveillance PPI Scan	Volume Scan					RHI Scan
Repeated Cycle (min.)	30	6					6
Times in One Cycle	1	1					3
PRF(s) (Hz)	400	dual PRF (ray alternative)					1250
		667	833	938	1250	1333	
Azimuth (deg)	Full Circle					Option	
Bin Spacing (m)	150						
Max. Range (km)	300	150	100	60	100		
Elevation Angle(s) (deg.)	0.5	0.5	1.0, 1.8, 2.6, 3.4, 4.2, 5.1, 6.2, 7.6, 9.7, 12.2, 15.2	18.7, 23.0, 27.9, 33.5, 40.0	0.0~ 60.0		

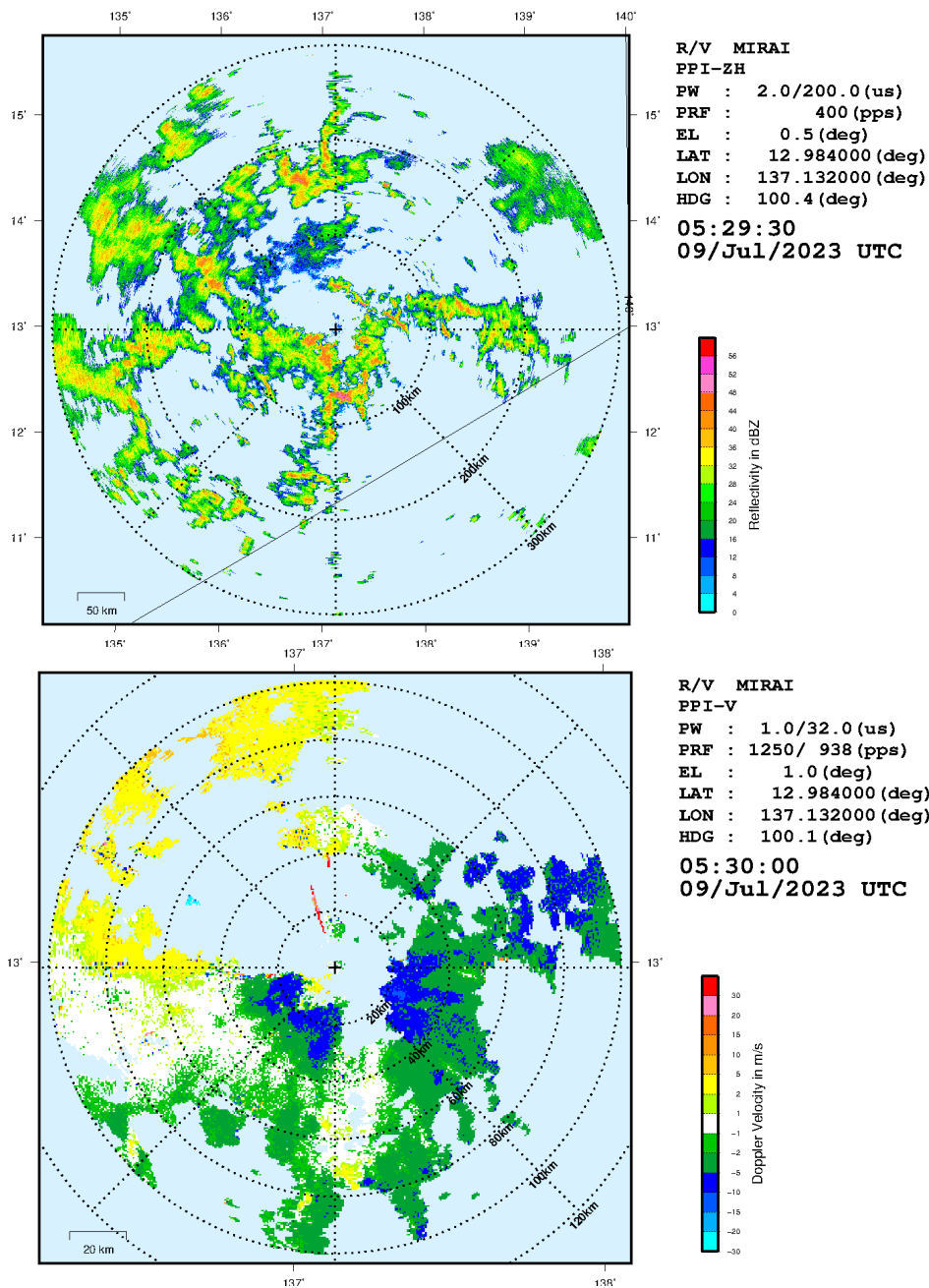


Figure 3.8-1 Example of the obtained data by the PPI scans at (around) 0530UTC on Jul.09, 2023. The upper panel is for the radar reflectivity by the surveillance PPI scan (at the elevation of 0.5° within a 300-km range distance), whereas the lower panel is for the Doppler velocity by the volume scan (at the elevation of 1.0° within a 100-km range distance).

### **3.9 Disdrometer observation**

#### **3.9.1 Optical disdrometer**

Masaki KATSUMATA (JAMSTEC) - Principal investigator

##### (1) Objectives

The disdrometer can continuously obtain size distribution of raindrops. The objective of this observation is (a) to reveal microphysical characteristics of the rainfall, depends on the type, temporal stage, etc. of the precipitating clouds, and (b) to retrieve the coefficient to convert radar data (especially from C-band radar in Section 3.8) to the rainfall amount

##### (2) Instrumentations and Methods

A “Laser Precipitation Monitor (LPM)” (Adolf Thies GmbH & Co) are utilized. It is an optical disdrometer. The instrument consists of the transmitter unit which emit the infrared laser, and the receiver unit which detects the intensity of the laser come thru the certain path length in the air. When a precipitating particle fall thru the laser, the received intensity of the laser is reduced. The receiver unit detect the magnitude and the duration of the reduction and then convert them onto particle size and fall speed. The sampling volume, i.e. the size of the laser beam “sheet”, is 20 mm (W) x 228 mm (D) x 0.75 mm (H). The LPM is installed at the starboard side on the top (roof) of the anti-rolling system.

The particles are categorized by the detected size and fall speed and counted the number in each category every minutes. The categories are shown in Table 3.9.1-1.

##### (3) Preliminary Results

The data have been obtained all through the cruise, except in the territorial water of the Republic of Palau. The further analyses for the rainfall amount, drop-size-distribution parameters, etc., will be carried out after the cruise.

##### (5) Data Archive

All data obtained during this cruise will be submitted to the JAMSTEC Data Management Group (DMG).

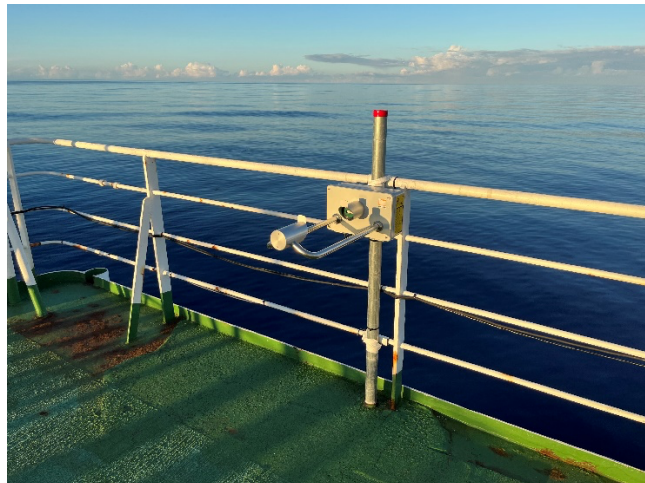


Figure 3.9.1-1 LPM sensor during MR23-05.

Table 3.9.1-1 Categories of the particle size and the fall speed.

Particle Size			Fall Speed		
Class	Diameter [mm]	Class width [mm]	Class	Speed [m/s]	Class width [m/s]
1	$\geq 0.125$	0.125	1	$\geq 0.000$	0.200
2	$\geq 0.250$	0.125	2	$\geq 0.200$	0.200
3	$\geq 0.375$	0.125	3	$\geq 0.400$	0.200
4	$\geq 0.500$	0.250	4	$\geq 0.600$	0.200
5	$\geq 0.750$	0.250	5	$\geq 0.800$	0.200
6	$\geq 1.000$	0.250	6	$\geq 1.000$	0.400
7	$\geq 1.250$	0.250	7	$\geq 1.400$	0.400
8	$\geq 1.500$	0.250	8	$\geq 1.800$	0.400
9	$\geq 1.750$	0.250	9	$\geq 2.200$	0.400
10	$\geq 2.000$	0.500	10	$\geq 2.600$	0.400
11	$\geq 2.500$	0.500	11	$\geq 3.000$	0.800
12	$\geq 3.000$	0.500	12	$\geq 3.400$	0.800
13	$\geq 3.500$	0.500	13	$\geq 4.200$	0.800
14	$\geq 4.000$	0.500	14	$\geq 5.000$	0.800
15	$\geq 4.500$	0.500	15	$\geq 5.800$	0.800
16	$\geq 5.000$	0.500	16	$\geq 6.600$	0.800
17	$\geq 5.500$	0.500	17	$\geq 7.400$	0.800
18	$\geq 6.000$	0.500	18	$\geq 8.200$	0.800
19	$\geq 6.500$	0.500	19	$\geq 9.000$	1.000
20	$\geq 7.000$	0.500	20	$\geq 10.000$	10.000
21	$\geq 7.500$	0.500			
22	$\geq 8.000$	unlimited			

### 3.9.2 Micro rain radar

Masaki KATSUMATA (JAMSTEC) - Principal investigator

#### (1) Objectives

The micro rain radar (MRR) is a compact vertically-pointing Doppler radar, to detect vertical profiles of rain drop size distribution. The objective of this observation is to understand detailed vertical structure of the precipitating systems.

#### (2) Instruments and Methods

The MRR-2 (METEK GmbH) was utilized. The specifications are in Table 3.9.2-1. The antenna unit was installed at the starboard side of the anti-rolling systems (see Fig. 3.9.2-1), and wired to the junction box and laptop PC inside the vessel.

The data was averaged and stored every 1 minute. The vertical profile of each parameter was obtained every 100 meters in range distance (i.e., height) up to 3100 meters. The recorded parameters were; Drop size distribution, radar reflectivity, path-integrated attenuation, rain rate, liquid water content and fall velocity.

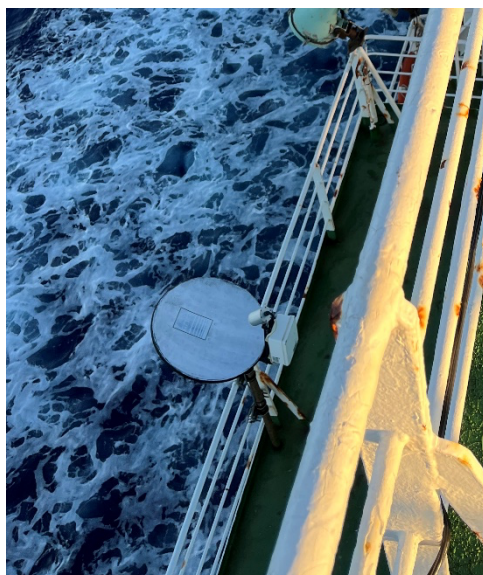


Figure 3.9.2-1 Onboard MRR sensor during MR23-05.

Table 3.9.2-1 Specifications of the MRR-2.

Transmitter power	50 mW
Operating mode	FM-CW
Frequency	24.230 GHz (modulation 1.5 to 15 MHz)
3dB beam width	1.5 degrees
Spurious emission	< -80 dBm / MHz
Antenna Diameter	600 mm
Gain	40.1 dBi

#### (3) Preliminary Results

The data have been obtained all through the cruise, except in the territorial water of the Republic of Palau. The further analyses will be after the cruise.

#### (4) Data Archive

All data obtained during this cruise will be submitted to the JAMSTEC Data Management Group (DMG).

### 3.10 Microwave radiometer observation

Masaki KATSUMATA	(JAMSTEC)	
Akira KUWANO-YOSHIDA	(Kyoto University)	- not on board
Masahiro MINOWA	(Furuno Electric Co., Ltd.)	- not on board

#### (1) Objective

To retrieve the total column integrated water vapor, and the vertical profiles of water vapor and temperature, in the atmosphere

#### (2) Method

Two microwave radiometers (hereafter MWR; manufactured by Furuno Electric Co., Ltd.) are used. The MWRs received natural microwave within the angle of 20 deg. from zenith. One of the MWRs for the water vapor observes at the frequencies around 22 GHz, to retrieve the column integrated water vapor (or precipitable water), and the vertical profile of the water vapor. The other MWR measures at the frequencies around 55 GHz to retrieve vertical profile of the air temperature.

The observation was made approximately every 20 seconds except when periodic auto-calibration was on-going (once in several minutes). The rain sensor is equipped to identify the period of rainfall.

In addition to the MWRs, the whole sky camera was installed beside the MWR. This is to monitor cloud cover, which also affects the microwave signals. The camera obtained the whole-sky image every 2 minutes.

Both instruments were installed at the top of the roof of aft wheelhouse, as in Fig. 3.10-1. The data were continuously obtained all through the cruise period.

#### (3) Results

The data have been obtained all through the cruise, except in the territorial water of the Republic of Palau. The further analyses for the water vapor (column-integrated amount and vertical profile), the air temperature (vertical profile), etc., will be carried out after the cruise.

#### (4) Data archive

The data will be submitted to the JAMSTEC Data Management Group (DMG).

#### (5) Acknowledgment

The observation was supported by the JSPS KAKENHI Grant 23H00519.



Figure 3.10-1 Outlook of the instruments installed at the roof of the aft wheelhouse; the microwave radiometer for the air temperature (right), microwave radiometer for the water vapor (middle), and the whole-sky camera (left).

### 3.11 Atmospheric composition in the marine boundary layer

#### 3.11.1 Trace gases and aerosols in the marine boundary layer

Fumikazu TAKETANI	(JAMSTEC)	
Takashi SEKIYA	(JAMSTEC)	
Cui TIANCHANG	(Hokkaido University/JAMSTEC)	
Yugo KANAYA	(JAMSTEC)	- not on board
Atsushi OOKI	(Hokkaido University)	- not on board
Hisahiro Takashima	(Fukuoka University/JAMSTEC)	- not on board
Yoko IWAMOTO	(Hiroshima University)	- not on board
Kazuhiko TAKEDA	(Hiroshima University)	- not on board
Minako KURISU	(JAMSTEC)	- not on board

Observation was supported by Nippon Marine Enterprises, Ltd.

#### (1) Objectives

To investigate halogen chemistry in the marine atmosphere over the Western Pacific warm pool.

To investigate the spatiotemporal behavior and sources of gas/aerosol components over the subtropical Northwest Pacific Ocean during the summer season.

To investigate the transport process of short-lived climate forcers from the continent to the Northwestern Pacific Ocean during the summer season.

To investigate influence of the wet/dry deposition to the marine ecosystem over the subtropical Northwestern Pacific Ocean during the summer season.

#### (2) Parameters

- Surface ozone(O<sub>3</sub>), carbon monoxide (CO) and Nitrogen dioxide (NO<sub>2</sub>) mixing ratios
- Vertical distributions of NO<sub>2</sub> and other gases (including IO) in the troposphere
- Aerosol optical depth (AOD) vertical distribution in the troposphere
- Surface aerosol particle size distributions and number density
- Surface aerosol chemical composition of fine and coarse mode aerosols
- Chemical composition of rain water
- Concentrations of organohalogen compounds in the ambient air

#### (3) Instruments and methods

(3-1) Continuous surface aerosol/gas observations during the cruise:

(3-1-1) Particle size distributions:

The size-resolved number concentration of particles was measured by a handheld optical particle counter (OPC) (KR-12A, RION) installed on the compass deck for the size range between 0.3 and 5 μm in diameter.

(3-1-2) CO, O<sub>3</sub>, and NO<sub>2</sub>:

Ambient air was continuously sampled on the compass deck and drawn through Teflon tubes connected to a nondispersive infrared (NDIR) CO analyzer (Model 48i-TLE, Thermo Fisher Scientific), a UV photometric ozone analyzer (model 205, 2B Technologies) and a NO<sub>2</sub> monitor

(CAPS-NO<sub>2</sub>-HS, Shoreline science), located in the environmental research room.

### (3-1-3) MAX-DOAS:

Multi-Axis Differential Optical Absorption Spectroscopy (MAX-DOAS), a passive remote sensing technique measuring spectra of scattered visible and ultraviolet (UV) solar radiation, was used for atmospheric aerosol and gas profile measurements. Our MAX-DOAS instrument consists of two main parts: an outdoor telescope unit and an indoor spectrometer (Acton SP-2358 with Princeton Instruments PIXIS-400B), connected to each other by a 14-m bundle optical fiber cable. The line of sight was in the directions of the portside of the vessel and the scanned elevation angles were 2, 3, 4, 6, 10, 20, and 90 degrees in the 30-min cycle. The roll motion of the ship was measured to autonomously compensate additional motion of the prism, employed for scanning the elevation angle.

For the selected spectra recorded with elevation angles with accurately measured elevation angle, DOAS spectral fitting was performed to quantify the slant column density (SCD) of NO<sub>2</sub> (and other gases) and O<sub>4</sub> (O<sub>2</sub>-O<sub>2</sub>, collision complex of oxygen) for each elevation angle. Then, the O<sub>4</sub> SCDs were converted to the aerosol optical depth (AOD) and the vertical profile of aerosol extinction coefficient (AEC) using an optimal estimation inversion method with a radiative transfer model. The tropospheric vertical column/profile of NO<sub>2</sub> and other gases (including IO) were retrieved using derived aerosol profiles.

### (3-2) Aerosol sampling:

Samplings of aerosol particles in the marine atmosphere for the chemical composition analyses were performed using High-volume air samplers and filter pack sampler on the compass deck. Aerosol particles were collected on the filter along cruise track using three high-volume air samplers (HVSs 1, 2 and 3) and filter pack sampler located on the compass deck to analyze the chemical composition. To avoid collecting particles derived from the research vessel's own exhaust, the pumping by the samplers were automatically controlled using a "wind-direction selection system". These samplings were carried out same period. The sampling logs are listed in Table 3.11.1-1. All the samples will be analyzed in the laboratories at JAMSTEC.

HVS1: HV-700F (SIBATA Sci.) with a single-stage impactor for analyzing mode-segregated inorganic ions and carbonaceous species (elemental and organic carbon, etc.) of collected aerosols. Prebaked quartz fiber filters (QR-100, Advantec, Japan) (3 hrs at 900°C) were employed for the sampling. Fine (PM<sub>2.5</sub>) and Coarse (TSP - PM<sub>2.5</sub>) mode particles were separately collected on the two QFF filters at the sampling rate of approximately 500 L/min.

HVS2: HV-700F (SIBATA Sci.) with a single-stage impactor for analyzing mode-segregated metal species (Fe etc.) of collected aerosols. For coarse particles, a PTFE filters (PF020, Advantec, Japan) washed by soaking into 3 mol/L HCl overnight and rinsed carefully with ultrapure water before use were used for the sampling. For fine particles, PTFE filters (WP-500-50, Sumitomo-Electric) were used for the sampling. Fine (PM<sub>2.5</sub>) and Coarse (TSP - PM<sub>2.5</sub>) mode particles were separately collected on the two PTFE filters at the sampling rate of approximately 500 L/min.

HVS3: 120SL (Kimoto Electric) for analyzing iodine species of collected aerosols. A prebaked quartz fiber filters (Tokyo direc) (3 hrs at 900°C) and activated carbon filter (CP-20, Advantec) were used for the sampling. Aerosol particles and gases were separately collected on the quartz

and activated carbon filters, respectively at the sampling rate of approximately 600 L/min.

Filter pack: Ambient particles/gases were collected on the 4 filters ( $\phi=47\text{mm}$ ) using multistage sampler to analyze their composition along cruise track operated at flow rate of 20 L/min. The filter pack contains for filters, PTFE (Whatman), Nylon filter (Nylasorb), alkaline impregnated cellulose filter (6%  $\text{K}_2\text{CO}_3+2\%$  Glycelin / $\text{H}_2\text{O}$ ) and phosphoric acid impregnated cellulose filter (6%  $\text{H}_3\text{PO}_4+2\%$  Glyceline / $\text{H}_2\text{O}$ ).

### (3-3) Rain sampling:

Rainwater was collected using hand-made rain samplers. These samples were analyzed in the R/V MIRAI and laboratory at JAMSTEC to investigate the chemical composition including nutrients over Northwestern Pacific region. Sampling logs are listed in Table 3.11.1-2.

### (3-4) Air sampling:

Air samplings were performed in order to investigate the concentrations of organohalogen compounds in the marine air. The marine air was collected in stainless steel canister with a volume of 6 L at a pressure of 1.5 atm using a metal bellows pump. These sampling logs are listed in Table 3.11.1-3. Analysis will be performed in the laboratory after the cruise using a preconcentration/capillary gas chromatography-mass spectrometry (GC-MS) system developed for automated measurement of atmospheric halocarbons  $\text{CH}_3\text{I}$  and other halocarbons will be measured by the analytical system.

### (4) Data archives

All data obtained during this cruise will be submitted to Data Management Group (DMG) of JAMSTEC after the sample analysis and validation. The data will be opened to the public via “Data Research System for Whole Cruise Information (DARWIN)” in JAMSTEC web site.

Table 3.11.1-1 Sampling logs for 4 aerosol samplers at compass deck.

On board ID	Date Collected					Latitude			Longitude		
	YYYY	MM	DD	hh:mm	UTC/JS T	Deg.	Min.	N/S	Deg.	Min.	E/W
MR2305leg1-001	2023	06	28	2:25	UTC	34	37	N	138	42.3	E
MR2305leg1-002	2023	07	01	1:26	UTC	29	33.9	N	144	38.5	E
MR2305leg1-003	2023	07	03	1:27	UTC	21	49.76	N	141	50.23	E
MR2305leg1-004	2023	07	05	1:00	UTC	13	9.37	N	136	58.29	E
MR2305leg1-005	2023	07	07	7:04	UTC	12	54.76	N	136	49.57	E
MR2305leg1-006	2023	07	09	9:34	UTC	13	29.34	N	136	52.05	E
MR2305leg1-007	2023	07	13	9:10	UTC	7	55.74	N	134	12.65	E
MR2305leg1-008	2023	07	15	7:12	UTC	14	56.86	N	134	52.82	E
MR2305leg1-009	2023	07	17	1:50	UTC	22	25.01	N	136	32.38	E

Table 3.11.1-2 Logs for rain sampling.

On board ID	Date Collected					Latitude			Longitude		
	YYYY	MM	DD	hh:mm	UTC/JS T	Deg.	Min.	N/S	Deg.	Min.	E/W
MR2305/R001	2023	07	02	7:24	UTC	24	38.57	N	144	39.52	E
MR2305/R002	2023	07	04	2:25	UTC	16	59.05	N	138	57.3	E
MR2305/R003	2023	07	05	9:30	UTC	12	58.6	N	136	57.38	E
MR2305/R004	2023	07	06	8:55	UTC	12	58.81	N	137	2.51	E
MR2305/R005	2023	07	06	9:20	UTC	12	58.81	N	137	2.51	E
MR2305/R006	2023	07	07	22:00	UTC	13	12.71	N	136	33.64	E
MR2305/R007	2023	07	08	7:21	UTC	12	59.35	N	137	4.91	E
MR2305/R008	2023	07	09	7:10	UTC	13	6.28	N	137	4.71	E
MR2305/R009	2023	07	10	22:30	UTC	10	1.24	N	134	55.34	E
MR2305/R010	2023	07	13	9:10	UTC	7	55.54	N	134	12.65	E

Table 3.11.1-3 Logs for Canister grab sampling.

On board ID	Date Collected					Latitude			Longitude		
	YYYY	MM	DD	hh:mm	UTC/JS T	Deg.	Min.	N/S	Deg.	Min.	E/W
MR2305/AIR01	2023	06	29	0.3	JST	32	41.9	N	143	10.45	E
MR2305/AIR02	2023	06	30	0.2799	JST	32	27.46	N	144	31.97	E
MR2305/AIR03	2023	07	01	0.2896	JST	30	18.3	N	144	35.25	E
MR2305/AIR04	2023	07	02	0.2924	JST	25	6.62	N	144	59.24	E
MR2305/AIR05	2023	07	03	0.2924	JST	22	20.92	N	142	21.61	E
MR2305/AIR06	2023	07	04	0.2896	JST	18	0.58	N	139	27.49	E
MR2305/AIR07	2023	07	05	0.2882	JST	13	35.76	N	137	15.03	E
MR2305/AIR08	2023	07	06	0.2931	JST	12	58.69	N	136	57.4	E
MR2305/AIR09	2023	07	07	0.2882	JST	12	59	N	136	52.22	E
MR2305/AIR10	2023	07	08	0.2083	JST	13	5.97	N	136	49.84	E
MR2305/AIR11	2023	07	08	0.2931	JST	13	6.25	N	136	53.4	E
MR2305/AIR12	2023	07	09	0.2083	JST	12	59.03	N	137	3.54	E
MR2305/AIR13	2023	07	09	0.2917	JST	12	59.26	N	137	8.03	E
MR2305/AIR14	2023	07	10	0.2924	JST	13	30.93	N	137	0.24	E
MR2305/AIR15	2023	07	11	0.2882	JST	13	11.57	N	135	40.87	E
MR2305/AIR16	2023	07	12	0.4896	JST	9	20.41	N	134	42.67	E
MR2305/AIR17	2023	07	14	0.2924	JST	10	30.6	N	134	41.38	E
MR2305/AIR18	2023	07	15	0.3076	JST	14	39.93	N	134	59.75	E
MR2305/AIR19	2023	07	16	0.2924	JST	18	1.22	N	135	31.31	E
MR2305/AIR20	2023	07	17	0.2917	JST	21	54.32	N	136	26.73	E
MR2305/AIR21	2023	07	18	0.2924	JST	26	42.71	N	137	10.36	E
MR2305/AIR22	2023	07	19	0.2903	JST	32	7.81	N	137	56.76	E

### 3.11.2 Experiment for ozone reaction with seawater

Cui TIANCHANG	(Hokkaido University/JAMSTEC)	
Atsushi OOKI	(Hokkaido University)	- not on board
Fumikazu TAKETANI	(JAMSTEC)	
Takashi SEKIYA	(JAMSTEC)	
Yugo KANAYA	(JAMSTEC)	- not on board
Hisahiro TAKASHIMA	(Fukuoka University/JAMSTEC)	- not on board
Yoko IWAMOTO	(Hiroshima University)	- not on board
Kazuhiko TAKEDA	(Hiroshima University)	- not on board

#### (1) Objectives

To investigate ozone reaction with iodine in seawater.

To investigate productions of organic iodine gases by the ozone reaction with iodine in seawater.

#### (2) Methods

Surface seawater was collected from a Niskin bottle by CTD observation (Stations KEO and KEOS). The sample seawater was put in a glass bottle with a volume of 600 mL and stirred in the bottle. Ozone at concentrations of 25 ppb or 50 ppb was introduced the glass bottle at a flow rate of 4 mL/min for 24 hr. Organic iodine gases in head space of the glass bottle were collected in a cold trap with TenaxTA using air pump and mass flow controller. The cold-trap sample will be analyzed after the cruise with GC/MS system. The seawater samples (10 mL and 32 mL) were collected in a tube for inorganic iodine analysis and a glass bottle for organic iodine analysis. These samples will be analyzed after the cruise. A schematic diagram of experiment is shown in Fig. 3.11.2-1.

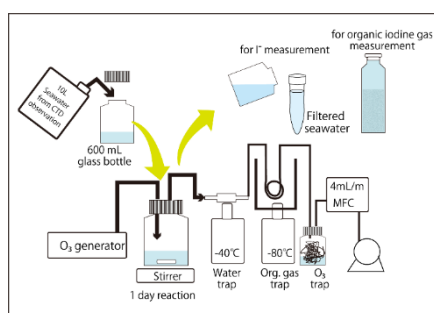


Figure 3.11.2-1 Schematic diagram of ozone reaction experiment.

#### (3) Experiment

The experiments were conducted 20 times during the cruise.

#### (4) Data archives

All data obtained during this cruise will be submitted to Data Management Group (DMG) of JAMSTEC after the sample analysis and validation. The data will be opened to the public via “Data Research System for Whole Cruise Information (DARWIN)” in JAMSTEC web site.

### 3.11.3 Greenhouse gases observation

Yasunori TOHJIMA	(NIES)	- not on board
Shigeyuki ISHIDOYA	(AIST)	- not on board
Fumikazu TAKETANI	(JASTEC)	- not on board
Shinji MORIMOTO	(Tohoku University)	- not on board
Daisuke GOTO	(NIPR)	- not on board
Prabir PATRA	(JAMSTEC)	- not on board

#### (1) Objective

##### Continuous observation onboard R/V MIRAI

Carbon dioxide (CO<sub>2</sub>) and methane (CH<sub>4</sub>) are the first- and second-most-important anthropogenic greenhouse gases (GHGs) in the atmosphere. Recent systematic measurements of the atmospheric mixing ratios of these GHGs have clearly shown the steady increases, reflecting imbalances between the sources and sinks of the GHGs. The CO<sub>2</sub> emissions from fossil fuel combustion and land use change are major drivers of the atmospheric CO<sub>2</sub> increase while the ocean and land biosphere act as the sink of CO<sub>2</sub>, taking up about half of the anthropogenic CO<sub>2</sub> emissions. However, there are still large uncertainties of the present and future levels of these sink strengths, making it uncertain to predict the future atmospheric CO<sub>2</sub> growth. As for CH<sub>4</sub>, there are lots of anthropogenic sources including fugitive emissions from fossil fuel exploitation, paddy fields, landfill, and so on. Since these emissions and the distributions have large uncertainties, the prediction of the future CH<sub>4</sub> levels is also difficult. To reduce these uncertainties atmospheric inversion approach based on atmospheric transport models and the atmospheric observed data are useful. However, since the atmospheric observations are still limited, extending the observation network is highly required. Therefore, we measured the atmospheric CO<sub>2</sub> and CH<sub>4</sub> mole fractions aboard the R/V MIRAI during MR23-05 Leg1 cruise to clarify the distributions across the Pacific and fill the observation gap.

##### Discrete flask sampling

In order to clarify spatial variations and air-sea exchanges of the greenhouse gases in the Pacific region, whole air samples were collected into 3 stainless-steel flasks on-board the R/V MIRAI during MR23-05 Leg1 cruise. The collected air samples will be analyzed for the mixing ratios of CO<sub>2</sub>, O<sub>2</sub>, Ar, CH<sub>4</sub>, CO, N<sub>2</sub>O and SF<sub>6</sub> and the stable isotope ratios of CO<sub>2</sub> and CH<sub>4</sub>.

#### (2) Apparatus

##### Continuous observation onboard R/V MIRAI

Atmospheric CO<sub>2</sub>, CH<sub>4</sub>, and CO mixing ratios were measured by a wavelength-scanned cavity ring-down spectrometer (WS-CRDS, Picarro,



**Photo 3.11.3-1.** Flask sampling system (left) and atmospheric CO<sub>2</sub>, CH<sub>4</sub> and CO measurement system (right) based on a cavity ring-down spectrometer (Picarro G2401).

G2401, see Photo 3.11.3-1). An air intake, capped with an inverted stainless-steel beaker covered with stainless steel mesh, was placed on the right-side of the upper deck. A diaphragm pump (GAST, MOA-P108) was used to draw in the outside air at a flow rate of  $\sim 8 \text{ L min}^{-1}$ . Water vapor in the sample air was reduced to a dew point of about  $-35^\circ\text{C}$  by passing it consecutively through a thermoelectric dehumidifier (KELK, DH-109) and a Nafion drier (PERMA PURE, PD-50T-24), respectively. Then, the dried sample air was introduced into the WS-CRDS at a flow rate of  $100 \text{ ml min}^{-1}$ . The WS-CRDS were automatically calibrated every 50 hours by introducing 3 standard airs with known  $\text{CO}_2$ ,  $\text{CH}_4$  and  $\text{CO}$  mixing ratios. The analytical precisions for  $\text{CO}_2$ ,  $\text{CH}_4$  and  $\text{CO}$  mixing ratios are about 0.02 ppm, 0.3 ppb and 3 ppb, respectively.

#### Discrete flask sampling

The air sampling equipment consisted of an air intake, a diaphragm pump (GAST MOA), a Stirling cooler (Twinbird) with a water trap, solenoid valves (CKD), a flow meter and a back pressure valve. Ambient air was pumped using the diaphragm pump from an air intake, dried cryogenically and filled into a 1 L stainless-steel flask at a pressure of 0.27 MPa.

#### (3) Results

The atmospheric  $\text{CO}_2$ ,  $\text{CH}_4$ , and  $\text{CO}$  mixing ratios were observed without any problems during the entire cruise period. The time series of the atmospheric  $\text{CH}_4$ ,  $\text{CO}_2$ , and  $\text{CO}$  mixing ratios observed during the entire cruise are shown in Fig. 3.11.3-1. Sampling logs of the discrete flask sampling are listed in Table 3.11.3-1.

Table 3.11.3-1: Sampling logs of the discrete flask sampling during MR23-05 Leg1 cruise.

On board ID	Date Collected					Latitude			Longitude		
	YYYY	MM	DD	Mh:mm:ss	UTC/AST	Deg.	Min.	N/S	Deg.	Min.	E/W
MR2305leg1-B001	2023	07	13	23:55	UTC	10	54.12	N	134	45.54	E
MR2305leg1-B002	2023	07	15	23:41	UTC	18	22.34	N	135	37.73	E
MR2305leg1-B003	2023	07	18	6:32	UTC	28	28.77	N	137	25.83	E

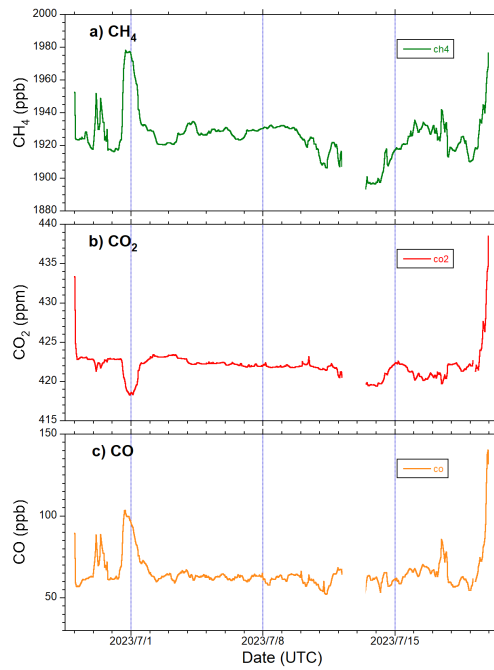


Figure 3.11.3-1: The time series of the atmospheric (top) CH<sub>4</sub>, (middle) CO<sub>2</sub>, and (bottom) CO mixing ratios observed during the entire period of MR23-05 Leg1 cruise.

### 3.12 GNSS precipitable water

Mikiko FUJITA	(JAMSTEC)	- not onboard
Masaki KATSUMATA	(JAMSTEC)	

#### (1) Objectives

Getting the GNSS satellite data to estimate the total column integrated water vapor content of the atmosphere.

#### (2) Instruments and Methods

The GNSS satellite data was archived to the receiver (Trimble NetR9 and SEKIREI-L9P) with 5 sec intervals. The GNSS antenna (HX-CGX611A and Hemisphere A45) was set on the roof of aft wheel house. The observations were carried out all through the cruise.

#### (3) Preliminary Results

We will calculate the total column integrated water from observed GNSS satellite data after the cruise.

#### (4) Data Archive

Raw data is recorded as T02 and UBX format and stream data every 5 seconds. These raw datasets are available from Mikiko Fujita of JAMSTEC. Corrected data will be submitted to JAMSTEC Marine-Earth Data and Information Department and will be archived there.

### 3.13 Lidar observation

Masaki KATSUMATA	(JAMSTEC)	
Kyoko TANIGUCHI	(JAMSTEC)	- not on board
Yutaro MURAKAMI	(NME)	
Ryo OYAMA	(NME)	

#### (1) Objective

The objective of this observation is to capture the vertical distribution of clouds, aerosols, and water vapor in high spatio-temporal resolution.

#### (2) Parameters

- 355nm Mie scattering signal
- 532nm Mie scattering signal
- 1064nm Mie scattering signal
- 387nm Raman nitrogen scattering signal (nighttime only)
- 408nm Raman water vapor scattering signal (nighttime only)
- 607nm Raman nitrogen scattering signal (nighttime only)
- 660nm Raman water vapor scattering signal (nighttime only)

#### (3) Instruments and methods

The MIRAI lidar system transmits a 10-Hz pulse laser in three wavelengths: 1064nm, 532nm, 355nm. For cloud and aerosol observation, the system detects Mie scattering at these wavelengths. The separate detections of polarization components at 532 nm and 355 nm obtain additional characteristics of the targets. The system also detects Raman water vapor signals at 660 nm and 408nm, Raman nitrogen signals at 607 nm and 387nm at nighttime. Based on the signal ratio of Raman water vapor to Raman nitrogen, the system offers water vapor mixing ratio profiles.

#### (4) Preliminary Results

The lidar system observed the lower atmosphere throughout the cruise (28 June to 19 July, 2023), except on the territorial waters of Palau Republic. All data will be reviewed after the cruise to maintain data quality.

#### (5) Data Archive

The obtained data will be submitted to the Data Management Group of JAMSTEC.

### 3.14 Aerosol optical characteristics measured by shipborne sky radiometer

Kazuma AOKI (University of Toyama) - not on board  
Sky radiometer operation was supported by Nippon Marine Enterprises, Ltd.

#### (1) Objectives

Objective of this observation is to study distribution and optical characteristics of marine aerosols by using a ship-borne sky radiometer (POM-01 MK-III: PREDE Co. Ltd., Japan). Furthermore, collections of the data for calibration and validation to the remote sensing data were performed simultaneously.

#### (2) Instruments and methods

##### i) Sky radiometer measurement

The sky radiometer measures the direct solar irradiance and the solar aureole radiance distribution with seven interference filters (0.315, 0.4, 0.5, 0.675, 0.87, 0.94, and 1.02  $\mu\text{m}$ ). Analysis of these data was performed by SKYRAD.pack version 4.2 developed by Nakajima et al. 1996 and 2020.

##### ii) Parameters

- Aerosol optical thickness at five wavelengths (400, 500, 675, 870 and 1020 nm)
- Ångström exponent
- Single scattering albedo at five wavelengths
- Size distribution of volume (0.01  $\mu\text{m}$  – 20  $\mu\text{m}$ )
- # GPS provides the position with longitude and latitude and heading direction of the vessel, and azimuth and elevation angle of the sun. Horizon sensor provides rolling and pitching angles.

#### (3) Data archive

Aerosol optical data are to be archived at University of Toyama (K.Aoki, SKYNET/SKY: <http://skyrad.sci.u-toyama.ac.jp/sobs/>) after the quality check and will be submitted to JAMSTEC.

#### (4) References

Nakajima, T., G.Tonna, R.Rao, P.Boi, Y.Kaufman and B.Holben (1996) Use of sky brightness measurements from ground for remote sensing of particulate polydispersions, *Appl. Opt.*, 35, 2672–2686, <https://doi.org/10.1364/AO.35.002672>.

Aoki, K., T.Takemura, K.Kawamoto, and T.Hayasaka (2013), Aerosol climatology over Japan site measured by ground-based sky radiometer, *AIP Conf. Proc.* 1531, 284-287 (2013); doi: 10.1063/1.4804762.

Nakajima, T., Campanelli, M., Che, H., Estellés, V., Irie, H., Kim, S.-W., Kim, J., Liu, D., Nishizawa, T., Pandithurai, G., Soni, V.K., Thana, B., Tugjurn, N.-U., Aoki, K., Hashimoto, M., Higurashi, A., Kazadzis, S., Khatrri, P., Kouremeti, N., Kudo, R., Marenco, F., Momoi, M., Ningombam, S. S., Ryder, C.L., and Uchiyama, A. (2020) An overview and issues of the sky radiometer technology and SKYNET, *Atmos. Meas. Tech.*, 13, 4195–4218, 2020, <https://doi.org/10.5194/amt-13-4195-2020>.

### 3.15 Three-dimensional wind and sonic temperature observation for eddy-covariance momentum and heat fluxes observation

Iwao UEKI	(JAMSTEC)	- Principal investigator
Tatsuya FUKUDA	(JAMSTEC)	- not on board
Biao GENG	(JAMSTEC)	- not on board
Ryo OYAMA	(NME)	
Yutaro MURAKAMI	(NME)	

#### (1) Objectives

Exchange of momentum, heat, and mass between the ocean and atmosphere is widely recognized as important processes for atmospheric and oceanic circulation, but observational approaches to detailed processes are still insufficient, and understanding those processes through observation is widely required. According to those background, we have been enhancing our observations to improve our understanding of fundamental processes between the atmosphere and the ocean. As a part of those efforts, we intend to establish momentum and heat fluxes observation based on eddy-covariance method.

#### (2) Parameters

- Three-dimensional wind speed
- Sonic temperature
- Air temperature
- Barometric pressure

#### (3) Methods

We installed a three-dimensional sonic anemometer of IRGASON (Campbell Scientific) with a GNSS/INS system of Spatial (Advanced Navigation) for accurate position, velocity, acceleration and orientation of IRGASON at the foremast (Fig. 3.15-1).

IRGASON and Spatial observed three-dimensional wind speed and parameters associated with attitude of IRGASON at 20 Hz. Using those variables, we plan to develop algorithms for kinematic and movement corrections and removal of apparent wind speed.

#### (4) Data archive

Three-dimensional wind speed data obtained in this cruise will be submitted to the Data Management Group of JAMSTEC, and will be opened to the public via “Data Research System for Whole Cruise Information in JAMSTEC (DARWIN)” in JAMSTEC web site.

<http://www.godac.jamstec.go.jp/darwin/e>

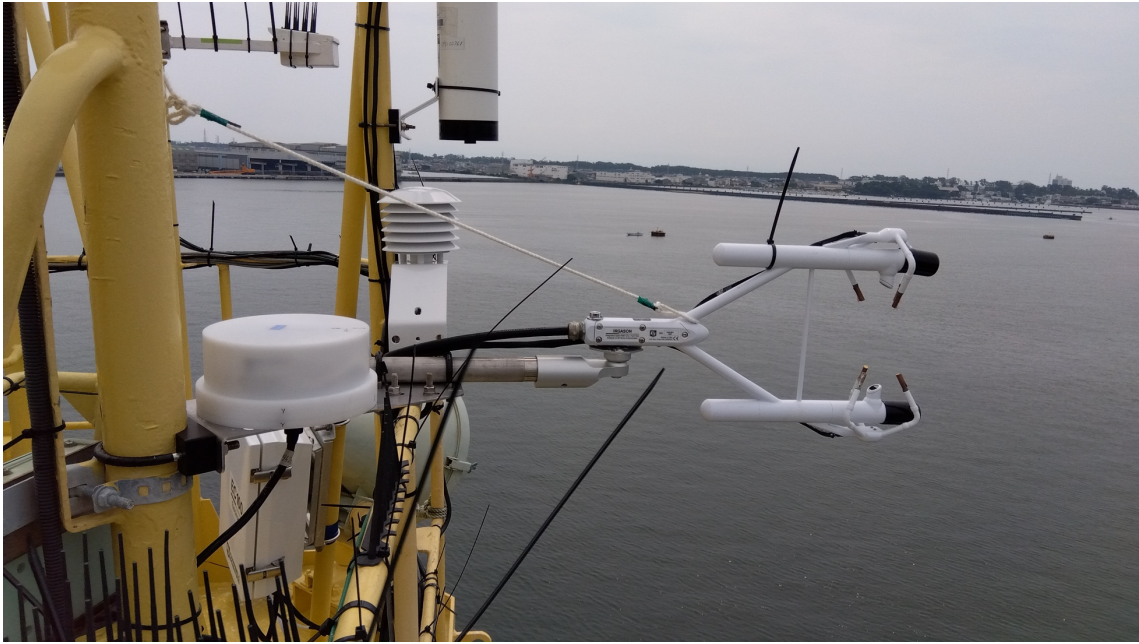


Figure 3.15-1 IRGASON with Spatial at the foremast

#### **4. Notice on using**

This cruise report is a preliminary documentation as of the end of cruise.

This report is not necessarily corrected even if there is any inaccurate description (i.e., taxonomic classifications). This report is subject to be revised without notice. Some data on this report may be raw or unprocessed. If you are going to use or refer the data on this report, it is recommended to ask the Chief Scientist for latest status.

Users of information on this report are requested to submit Publication Report to JAMSTEC.

<http://www.godac.jamstec.go.jp/darwin/explain/1/e#report>

E-mail: [submit-rv-cruise@jamstec.go.jp](mailto:submit-rv-cruise@jamstec.go.jp)